

# SILOXANE REMOVAL IN THE ENERGY RECOVERY OF BIOGAS: SEQUENTIAL ADSORPTION/OXIDATION PROCESSES

**Alba Cabrera-Codony**

Per citar o enllaçar aquest document:

Para citar o enlazar este documento:

Use this url to cite or link to this publication:

<http://hdl.handle.net/10803/399731>

**ADVERTIMENT.** L'accés als continguts d'aquesta tesi doctoral i la seva utilització ha de respectar els drets de la persona autora. Pot ser utilitzada per a consulta o estudi personal, així com en activitats o materials d'investigació i docència en els termes establerts a l'art. 32 del Text Refós de la Llei de Propietat Intel·lectual (RDL 1/1996). Per altres utilitzacions es requereix l'autorització prèvia i expressa de la persona autora. En qualsevol cas, en la utilització dels seus continguts caldrà indicar de forma clara el nom i cognoms de la persona autora i el títol de la tesi doctoral. No s'autoritza la seva reproducció o altres formes d'explotació efectuades amb finalitats de lucre ni la seva comunicació pública des d'un lloc aliè al servei TDX. Tampoc s'autoritza la presentació del seu contingut en una finestra o marc aliè a TDX (framing). Aquesta reserva de drets afecta tant als continguts de la tesi com als seus resums i índexs.

**ADVERTENCIA.** El acceso a los contenidos de esta tesis doctoral y su utilización debe respetar los derechos de la persona autora. Puede ser utilizada para consulta o estudio personal, así como en actividades o materiales de investigación y docencia en los términos establecidos en el art. 32 del Texto Refundido de la Ley de Propiedad Intelectual (RDL 1/1996). Para otros usos se requiere la autorización previa y expresa de la persona autora. En cualquier caso, en la utilización de sus contenidos se deberá indicar de forma clara el nombre y apellidos de la persona autora y el título de la tesis doctoral. No se autoriza su reproducción u otras formas de explotación efectuadas con fines lucrativos ni su comunicación pública desde un sitio ajeno al servicio TDR. Tampoco se autoriza la presentación de su contenido en una ventana o marco ajeno a TDR (framing). Esta reserva de derechos afecta tanto al contenido de la tesis como a sus resúmenes e índices.

**WARNING.** Access to the contents of this doctoral thesis and its use must respect the rights of the author. It can be used for reference or private study, as well as research and learning activities or materials in the terms established by the 32nd article of the Spanish Consolidated Copyright Act (RDL 1/1996). Express and previous authorization of the author is required for any other uses. In any case, when using its content, full name of the author and title of the thesis must be clearly indicated. Reproduction or other forms of for profit use or public communication from outside TDX service is not allowed. Presentation of its content in a window or frame external to TDX (framing) is not authorized either. These rights affect both the content of the thesis and its abstracts and indexes.



DOCTORAL THESIS

Siloxane removal in the energy recovery of biogas:  
Sequential adsorption/oxidation processes

Alba Cabrera i Codony

2016

Supervised by

Dr. Maria J. Martín Sánchez and Dr. Rafael González Olmos

Thesis submitted in fulfilment of the requirements for the degree of  
Doctor from the University of Girona  
Experimental Sciences and Sustainability Doctoral Programme



MARIA J. MARTÍN SÁNCHEZ

Professora del Departament d'Enginyeria Química, Agrària i Tecnologia Agroalimentària de la Universitat de Girona.

RAFAEL GONZÁLEZ OLMOS

Professor del Departament d'Enginyeria Química i Ciència dels Materials, de l'Institut Químic de Sarrià, Universitat Ramon Llull.

Certifiquem:

Que la llicenciada en Ciències ambientals Alba Cabrera Codony ha dut a terme sota la nostra direcció el treball titulat *Siloxane removal in the energy recovery of biogas: Sequential adsorption/oxidation processes* que es presenta en aquesta memòria, la qual constitueix la seva Tesi per optar al Grau de Doctor per la Universitat de Girona.

A Girona, 30 de juny de 2016

Dra. Maria J. Martín Sánchez

Dr. Rafael González Olmos



# Table of Content

---

Table of Content .....	ix
List of Tables .....	xiii
List of Figures .....	xv
List of Acronyms .....	xxi
Publications and Communications .....	xxv
Summary .....	xxvii
Summary in Catalan .....	xxxii
Summary in Spanish .....	xxxv
1 Introduction.....	1
1.1 Biogas as renewable energy source.....	3
1.2 Siloxanes in biogases.....	7
1.3 Siloxane removal from biogas.....	9
1.4 Adsorption/oxidation technologies.....	11
1.4.1 Adsorption.....	11
1.4.2 Activated carbon .....	12
1.4.3 Zeolites.....	13
1.4.4 Regeneration of adsorbents.....	15
1.5 State of the art .....	17
2 Objectives.....	23
3 Materials and methods.....	27
3.1 Adsorbents .....	29
3.1.1 Activated carbons.....	29
3.1.2 Zeolites.....	29
3.2 Adsorbents characterization.....	30
3.2.1 Textural characterization .....	31
3.2.2 Thermal programmed desorption (TPD).....	31
3.2.3 X-ray Photoelectron Spectroscopy (XPS) .....	32

3.2.4	Elemental Analysis (EA) .....	32
3.2.5	Energy-dispersive X-ray spectroscopy and SEM analysis (EDX/SEM) .....	32
3.2.6	Fourier transform infrared spectroscopy (FT-IR) .....	33
3.2.7	pH <sub>slurry</sub> of the ACs .....	33
3.2.8	Zeolites acidity determination.....	33
3.3	Adsorption tests .....	34
3.3.1	Static adsorption tests .....	34
3.3.2	Dynamic adsorption tests .....	34
3.3.3	Analysis of exhausted AC .....	37
3.3.4	Analysis of exhausted zeolites.....	37
3.4	Regeneration tests.....	38
3.4.1	Regeneration with H <sub>2</sub> O <sub>2</sub> .....	38
3.4.2	Ozonation in batch experiments .....	39
4	Octamethylcyclotetrasiloxane adsorption into activated carbon .....	43
4.1	Overview .....	45
4.2	Methodology.....	46
4.3	Results and Discussion.....	46
4.3.1	D4 adsorption on commercial ACs.....	46
4.3.2	Influence of the AC textural properties on D4 adsorption .....	48
4.3.3	Influence of the AC surface chemistry on D4 adsorption .....	51
4.3.4	Polymerization of the adsorbed D4 on ACs.....	55
4.4	Final remarks.....	60
5	Regeneration of siloxane-exhausted AC by AOPs.....	61
5.1	Overview .....	63
5.2	Methodology.....	64
5.3	Results and Discussion.....	65
5.3.1	Regeneration of D4-exhausted AC by O <sub>3</sub> .....	65
5.3.2	Regeneration of D4-exhausted AC by H <sub>2</sub> O <sub>2</sub> .....	68
5.3.3	Regeneration of Fe-AC with H <sub>2</sub> O <sub>2</sub> .....	71
5.4	Final remarks.....	76

6	Zeolites as recyclable adsorbent/catalysts for D4 removal .....	77
6.1	Overview.....	79
6.2	Methodology.....	80
6.3	Results and Discussion.....	81
6.3.1	D4 uptake by zeolites.....	81
6.3.2	D4 uptake mechanisms.....	83
6.3.3	Regeneration of D4-exhausted zeolites by wet procedures.....	90
6.3.4	Regeneration with aqueous ozone.....	95
6.4	Finals remarks.....	97
7	Towards real scenario implementation.....	99
7.1	Overview.....	101
7.2	Methodology.....	102
7.3	Problem statement in a case of study.....	103
7.3.1	Biogas sampling and analysis.....	103
7.3.2	Exhausted AC analysis.....	103
7.3.3	Effectiveness of thermal desorption.....	105
7.4	Approaching a real scenario.....	107
7.4.1	Influence of the D4 concentration.....	107
7.4.2	Effect of the gas matrix composition.....	108
7.4.3	Adsorption of other siloxanes.....	110
7.4.4	Competitive multicomponent adsorption.....	111
7.5	Finals remarks.....	117
8	General discussion .....	119
9	General conclusions.....	129
10	References.....	133
11	Appendices.....	145



## List of Tables

---

### Chapter 1: Introduction

<b>Table 1.1</b> Composition of sewage sludge and landfill gas.....	5
<b>Table 1.2</b> Most common organic silicon compounds found in biogases and their properties (Schweigkofler and Niessner (2001);McBean (2008);Rasi <i>et al.</i> (2010)).....	7
<b>Table 1.3</b> Siloxane removal technologies already commercial and under development and main features resumed.....	10
<b>Table 1.4</b> Review of the studies concerning siloxane removal by adsorption on different porous materials.....	19

### Chapter 3: Materials and methods

<b>Table 3.1</b> Commercial name, origin and activation process undergone for the aAC.....	29
<b>Table 3.2</b> Properties of commercial zeolites considered. ....	30
<b>Table 3.3</b> AC characterization techniques and their purpose. ....	30
<b>Table 3.4</b> Groups decomposed at each temperature by TPD analysis.....	31
<b>Table 3.5</b> Assignment of peaks corresponding to each binding energy on XPS analysis.....	32

### Chapter 4: Octamethyltetrasiloxane adsorption into activated carbon

<b>Table 4.1</b> D4 adsorption capacity, textural properties of the ACs considered and $H_{MTZ}$ . ....	47
<b>Table 4.2</b> EDX elemental composition of AC samples analyzed by SEM.....	51
<b>Table 4.3</b> Results of $pH_{slurry}$ and XPS analyses of the ACs considered.....	53
<b>Table 4.4</b> Results of the TPD analyses of the activated carbons considered.....	53
<b>Table 4.5</b> Contribution of D5, D6 and D7 on the long-term polymerization of each AC.....	56

Chapter 5: Regeneration of siloxane-exhausted activated carbon

<b>Table 5.1</b> Physico-chemical properties of the AC tested in this work. ....	64
<b>Table 5.2</b> Iron concentration in each sample of Nuchar depending on the iron concentration of the solution of ferrous sulfate applied and Fe fraction retained in the AC. ....	72
<b>Table 5.3</b> Regeneration efficiency and Fe leached determined after each regeneration cycle of Fe-Nuchar.....	75

Chapter 6: Zeolites as recyclable adsorbent/catalysts for D4 removal

<b>Table 6.1</b> Physico-chemical properties of the tested zeolites and D4 uptake.....	82
<b>Table 6.2</b> List of identified compounds by GC-MS analysis after THF extraction of D4-exhausted zeolites.....	85

Chapter 7: Towards real scenario implementation

<b>Table 7.1</b> Isotherm equation constants of Langmuir model of D4 adsorption at 22°C.....	108
<b>Table 7.2</b> Origin, activation process and textural properties of Silpure and Silpure W .....	110
<b>Table 7.3</b> Multicomponent test gas composition, 200 ml min <sup>-1</sup> N <sub>2</sub> carrier.....	112
<b>Table 7.4</b> Results of the multicomponent removal efficiency in BV for the set of AC .....	115
<b>Table 7.5</b> Advantages and weaknesses of the adsorbent materials tested .....	118

## List of Figures

---

### Chapter 1: Introduction

<b>Figure 1.1</b> Scheme of the subsequence steps in the process of anaerobic digestion.....	3
<b>Figure 1.2</b> Primary energy production of biogas in the European Union, Germany, UK and Spain in 2008, 2011, 2012 and 2013. ....	4
<b>Figure 1.3</b> Scheme of the biogas generation and cleaning requirements depending on the final use.....	6
<b>Figure 1.4</b> Molecular configuration of lineal and cyclic siloxanes. ....	7
<b>Figure 1.5</b> Oxygen functional groups in ACs surface.....	13
<b>Figure 1.6</b> Frameworks types of BEA, MFI, FAU and HEU zeolites .....	14

### Chapter 3: Materials and Methods

<b>Figure 3.1</b> Schematic of the dynamic adsorption experiment.....	35
---	----

### Chapter 4: Octamethylcyclotetrasiloxane adsorption into activated carbon

<b>Figure 4.1</b> Dynamic adsorption breakthrough curves for D4 onto different commercial activated carbons.....	47
<b>Figure 4.2</b> Correlation between D4 adsorption capacity (x/M) of the tested ACs vs $S_{BET}$ surface area; Total pore volume; Mesopore volume; Total micropore volume; and Narrow micropore volume.....	50
<b>Figure 4.3</b> Correlation between $S_{BET}$ and Total pore volume and the $H_{MTZ}$ .....	51
<b>Figure 4.4</b> Relation between O/C ratio obtained by XPS and the D4 adsorption capacity of the ACs studied.....	52
<b>Figure 4.5</b> Concentrations of Carboxylic acid, Lactone, Carboxylic anhydride, Phenolic, Carbonyl / Quinone and Ether groups obtained by TPD related with adsorption capacity of each AC.....	54

<b>Figure 4.6</b> FT-IR spectra of fresh and D4-saturated MWV-2 compared to the spectrum of pure D4 in liquid phase.....	55
<b>Figure 4.7.</b> Short and long term polymerization ratio of D4 adsorbed on ACs.....	57
<b>Figure 4.8</b> Correlation between chemical surface properties O/C ratio obtained by XPS ratio, ad O/C ratio obtained by TPD.....	58
<b>Figure 4.9</b> Correlation between chemical surface properties phenolic groups and carboxylic groups and the long term polymerization ratio of ACs.....	58
<b>Figure 4.10</b> Influence of the pH <sub>slurry</sub> of the AC in the short and long term PR.....	59
<b>Figure 4.11.</b> Proposed mechanism for the polymerization of cyclosiloxanes AC surfaces.....	59

## Chapter 5: Regeneration of siloxane-exhausted activated carbon

<b>Figure 5.1</b> Nuchar and Organosorb RE obtained with the O <sub>3</sub> treatment at different exposition times. Experiments were conducted with 0.250 g of AC, in 500 ml solution, O <sub>3</sub> flow of 70 mg min <sup>-1</sup> , room temperature, and free pH.....	65
<b>Figure 5.2</b> IR spectra of Nuchar 1) Fresh, 2) after O <sub>3</sub> regeneration (15 minutes), 3) after H <sub>2</sub> O <sub>2</sub> regeneration (1% w/v), 4) D4-exhausted after O <sub>3</sub> regeneration, 5) D4-exhausted after H <sub>2</sub> O <sub>2</sub> regeneration, 6) D4-exhausted first cycle, and spectrum of 7) D4 and 8) SiO <sub>2</sub> .....	67
<b>Figure 5.3</b> H <sub>2</sub> O <sub>2</sub> decomposition of fresh and D4-exhausted Nuchar and Organosorb.....	69
<b>Figure 5.4</b> Nuchar and Organosorb regeneration efficiency obtained with different H <sub>2</sub> O <sub>2</sub> concentrations.....	70
<b>Figure 5.5</b> Chromatogram obtained by GC-MS analysis of the liquid phase of the H <sub>2</sub> O <sub>2</sub> oxidation of D4-exhausted Nuchar.....	71
<b>Figure 5.6</b> H <sub>2</sub> O <sub>2</sub> decomposition for fresh Nuchar, fresh Fe-amended Nuchar with different iron content, and fresh and D4-exhausted Fe-Nuchar.....	73
<b>Figure 5.7</b> Nuchar and Fe-Nuchar regeneration efficiency obtained with different H <sub>2</sub> O <sub>2</sub> concentrations.....	73

**Figure 5.8** FT-IR spectra of Fresh Fe-Nuchar, Fe-Nuchar after H<sub>2</sub>O<sub>2</sub> oxidation treatment, D4-exhausted Fe-Nuchar after H<sub>2</sub>O<sub>2</sub> oxidation treatment and 4) D4-exhausted Fe-Nuchar after first use.....75

Chapter 6: Zeolites as recyclable adsorbent/catalysts for siloxane removal

**Figure 6.1** Dynamic adsorption breakthrough curves obtained for tested zeolites..... 81

**Figure 6.2** Relation between S<sub>BET</sub> surface area and D4 uptake at bed exhaustion of the zeolites considered at D4 inflow concentration of 3000 mg m<sup>-3</sup> .....83

**Figure 6.3** Differential FT-IR spectra of D4-exhausted zeolites .....84

**Figure 6.4** Percentage of D4 recovered or transformed to other cyclic siloxanes and α-ω-silanediods from THF extracts of exhausted zeolites.....85

**Figure 6.5** Correlation between content of Brønsted acidic sites and D4 uptake .....86

**Figure 6.6** Correlation between content of Brønsted acidic sites and A% yield of D4 into extractable α-ω-silanediods for BEA zeolites and other zeolites.....88

**Figure 6.7** FT-IR spectra of zeolites considered using pyridine as probe molecule for the determination of BAS and LAS.....89

**Figure 6.8** Regeneration efficiencies obtained for Fe-BEA in four adsorption/regeneration cycles at different H<sub>2</sub>O<sub>2</sub> concentrations.....90

**Figure 6.9** Differential FT-IR spectra of Fe-BEA zeolite after various regeneration cycles. Values between brackets refer to the carbon content (wt%) in the exhausted or regenerated materials determined by EA..... 92

**Figure 6.10** H<sub>2</sub>O<sub>2</sub> decomposed after 24 hours in catalyst suspension of fresh Fe-BEA and D4-exhausted Fe-BEA during 5 treatment cycles .....93

**Figure 6.11** FT-IR spectra of Fe-BEA zeolite using pyridine as probe molecule for the determination of BAS after 4 adsorption/regeneration cycles by H<sub>2</sub>O<sub>2</sub> or O<sub>3</sub> as compared to fresh Fe-BEA.....94

**Figure 6.12** Regeneration efficiencies obtained after various adsorption/oxidation cycles with different ozonation times for D4-exhausted Fe-BEA zeolite.....96

Chapter 7: Towards real scenario implementation

<b>Figure 7.1</b> Scheme of a Capstone biogas treatment unit.....	101
<b>Figure 7.2</b> GC-MS chromatograms obtained from the analysis of the THF extraction of exhausted Airpel samples used in biogas filters.....	104
<b>Figure 7.3</b> GC-MS chromatograms obtained in the analysis of the outlet flow during the thermal desorption of real exhausted Airpel after 10, 55 and 220 minutes. ....	106
<b>Figure 7.4</b> D4 adsorption isotherms obtained in static adsorption tests with Airpel and Nuchar AC, fitting the Langmuir model. ....	108
<b>Figure 7.5.</b> Adsorption breakthrough curves obtained for MVW-2 with a 1000 ppm v/v D4 flow with nitrogen, wet and dry air and synthetic biogas as carrier gases.....	109
<b>Figure 7.6</b> Correlation between pore volume of the AC tested with D5, D4 and L2 x/M.....	111
<b>Figure 7.7</b> Dynamic multicomponent adsorption breakthrough curves obtained for Airpel ..	113
<b>Figure 7.8</b> Dynamic multicomponent adsorption breakthrough curves for Nuchar .....	113
<b>Figure 7.9</b> Competitive adsorption capacities reported at L2 breakthrough and at bed exhaustion .....	115
<b>Figure 7.10</b> Multicomponent adsorption in presence of 35% humidity.....	115
<b>Figure 7.11</b> Comparative cost of siloxane removal per volume of biogas treated at the conditions tested at dry N <sub>2</sub> matrix gas (BD) and with 35% humidity.....	116

Appendice A: GC-FID Calibration curves

<b>Figure 11.1</b> Calibration curve of D4 in N <sub>2</sub> gas matrix.....	147
<b>Figure 11.2</b> Calibration curve of L2 in N <sub>2</sub> gas matrix.....	147
<b>Figure 11.3</b> Calibration curve of D5 in N <sub>2</sub> gas matrix.....	148
<b>Figure 11.4</b> Calibration curve of Toluene in N <sub>2</sub> gas matrix.....	148
<b>Figure 11.5</b> Calibration curve of Limonene in N <sub>2</sub> gas matrix.....	148

Appendice B: GC-MS Calibration curves

<b>Figure 11.6</b> Calibration curve of D4 in THF dissolution .....	149
<b>Figure 11.7</b> Calibration curve of L2 in THF dissolution.....	149
<b>Figure 11.8</b> Calibration curve of D5 in THF dissolution.....	150
<b>Figure 11.9</b> Calibration curve of Toluene in THF dissolution .....	150
<b>Figure 11.10</b> Calibration curve of limonene in THF dissolution.....	150

Appendice C: UV-VIS Calibration curves

<b>Figure 11.11</b> Calibration curve of H <sub>2</sub> O <sub>2</sub> (λ=410 nm) .....	151
<b>Figure 11.12</b> Calibration curve of Fe(II/III) (λ=504 nm).....	151

Appendice D: Characterization of ACs

<b>Figure 11.13</b> EDX spectra of fresh MWV-2 and D4-saturated MWV-2 .....	152
<b>Figure 11.14</b> SEM image of fresh MWV-2 and D4-saturated MWV-2.....	152
<b>Figure 11.15</b> XPS oxygen (1s) spectrum of activated carbons.....	153
<b>Figure 11.16</b> XPS carbon (1s) spectrum of activated carbons.....	153
<b>Figure 11.17</b> CO desorption curve for all the activated carbons considered .....	154
<b>Figure 11.18</b> CO <sub>2</sub> desorption curve for all the activated carbons considered.....	154



## List of acronyms

---

AC	Activated carbon
ACA	Catalan Water Agency
AD	Anaerobic digestion
AOP	Advanced oxidation processes
$b_A$	Langmuir constant of adsorption rate
BAS	Brønsted acidic sites
BEA	Beta type zeolites
BV	Bed volume treated
CLG	<i>Calgon Carbon</i>
CMV	<i>Chemviron Carbon</i>
D3	Hexamethylcyclotrisiloxane
D4	Octamethylcyclotetrasiloxane
D5	Decamethylcyclopentasiloxane
D6	Dodecamethylcyclohexasiloxane
D7	Tetradecamethylcycloheptasiloxane
DR	Dubinin-Redushkevich
DST	<i>Desotec Activated carbon</i>
EA	Elemental analysis
EDX	Energy-dispersive X-ray spectroscopy
EPS	Extracellular polymeric substances
ERS	Energy recovery systems
FAU	Faujasite zeolite type
FID	Flame ionization detector
FT-IR	Fourier transformed infrared spectroscopy

GC	Gas chromatography
HC	Hydrocarbon compounds
H <sub>MTZ</sub>	Height of the mass transfer zone
ICP-AES	Inductively coupled plasma atomic emission spectroscopy
IZA	International Zeolite Association
JCB	<i>Jacobi Carbons</i>
L2	Hexamethyldisiloxane
L3	Octamethyltrisiloxane
L4	Decamethyltetrasiloxane
L5	Dodecamethylpentasiloxane
LAS	Lewis acidic sites
MOR	Mordenite zeolite type
MS	Mass spectrometry
MW	Molecular weight [mg mmol <sup>-1</sup> ]
MWV	<i>MeadWestvaco</i>
NRT	<i>Norit Activated carbon</i>
O <sub>3</sub>	Ozone
·OH	Hydroxyl radical
O/C <sub>XPS</sub>	Oxygen content
O/C <sub>TPD</sub>	Oxygen content
PDM	Polydimethylsiloxanes

Q	Gas flow [ml min <sup>-1</sup> ]
Q <sub>M</sub>	Langmuir constant for adsorption capacity
RE	Regeneration efficiency
RH	Relative Humidity [%]
R <sub>L</sub>	Langmuir partition coefficient
S <sub>BET</sub>	BET specific surface area [m <sup>2</sup> g <sup>-1</sup> ]
SEM	Scanning electron microscopy
THF	Tetrahydrofuran
TPD	Thermal programmed desorption
VDR <sub>CO<sub>2</sub></sub>	Narrow micropore volume
VDR <sub>N<sub>2</sub></sub>	Total micropore volume
V <sub>meso</sub>	Mesopore volume
V <sub>t</sub>	Total pore volume
VOC	Volatile organic compound
x/M	Adsorption capacity [mg g <sup>-1</sup> ]
XPS	X-ray photoelectron spectroscopy
WWTP	Wastewater treatment plant



## Publications and Communications

---

Journal publications resulting from this PhD thesis:

- Biogas upgrading: Optimal activated carbon properties for siloxane removal. Alba Cabrera-Codony, Miguel A. Montes-Morán, Manuel Sanchez-Polo, Maria J. Martin, Rafael Gonzalez-Olmos. *Environmental Science & Technology*, 48 (2014) 7187-7195.
- Regeneration of siloxane-exhausted activated carbon by advanced oxidation processes. Alba Cabrera-Codony, Rafael Gonzalez-Olmos, Maria J. Martin. *Journal of Hazardous Materials*, 285 (2015) 501-508.
- Zeolites as recyclable adsorbents/catalysts for biogas purification: removal of octamethylcyclotetrasiloxane. Alba Cabrera-Codony, Anett Georgi, Rafael Gonzalez-Olmos, Héctor Valdés, Maria J. Martín. *Submitted for publication*.

Communications resulting from this PhD thesis:

- Continuous gas-phase siloxane removal: Adsorption and regeneration by AOPs. Alba Cabrera-Codony, Alba Anfruns, Rafael Gonzalez-Olmos, Maria J. Martín. *The annual world conference on carbon – CARBON 2012*. Krakow, Poland, June 17-22, 2012. Oral presentation.
- Eliminación de siloxanos en biogás mediante adsorción en carbón activo. Alba Cabrera-Codony, Rafael Gonzalez-Olmos, Maria J. Martín. *XII Reunión del grupo español del carbon – GEC 2013*. Madrid, Spain, October 20-13, 2013. Oral presentation.
- Advanced Oxidation Processes for the regeneration of siloxane exhausted adsorbents used for biogas purification. Alba Cabrera-Codony, Esther Vega, Rafael Gonzalez-Olmos, Maria J. Martín. *3rd European Conference on Environmental Application of AOPs – EAAOP-3*. Almeria, Spain, October 27-30, 2013. Poster presentation.
- Biogas upgrading: siloxane removal by adsorption and regeneration by AOPs. Alba Cabrera-Codony, Rafael Gonzalez-Olmos, Maria J. Martín. *13<sup>th</sup> Mediterranean*

*Congress of Chemical Engineering – 13MCCE*. Barcelona, September 30-October 3, 2014. Oral presentation.

- Advanced oxidation processes for the regeneration of siloxane-exhausted adsorbents. Alba Cabrera-Codony, Rafael Gonzalez-Olmos, Maria J. Martín. *22<sup>nd</sup> IOA World Congress*. Barcelona, June 28– July 3, 2015. Oral presentation.
- Siloxane removal for biogas upgrading: adsorption and regeneration by advanced oxidation processes. Alba Cabrera-Codony, Rafael Gonzalez-Olmos, Maria J. Martín. *The annual world conference on carbon - CARBON 2015*. Dresden, Germany, July 12-15, 2015. Oral presentation.
- AOP Regeneration of Adsorbents/Catalysts used for Siloxane Removal in Biogas Upgrading. Alba Cabrera-Codony, Rafael Gonzalez-Olmos, Maria J. Martín. *The 21st International Conference on Advanced Oxidation Technologies for Treatment of Water, Air and Soil – AOTs-21*. San Diego, USA, November 16-19, 2015. Oral presentation.
- Advanced oxidation processes for the regeneration of exhausted adsorbents. Alba Cabrera-Codony, Eric Santos-Clotas, Maria J. Martín. *The annual world conference on carbon - CARBON 2016*. Penn State, USA, July 10-15, 2016. Poster presentation.
- Activated carbons for the removal of siloxanes: sewage biogas upgrading. Alba Cabrera-Codony, Maria J. Martín. *The annual world conference on carbon - CARBON 2016*. Penn State, USA, July 10-15, 2016. Keynote lecture.

## Summary

---

Biogas generated from both anaerobic digesters in wastewater treatment plants (WWTP) and landfills can be used for the generation of energy. The predictable high percentage of methane present in biogas, with an energy content equivalent to approximately one-half of natural gas, has provided significant opportunities for many energy recovery systems (ERS). Moreover, the reuse of biogases as a renewable energy source contributes to initiatives to decrease greenhouse gases emissions.

Likewise, biogases contain several trace compounds that negatively affect ERS, such as hydrogen sulfide, which presents corrosive properties, and siloxanes. The term siloxane refers to a subgroup of silicones containing Si-O bonds with organic radicals attached to the atom of silicon, so they are a hybrid of both organic and inorganic compounds. Siloxanes are widely used in several industrial and household applications, so they arrive to wastewaters. Once there, they are hydrolyzed to compounds with lower molecular weight and soluble volatile methylsiloxanes, and subsequently volatilize during the anaerobic digestion of sewage sludge and in landfills. Recently, the production of silicon has risen as well as the siloxane concentration in sewage and landfill gas. During the combustion of biogas, the siloxanes are converted into abrasive microcrystalline silica, which has chemical and physical properties similar to those of glass, leading to abrasion of engine parts or the build-up layers that inhibit essential heat conduction or lubrication. Thus, ERS manufacturers strive to limit the concentrations of siloxanes in biogas to improve energy applications.

The most widely used method to reduce siloxanes concentrations is the non-regenerative adsorption into activated carbons (ACs), although other solids, such as silica, zeolites or polymeric resins may also give interesting results. Despite the wide spread industrial use of adsorption for biogas upgrading, little is known about the mechanism involved in the removal of these trace compounds. Thus, the aim of this dissertation is to establish the siloxane adsorption mechanisms in order to enhance the yield of the sequential adsorption/regeneration technologies for siloxane abatement in biogas. For this purpose, we used activated carbon and inorganic materials as adsorbents, and different advanced oxidative systems based on H<sub>2</sub>O<sub>2</sub> and/or O<sub>3</sub> to favor a partial attack of siloxanes and produce water-soluble silanols. Furthermore, we studied the tuning of adsorbents/catalyst

to improve the activity of the advanced oxidation processes (AOPs), i.e., to promote the generation of oxidant species. In that sense, a compromise between the capacity of the adsorbents and the catalytic activity is pursued.

Twelve commercial activated carbons (ACs) were tested in D4 dynamic adsorption experiments using different carrier gases and octamethylcyclotetrasiloxane (D4) concentrations as a representative siloxane typically found in biogas. A comprehensive characterization of the ACs was carried out, aiming to find relationships between their physical and chemical properties and their adsorption capacity ( $x/M$ ) obtained in adsorption tests at lab-scale with D4 at a high concentration in a dry  $N_2$  gas matrix. The D4 adsorption capacities were strongly related with the textural porosity of the ACs. Results showed that the optimum adsorbents for D4 are wood-based chemically activated carbons.

The polymerization of D4 over the surface of all ACs was also investigated, and it was observed to be relevant after prolonged contact times. The presence of phenolic and carboxylic groups over the surface of ACs, especially the ones chemically activated, catalyze the ring-opening of the D4, leading to hydrolysis and condensation reactions that form silanols and cyclic siloxanes of lower molecular weight. This way, the polymerization ratio was established, which depends in the contact time and also in the quantity of oxygenated functional groups over ACs surface. The formation of cyclic compounds of higher molecular weight reduces the possibility of regenerating the materials by means of thermal desorption, whereas the formation of silanols, soluble compounds, offers an opportunity for wet regeneration of exhausted materials. In this sense, the wet regeneration of a D4-exhausted ACs was studied under different concentrations of  $O_3$  and  $H_2O_2$ . In order to refine the yield of the process, the AC with the highest  $x/M$ , Nuchar ( $1732 \text{ mg g}^{-1}$ ), was doped with iron for conducting a Fenton reaction. Almost a total regeneration of the adsorbent was achieved in the first cycle, but the textural properties of the carbon were affected due to the oxidants attack, impeding an efficient reutilization of the material during more cycles.

In this context, zeolites are presented as inorganic adsorbents resistant to the oxidation that, without achieving siloxane adsorption capacities as high as ACs and representing higher costs, may be recyclables during further adsorption/regeneration cycles. Six

synthetic zeolites and a natural one were studied in D4 adsorption tests. Adsorption capacity in zeolites is not only related to their porous structure, but also to their catalytic capacity to form silanediols from the D4 ring-opening, that can diffuse in their structural channels. This reaction is well correlated to Lewis and Brønsted acid content, and BEA-type zeolites resulted to be the best zeolite for D4 siloxane removal (143 mg g<sup>-1</sup>). Wet treatments with O<sub>3</sub> and H<sub>2</sub>O<sub>2</sub> were optimized for recovering almost completely the adsorption capacity of Fe-BEA after its first use. Nevertheless, in further cycles, the accumulation of D4 and/or by-products led to a successive decline in the catalytic activity of the zeolites, hampering not only the capacity to transform D4 into lineal silanediols, hence reducing the adsorption capacity, but also the catalytic activity towards promoting Fenton-like reactions during regeneration. Then, improving and extending their catalytic capacity for increasing the transformation from cyclic siloxanes to soluble silanols will be essential for a better yield in wet regeneration.

The knowledge obtained from the D4 uptake in dry nitrogen flows allowed our investigation in the effect over more complex matrices in adsorption processes, including CH<sub>4</sub> and CO<sub>2</sub> as carrier gases, humidity presence and also the competence among different siloxanes and volatile organic organic compounds (VOCs). Considering all these parameters, the implementation of the improvements in a case study of a real Catalan WWTP was evaluated.

D4 adsorption isotherms were obtained to ascertain the influence of the adsorbate concentration as well as the observed trend, reaffirming that chemically activated carbons have higher D4 adsorption capacities than physically activated ACs, due to the development of their porous structure. The experiments carried out with synthetic biogas have a limited repercussion in x/M, since CH<sub>4</sub> and CO<sub>2</sub> presence suppose an adsorption competitiveness and/or a decrease in diffusivity of D4 molecules, corresponding to an x/M reduction of 17%. Humidity at values down to 20% resulted negligible, although values up to 80% led to a 16% decrease in the capacity, due to formation of hydrogen bonds in the porous structure of the AC, hence blocking the adsorption sites.

Finally, the competitive adsorption of different siloxanes (L2, D4, D5) in presence of volatile organic compounds typically found in biogases (toluene and limonene) was investigated. Two clear and different trends were detected in the adsorption of compounds depending

on the activation process of the ACs studied. Whereas physically activated ACs present higher capacity for VOCs, chemically activated carbons have more affinity for siloxanes. In this sense, the efficiency of the materials was evaluated according to the breakthrough time of the first siloxane. It was concluded that the use of ACs activated with phosphoric acid might prolong the lifespan of the adsorbent used in the case study WWTP up to a 120%, leading to significant savings in the current adsorbent material costs.

## Summary in Catalan

---

El biogàs produït a partir de la digestió anaeròbica en estacions depuradores d'aigües residuals i d'abocadors es pot utilitzar per a la generació d'energia. L'alt percentatge de metà present en el biogàs, que té contingut energètic equivalent aproximadament a la meitat que el del gas natural, presenta moltes oportunitats a partir de la seva utilització en sistemes de recuperació d'energia (SRE). A més la utilització del biogàs com a font d'energia renovable contribueix als esforços per reduir les emissions de gasos d'efecte hivernacle.

Tanmateix, els biogasos contenen diversos compostos que afecten de forma negativa als SRE, com ara el sulfur d'hidrogen, que té efectes corrosius, i els siloxans. El mot 'siloxà' fa referència a un grup de compostos que contenen enllaços Si-O amb radicals orgànics units als àtoms de silici, per tant són un híbrid entre compostos orgànics i inorgànics. Els siloxans s'utilitzen àmpliament en diverses aplicacions industrials i domèstiques, de manera que arriben a les aigües residuals i s'hidrolitzen en forma de polimetilsiloxans, de baix pes molecular i baixa solubilitat. Per aquesta raó es volatilitzen durant la digestió anaeròbia dels fangs de depuradora i en els abocadors. Com que la utilització de siloxans ha augmentat els últims anys, la seva concentració en biogasos s'ha incrementat en conseqüència. Durant la combustió de biogàs, els siloxans es converteixen en sílice microcristal·lina abrasiva, que té propietats químiques i físiques similars a les de vidre, produint l'abradió de les parts dels SRE i inhibeix la conducció de la calor essencial o la lubricació dels seus components. Per tant, els fabricants dels SRE limiten les concentracions de siloxans en els biogasos per a millorar la seva aplicació.

El mètode més àmpliament utilitzat per reduir la concentració de siloxans és l'adsorció no-regenerativa en carbons activats (CA), encara que altres sòlids, com ara les zeolites o les resines polimèriques també poden donar resultats interessants. Malgrat l'ús industrial generalitzat de l'adsorció per a la millora del biogàs, els mecanismes implicats en l'eliminació d'aquests compostos són poc coneguts. L'objectiu d'aquest treball és, doncs, establir els mecanismes d'adsorció per tal de millorar el rendiment de les tecnologies seqüencials d'adsorció / regeneració per a l'eliminació de siloxans del biogàs. Amb aquesta finalitat, hem utilitzat diferents sistemes de regeneració humida amb tractaments oxidatius avançats basats en  $H_2O_2$  i/o en  $O_3$  per tal d'aconseguir un atac parcial dels

siloxans i produir silanols solubles en aigua. A més, vam estudiar la modificació dels adsorbents / catalitzadors per millorar l'activitat dels processos d'oxidació avançada (POA), és a dir, per millorar la generació d'espècies oxidants. En aquest sentit, es persegueix un compromís entre la capacitat dels adsorbents i la seva activitat catalítica.

Hem estudiat un conjunt de 12 CA comercials amb diferents propietats químiques i texturals en proves dinàmiques d'adsorció de octametilciclotetrasiloxà (D4) com a compost representatiu dels siloxans que es troben típicament als biogasos. Tots els carbons van ser exhaustivament caracteritzats per trobar les relacions entre les seves propietats i les capacitats d'adsorció ( $x/M$ ) obtingudes en proves d'adsorció realitzades a escala de laboratori amb D4 a alta concentració en una matriu de  $N_2$  sec. Vam poder concloure que la  $x/M$  està fortament relacionada amb el desenvolupament de la textura porosa dels CAs, de manera que els resultats van mostrar que els adsorbent òptims per l'eliminació de D4 són els carbons activats químicament a base de fusta.

Tanmateix, vam estudiar les transformacions que tenen lloc a la superfície dels CA, i vam descobrir que els grups fenòlics i carboxílics presents a la superfície dels CAs, especialment els activats químicament, catalitzen l'obertura de l'anell del D4, donant lloc a reaccions de hidròlisi i condensació que formen silanols i siloxans cíclics de més elevat pes molecular. Així vam establir la ràtio de polimerització, que és un fenomen que depèn del temps de contacte i de la quantitat de grups funcionals oxigenats a la superfície dels CAs. La formació de compostos cíclics de més elevat pes molecular redueix la possibilitat de la regeneració dels materials a través de desorció tèrmica, mentre que la formació de silanols, compostos solubles, obre una oportunitat per la regeneració humida dels adsorbents. En aquest sentit, la regeneració humida dels CA esgotat de D4 es va estudiar amb diferents concentracions de  $O_3$  i  $H_2O_2$ . Per millor el rendiment del procés, el CA amb més  $x/M$ , Nuchar ( $1732 \text{ mg g}^{-1}$ ), es va dopar amb ferro per dur a terme processos tipus Fenton. Tot i que en aquest cas es va aconseguir una regeneració gairebé total de l'adsorbent en el primer cicle de regeneració, la degradació de les propietats texturals del carbó degut a l'atac dels oxidants va impedir la reutilització eficient del material durant més cicles.

En aquest context, les zeolites es presenten com a adsorbents inorgànics resistent a l'oxidació que, tot i que no aconseguen les elevades capacitats d'adsorció de siloxans

dels CA i tinguin preus més elevats, poden ser reciclables durant més cicles d'adsorció/regeneració. Vam fer un conjunt de proves d'adsorció de D4 amb sis zeolites sintètiques i una de natural, de preu molt més baix. La x/M de les zeolites no està relacionada només amb la seva estructura porosa, sinó amb la capacitat catalítica per formar silanediols, a partir de l'obertura de l'anell del D4, que es poden difondre en els canals estructurals. Aquesta reacció està relacionada amb el contingut d'àcids de Lewis i de Brønsted, i la zeolita amb millor rendiment va ser la Fe-BEA (143 mg g<sup>-1</sup>). Els tractaments humits amb O<sub>3</sub> i H<sub>2</sub>O<sub>2</sub> van ser optimitzats per recuperar gairebé completament la capacitat d'adsorció la zeolita Fe-BEA després de la primera utilització. No obstant, en els següents cicles, l'acumulació de D4 i de subproductes va conduir a una disminució successiva en l'activitat catalítica de la zeolita, afectant tant a la capacitat de transformació del D4 cap a silanediols lineals fonamentals pel procés d'eliminació de D4, com pel que fa a la promoció de reaccions tipus Fenton per millorar la regeneració humida. Per tant, per utilitzar aquests materials caldrà millorar i prolongar la seva capacitat catalítica per incrementar la transformació del siloxans cíclics cap a silanols solubles que millorin el rendiment de la regeneració humida.

El coneixement obtingut en l'estudi de l'eliminació de D4 en corrents de nitrogen sec ens va permetre investigar l'efecte de matrius més complexes en els processos d'adsorció, incloent el CH<sub>4</sub> i CO<sub>2</sub> com a gasos portadors, la presència d'humitat i la competència entre diferents siloxans i compostos orgànics volàtils. Tenint en compte aquests paràmetres, vam avaluar la implementació de millores en un cas d'estudi del sistema d'eliminació de siloxans del biogàs generat en una estació depuradora d'aigües residuals catalana.

Les isoterms d'adsorció de D4 obtingudes van permetre validar els resultats dels experiments a alta concentració i confirmen la tendència observada, reafirmant que els carbons químicament activats presenten capacitats d'eliminació de D4 molt més elevades que els activats físicament degut al desenvolupament de l'estructura porosa. Els experiments realitzats amb biogàs sintètic tenen una limitada repercussió en les capacitats d'adsorció, ja que la presència de CH<sub>4</sub> i CO<sub>2</sub> produeix una adsorció competitiva i/o una reducció en la difusió de les molècules de D4 corresponent a una reducció en la x/M del 17%. L'efecte d'humitat a nivells inferiors al 20 % va resultar menyspreable, tot i que l'increment a elevats nivells de fins al 80% produeix una reducció del 16% degut a la

formació de ponts d'hidrogen en l'estructura porosa del CA que bloqueja els llocs d'adsorció.

Finalment, vam investigar l'adsorció competitiva de diferents siloxans (L2, D4, D5) en presència de compostos orgànics volàtils (COV) típicament presents en els biogasos: toluè i limonè. Vam detectar dues tendències marcadament diferents en l'adsorció dels compostos en funció del procés d'activació dels carbons utilitzats. Mentre que els compostos activats físicament presenten major capacitat pels COVs que pels siloxans, el activats químicament adsorbeixen més quantitats de siloxans. En aquest sentit vam avaluar l'eficiència dels materials segons el temps de ruptura del primer siloxà, i vam concloure que la utilització de carbons activats amb àcid fosfòric permetrien allargar la vida útil dels llits adsorbents utilitzant en l'EDAR del cas estudiat fins a un 120%, generant estalvis en el cost del material adsorbent utilitzant actualment.

## Summary in Spanish

---

El biogás producido a partir de la digestión anaerobia en estaciones depuradoras de aguas residuales y vertederos se puede utilizar para la generación de energía. El alto porcentaje de metano presente en el biogás, cuyo contenido equivalente de energía es aproximadamente la mitad que el del gas natural, presenta muchas oportunidades para los sistemas de recuperación de energía (SRE). Asimismo el biogás posee un valor alto energético deseable y su utilización contribuye con los esfuerzos para reducir las emisiones de gases de efecto invernadero.

Sin embargo hay que tener en cuenta también que los biogases contienen varios compuestos que afectan de forma negativa a los SER, como el sulfuro de hidrogeno, que tiene efectos corrosivos, y los siloxanos. El término 'siloxano' se refiere a un subgrupo de siliconas que contienen enlaces Si-O con radicales orgánicos unidos a los átomos de silicio, por lo tanto son un híbrido entre compuestos orgánicos e inorgánicos. Los siloxanos se utilizan ampliamente en varias aplicaciones industriales y domésticas, de modo que llegan a aguas residuales, donde se hidrolizan a polimetilsiloxanos, que son compuestos con un menor peso molecular y solubilidad baja, y se volatilizan durante la digestión anaerobia de los lodos de depuradora y en los vertederos. Debido al aumento de utilización de siloxanos en los últimos años, su concentración en biogases se ha visto incrementada. Durante la combustión de biogás, los siloxanos se convierten en sílice microcristalina abrasiva, que tiene propiedades químicas y físicas similares a las del vidrio, produciendo la abrasión de las piezas del SRE e inhibe la conducción de calor esencial o la lubricación de sus componentes. Por lo tanto, los fabricantes de SRE limitan las concentraciones de siloxanos en los biogases para mejorar su aplicación.

El método más ampliamente utilizado para reducir la concentración de siloxanos es la adsorción no regenerativa en carbones activados (CA), aunque otros sólidos, tales como sílica y zeolitas o resinas poliméricas también pueden dar resultados prometedores. A pesar del uso industrial generalizado de la adsorción para la mejora del biogás, hay pocos estudios sobre los mecanismos implicados en la eliminación de estos compuestos. El objetivo de este trabajo consiste en establecer los mecanismos de adsorción de siloxanos con el fin de mejorar el rendimiento de las tecnologías secuenciales de adsorción / regeneración para la eliminación de siloxanos del biogás. Para este fin, hemos utilizado

diferentes sistemas de regeneración húmeda con tratamientos oxidativos avanzados basados en  $\text{H}_2\text{O}_2$  y/o  $\text{O}_3$  con tal de conseguir un ataque parcial de los siloxanos y producir silanoles solubles en agua. Además, se estudió la modificación de adsorbentes / catalizador para mejorar la actividad de los procesos de oxidación avanzada (POA), es decir, para mejorar la generación de especies oxidantes (principalmente el radical hidroxilo). En ese sentido, se persigue un compromiso entre la capacidad de los adsorbentes y la actividad catalítica.

Hemos estudiado un conjunto de 12 CAs comerciales con diferentes propiedades químicas y texturales en pruebas dinámicas de adsorción de octametilciclotetrasiloxano (D4) como compuesto representativo de los siloxanos que se encuentran comúnmente en los biogases. Todos los carbones fueron caracterizados exhaustivamente para encontrar relaciones entre sus propiedades y las capacidades de adsorción ( $x/M$ ) obtenidas en pruebas de adsorción realizadas a escala de laboratorio con D4 a alta concentración en una matriz de  $\text{N}_2$  seco. Pudimos concluir que la  $x/M$  está fuertemente relacionada con el desarrollo de textura porosa de los CAs, por lo que los resultados mostraron que los adsorbentes óptimos para el D4 son los carbones activados químicamente a base de madera.

También investigamos las transformaciones que tienen lugar en la superficie de los CAs, y descubrimos que los grupos fenólicos y carboxílicos presentes en la superficie de los CA, especialmente los activados químicamente, catalizan la apertura del anillo del D4, dando lugar a reacciones de hidrólisis y condensación que forman silanoles y siloxanos cíclicos de peso molecular más elevado. Así establecimos la ratio de polimerización, que es un fenómeno que depende del tiempo de contacto y de la cantidad de grupos funcionales oxigenados en la superficie de los CAs. La formación de compuestos cíclicos de mayor peso molecular reduce la posibilidad de la regeneración de los materiales mediante desorción térmica, mientras que la formación de silanoles, compuestos solubles, abre una oportunidad para la regeneración húmeda de los adsorbentes. En este sentido, la regeneración húmeda de los CAs agotados de D4 se estudió a diferentes concentraciones de  $\text{O}_3$  y  $\text{H}_2\text{O}_2$ . Para mejorar el rendimiento del proceso, el CA con más  $x/M$ , Nuchar ( $1732 \text{ mg g}^{-1}$ ), se dopó con hierro para llevar a cabo procesos tipo Fenton. Aunque en este caso se consiguió una regeneración casi total del adsorbente en el primer

ciclo de regeneración, la degradación de las propiedades texturales del carbón debido al ataque de los oxidantes, impidió la reutilización eficiente del material durante más ciclos.

En este contexto, las zeolitas se presentan como adsorbentes inorgánicos resistentes a la oxidación y aun no conseguir las elevadas capacidades de adsorción de siloxanos de los CAs y teniendo precios más elevados, pueden ser reciclables durante más ciclos de adsorción/regeneración. Se realizaron un conjunto de pruebas de adsorción de D4 de seis zeolitas sintéticas y una de natural, de precio muy reducido. La  $x/M$  de las zeolitas no está relacionada solo con su estructura porosa, sino también con la capacidad catalítica para formar silanedioles, a partir de la obertura del anillo del D4, que se puede difundir en los canales estructurales. Esta reacción está relacionada con en el alto contenido de ácidos de Lewis y de Brønsted, y la zeolita con mejor rendimiento fue Fe-BEA ( $143 \text{ mg g}^{-1}$ ). Los tratamientos húmedos con  $\text{O}_3$  y  $\text{H}_2\text{O}_2$  fueron optimizados para recuperar la mayor parte de la capacidad de adsorción de la zeolita Fe-BEA después del primer uso. No obstante, en los siguientes ciclos, la acumulación de D4 y de subproductos condujo a una disminución sucesiva en la actividad catalítica de la zeolita, afectando tanto a la capacidad de transformación del D4 hacia silanedioles lineales fundamentales para el proceso de eliminación de D4, como a la promoción de reacciones tipo Fenton para mejorar la regeneración húmeda. Por lo tanto, para utilizar estos materiales será necesario mejorar y prolongar su capacidad catalítica para incrementar la transformación de los siloxanos cíclicos hacia silanoles solubles que benefician el rendimiento de la regeneración húmeda.

El conocimiento obtenido a partir del estudio de eliminación de D4 en corrientes de nitrógeno seco nos permitió investigar el efecto en matrices más complejas en los procesos de adsorción, incluyendo el  $\text{CH}_4$  y  $\text{CO}_2$  como gases portadores, la presencia de humedad y la competencia entre diferentes siloxanos y compuestos volátiles. Teniendo en cuenta estos parámetros, evaluamos la implementación de mejoras en un caso de estudio del sistema de eliminación de siloxanos del biogás generado en una estación depuradora de aguas residuales catalanas.

Las isothermas de adsorción de D4 obtenidas permitieron validar los resultados experimentales a alta concentración y confirman la tendencia observada, reafirmando que los carbones químicamente activados presentan capacidades de eliminación de D4 mucho más elevadas que los activados físicamente debido al desarrollo de la estructura

porosa. Los experimentos realizados con biogás sintético tienen una repercusión limitada en las capacidades de adsorción, pues la presencia de CH<sub>4</sub> y CO<sub>2</sub> produce una adsorción competitiva y/o una reducción en la difusión de las moléculas de D4 correspondiendo a una reducción en la x/M del 17%. El efecto de la humedad a niveles inferiores al 20% resultaron menospreciables, aunque el incremento a niveles elevados de hasta el 80% produce una reducción del 16% debido a la formación de puentes de hidrógeno en la estructura porosa del CA que bloquea los lugares de adsorción.

Finalmente, investigamos la adsorción competitiva de distintos siloxanos (L2, D4, D5) en presencia de compuestos orgánicos volátiles (COV) típicamente presentes en los biogases: tolueno y limoneno. Se detectaron dos tendencias claramente diferentes en la adsorción de los compuestos en función del proceso de activación de los carbones utilizados. Mientras los carbones activados físicamente presentan mayor capacidad para los COVs que para los siloxanos, los químicamente activados adsorben más cantidad de siloxanos. En este contexto, se evaluó la eficiencia de los materiales según el tiempo de ruptura del primer siloxano, y se concluyó que la utilización de CA con ácido fosfórico permitiría alargar la vida útil de los lechos adsorbentes utilizados en la EDAR del caso estudiado hasta un 120%, suponiendo altos ahorros en el coste del material adsorbente utilizado actualmente.

---

Chapter 1

# INTRODUCTION



## 1.1 Biogas as renewable energy source

---

In a context of rising concerns regarding the depletion of fossil fuels combined with the climate change mitigation efforts, developing green technologies capable to efficiently transform waste into energy has become a fundamental social and research challenge. In this sense, the production of biogas has increased and many landfills and sewage treatment plants are collecting and using their biogas mixture to obtain energy (Schweigkofler and Niessner, 2001; Dewil *et al.*, 2006) as a renewable fuel for the production of electricity and heat.

In wastewater treatment plants, the disposal of the sludge produced represents a huge part of the operational costs. The large quantities of sludge have to be treated to reduce the volume by reducing the water content of raw sludge, to stabilize the organic matter and condition the residue for disposal under current legal requirements. The digestion of organic matter requires strict anaerobic conditions to allow a complex of microorganisms transform the organic material into  $\text{CH}_4$  and  $\text{CO}_2$ . The process is carried out in four successive stages depicted in Figure 1.1.

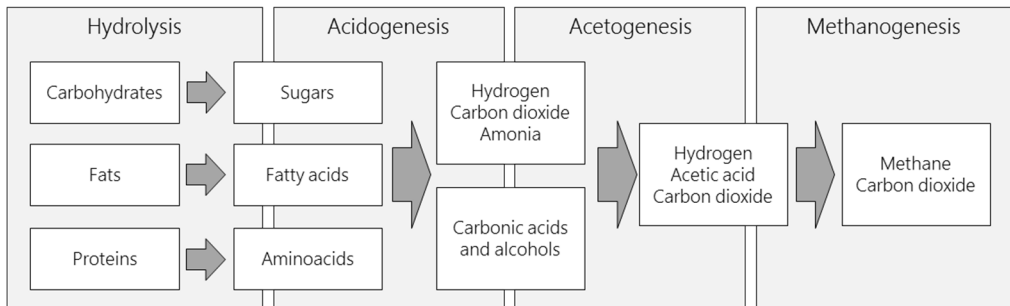


**Figure 1.1** Scheme of the successive steps in the process of anaerobic digestion.

During the hydrolysis step, the insoluble organic matter and high weight molecules are converted into soluble organic compounds, which are further split during acidogenesis. By the acetogenesis process, the organic acids and alcohols are converted into acetic acid,  $\text{H}_2$  and  $\text{CO}_2$ . The last step is carried out by two groups of methanogenic bacteria that i) split acetic acid into  $\text{CH}_4$  and  $\text{CO}_2$  and ii) use  $\text{H}_2$  and  $\text{CO}_2$  to produce  $\text{CH}_4$ .

pH, alkalinity and temperature determine the process. Temperature affects the growth of the microorganism's population and their metabolism. Digesters can be operated in mesophilic ranges (30-38°C) which has lower energy requirement, lower odor potential and less stability requirements. On the other hand, thermophilic digesters (50-57°C) present higher reaction rates and the digestion is faster, improve the dewatering reducing the solids and destroy more pathogenic organisms. Several pre-treatment processes have been studied in order to enhance the anaerobic digestion biogas production (Carlsson *et al.*, 2012; Bacenetti *et al.*, 2013; Cavinato *et al.*, 2013).

The worldwide production of biogas is known, but the Biogas Barometer studies of the European Union (EU) showed that it has steadily increase over the last years. In this sense the last European Biogas barometer published in 2014 (Euroobserver, 2015) points out that the primary energy production of biogas in the European Union was 156 Twh. In Figure 1.2 the energy produced in the EU from biogas sources is shown, expressed in kilotons of oil equivalent. Germany is the first European producer, followed by the UK, while Spain is in the seventh position. The data of EurObserver (Euroobserver, 2015) distinguishes between landfill gas, sewage sludge gas and other biogases, which include slurry, farming wastes and food-processing waste, being Germany and the UK the main producers.

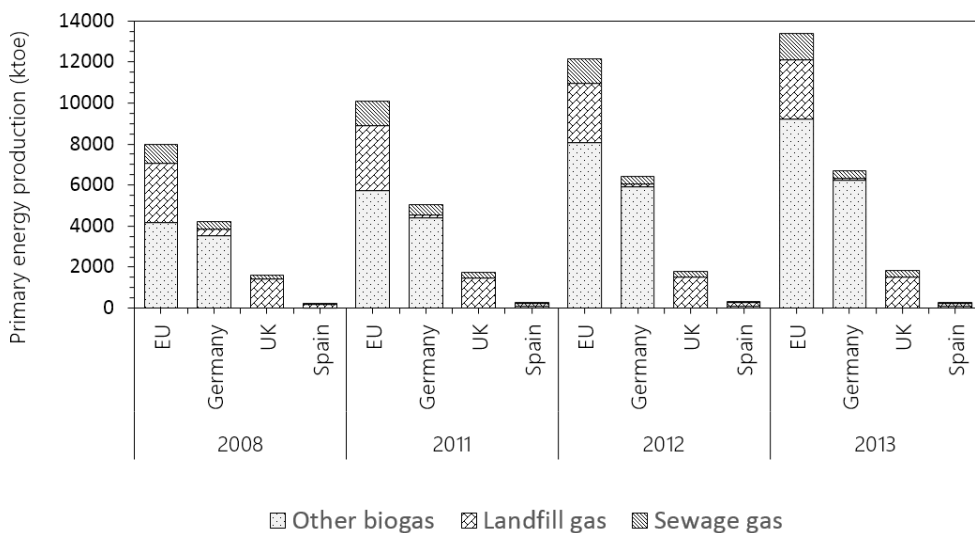


**Figure 1.2** Primary energy production of biogas in the European Union, Germany, UK and Spain in 2008, 2011, 2012 and 2013.

Production and use of biogas presents several environmental advantages since it is a renewable energy source, reduces the release of methane to the atmosphere compared to traditional manure management, it can be used as a substitute for fossil fuels and the high quality of the digested produced simultaneously with biogas can be used as fertilizer.

The CH<sub>4</sub> content determines the energy value of the biogas. Since it is obtained as a product of the anaerobic digestion, its composition (Table 1.1) is a mixture of methane (35-70%) and carbon dioxide (15-50%) with small amounts of other gases and by-products in concentrations under 2%, such as hydrogen, nitrogen, carbon monoxide, hydrogen sulfide (H<sub>2</sub>S) and ammonia depending on the source. Trace compounds usually include aromatic hydrocarbons, alkanes and alkenes, such as toluene, xylene, ethylbenzene or limonene. Halogenated compounds are not found in the biogases generated by anaerobic digestion (AD) of sewage sludge, but are often present in landfill gases. Siloxanes are also present as trace compounds in biogases from wastewater and landfill sources. Moreover this mix is usually saturated with water vapor at the digester temperature.

**Table 1.1**

Composition of sewage sludge and landfill gas (Rasi *et al.*, 2011; Tansel and Surita, 2014).

Compounds	Sewage sludge gas	Landfill gas
Methane (%vol)	60-70	35-65
Carbon dioxide (%vol)	30-40	15-50
Nitrogen	~0.2	5-40
Hydrogen	0	0-3
Oxygen	0	0-5
Hydrogen sulfide (ppm v/v)	0-4000	0-100
Ammonia (ppm v/v)	~100	~5
Halogenated species (ppm v/v)	<10	<90
Siloxanes (ppm v/v)	3-100	0-50

Biogas presents various sulfur compounds which are corrosive in the presence of H<sub>2</sub>O. H<sub>2</sub>S, produced in high concentrations from the anaerobic digestion of organic compounds, is a corrosive gas that also must be removed before the use of biogases. The abatement techniques applied depend on the H<sub>2</sub>S concentration, including biological treatment, absorption, chemical oxidation and catalytic adsorption onto impregnated activated carbons (Abatzoglou and Boivin, 2009). Besides the H<sub>2</sub>S abatement, the biogas upgrading must include the removal of siloxanes, whose study is the aim of this thesis,

since they are considered one of the most harmful compounds found on waste-derived fuels (Schweigkofler and Niessner, 2001).

The gas obtained can be used for the production of heat and steam, electricity generation or vehicle fuel, and the frameworks, tax systems and subsidies applied depend on the national regulations. Most of the European biogas is combusted in combined heat and power (CHP) internal combustion engines, gas micro-turbines (25-100kW) or large turbines (>100 kW), which is a reliable technology that does not require high biogas quality. Fuel cells, where energy is obtained directly through electrochemical reactions, can reach very high efficiencies and low emissions although their use required methane-rich biogas. Therefore, depending on the end use, different treatment steps are necessary, resumed in Figure 1.3. For some applications, where it is important to have a high energy content in the gas, e.g. as vehicle fuel or grid injection, the gas need to be upgraded by removing carbon dioxide. Hence, biogas generates new possibilities for its use since it can then replace natural gas.

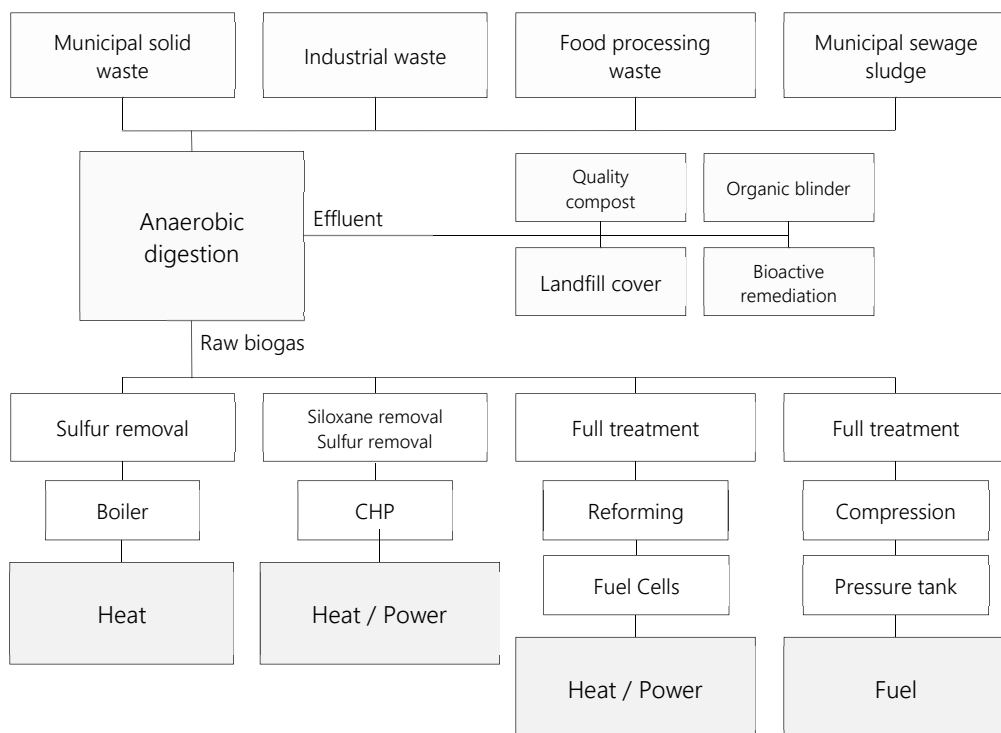


**Figure 1.3** Scheme of the biogas generation and cleaning requirements depending on the final use.

## 1.2 Siloxanes in biogases

Siloxanes are a group of manmade polymeric compounds of Si-O bonds with organic chains (methyl, ethyl or other functional groups) attached to the silicon atoms. Sources of siloxanes are substantial, and increasing. In the search for improved environmental cleaners and solvents, volatile methyl-siloxanes solvents are used due to their chemical and physical properties, including low surface tension, water repelling properties, low surface tension, resistance to temperature and high compressibility (Dudzina *et al.*, 2014). Table 1.1 resumes the physico-chemical properties of the organosilicon compounds most commonly found in biogas, which present low molecular weight and high vapor pressure, and are aroma-free, non-toxic and exempt from volatile organic compounds regulations. Volatile siloxanes molecular structure can be lineal (L abbreviation) or cyclic (D abbreviation).

**Table 1.2**

Most common organic silicon compounds found in biogases and their properties (Schweigkofler and Niessner, 2001);(McBean, 2008);(Rasi *et al.*, 2010).

Compound	Abbreviation	Molecular weight [g mol <sup>-1</sup> ]	Water solubility at 25°C [mg l <sup>-1</sup> ]	Boiling point [°C]	Vapor pressure at 25°C [kPa]
Trimethylsilanol	TMS	90	35000	70	2.13
Hexamethyldisiloxane	L2	162	0.93	107	4.12
Octamethyltrisiloxane	L3	236	0.035	153	0.52
Decamethyltetrasiloxane	L4	310	0.0067	194	0.07
Dodecamethylpentasiloxane	L5	384	0.0034	230	0.009
Hexamethylcyclotrisiloxane	D3	222	1.56	135	1.14
Octamethylcyclotetrasiloxane	D4	297	0.056	176	0.13
Decamethylcyclopentasiloxane	D5	371	0.017	211	0.02
Dodecamethylcyclohexasiloxane	D6	445	0.005	245	0.003

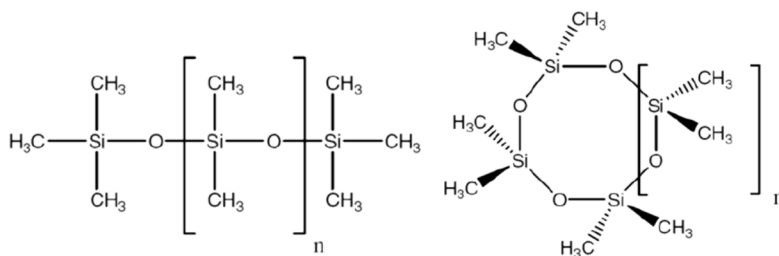


**Figure 1.4** Molecular configuration of lineal and cyclic siloxanes.

Siloxanes are ubiquitous in personal care products such as cosmetics, shampoos, deodorants, detergents and hairsprays. They are also present in pharmaceuticals, inks, adhesives, lubricants and heat transfer fluids (Dewil *et al.*, 2006). The most volatile siloxanes, such as hexamethyldisiloxane (L2) partially disperse into the atmosphere, and react with ·OH radicals to form OH-substituted silanols (Genualdi *et al.*, 2011), so that they are found at low concentrations. On the other hand, compounds like octamethylcyclotetrasiloxane (D4), decamethylcyclopentasiloxane (D5) and dodecamethylcyclohexasiloxane (D6) remain in wastewaters. They are not decomposed in the activated sludge process, have a significantly low water solubility and are more adsorptive than many organic compounds (Soreanu *et al.*, 2011). They do therefore not accumulate in the water phase, but are selectively attached to the sludge flocks where the extracellular polymeric substances (EPS) offer adsorbing sites (Dewil *et al.*, 2006).

Recent publications (Bletsou *et al.*, 2013; Xu *et al.*, 2013) have studied the degradation of linear and cyclic siloxanes in wastewater treatment plants in Greece and China. Bletsou *et al.* (2013) determined that about a 60% of the siloxanes that enter in a wastewater treatment plant are released with the sludge. Given the anaerobic conditions and high temperatures in the sludge digesters, generated biogases contain siloxanes, mainly D4 and D5 (Appels *et al.*, 2008). Larger molecules, such as dodecamethylhexasiloxane (D6), do not volatilize during sludge digestion due to its low vapour pressure and remain associated with the sludge (Dewil *et al.*, 2007). Volatile siloxanes are present in concentrations ranging from one to tens of ppm v/v in sewage biogas (Ohannessian *et al.*, 2008), far beyond the limits tolerated by several energy recovery systems manufacturers (Wheless, 2004).

During the combustion of biogas, the siloxanes are converted into abrasive microcrystalline silica, which has chemical and physical properties similar to those of glass, leading to the abrasion of engine parts or the build-up of silica layers that inhibit essential heat conduction or lubrication (Wheless, 2004). Therefore, the combustion of silicon-containing biogases causes serious damage to gas engines, microturbines and fuel cells, hampering the recovery of energy from biogas. The siloxane problem was given closer attention since the late 1990s, when the extent of the problem became more visible as the use of biogas increased due to public subsidies.

Consequently, growing importance is given to siloxane removal from biogas, as demonstrated by the increase in publications and patents filed in the last years (De Arespacochaga *et al.*, 2015) concluding that the application of techniques to remove siloxanes from biogas is required and a challenge for the effective recovery of energy from this renewable resource (Dewil *et al.*, 2006; Ajhar *et al.*, 2010).

### 1.3 Siloxane removal from biogas

---

Typical siloxane concentration reported in the literature range from 10 to 120 mg m<sup>-3</sup> (Piechota *et al.*, 2012; Raich-Montiu, 2014) while energy recovery systems (ERS) manufacturers have set the limits for siloxane concentrations from 0.03 to 28 mg m<sup>-3</sup>, being the lowest limits for turbines and microturbine and the internal combustion engines are the most tolerant (Wheless and Pierce, 2004). Therefore, siloxane removal is mandatory for the energy recovery from biogas and the number of publications regarding siloxanes abatement has increased in the past years, and the main features are resumed in Table 1.3. Emerging removal technologies, currently under investigation, include bio-tricking filters and membrane separation processes. Absorptive technologies are already commercial for the siloxanes abatement, consisting on scrubbing systems of concentrated acid solutions to cleavage the Si-O bond. These techniques achieve moderate siloxane removal efficiencies and are combined with pre and post-treatment methods (De Arespacochaga *et al.*, 2015). The most common pre-treatment applied is the refrigeration of the biogas in order to condensate water and other volatile compounds, achieving also a siloxane removal up to 18% (Schweigkofler and Niessner, 2001).

Among the commercial technologies, the most widely used to reduce siloxanes concentration in biogas is adsorption, since it is a low energy and low cost process, and effective at low pressure and low contaminant concentrations. At the same time, the most applied adsorbents are activated carbons (AC), although other solids, such as silica and zeolites or polymeric resins have given interesting results (Ajhar *et al.*, 2010). In spite of some scarce publications (Matsui and Imamura, 2010; Oshita *et al.*, 2010; Gislon *et al.*, 2013), little is known about the influence of the AC surface properties (i.e., porosity and surface chemistry) on the removal of these compounds.

**Table 1.3**

Siloxane removal technologies already commercial and under development and main features resumed.

	Technology	Main features	Ref.
Commercial	Adsorption	Activated carbon is the most widely used media to remove siloxanes from biogases. Loading capacity drops as a function of the relative humidity of the carrier gas and for the presence of sulphur-containing or halogenated compounds. Usually combined with a pre-drying step. Thermal desorption has limited efficiency (deposition of amorphous silica and polymerization products). Expenses for activated carbon replacement are the predominant part of operating costs.	[1,2]
	Absorption	Chemical absorption with strong acids and bases destroys siloxanes Only acidic liquids can be used as bases react to form carbonates but there are safety and corrosion concerns. Selexol™ process makes use of physical absorption in dimethyl ethers of polyethylene glycol.	[1,3]
	Deep chilling	At -30° C removal efficiencies between 50-90% have been reported Mere cooling to temperatures around 5°C has proven unsuitable for quantitative siloxanes removal. Generally regarded as economically suitable only at high flow rates and elevated siloxane load.	[1,4]
Development	Biological removal	Scarcely investigated and not proven yet. Suffer severe mass transfer limitations. The use of a second organic phase to enhance availability does not improve the efficiency (40%).	[5,6]
	Catalytic processes	High temperature (200-400°C) decomposition over metallic oxides and Silica. Testing performed at high concentrations of siloxanes (1400 mg/Nm <sup>3</sup> ) shows a 4-fold increase with respect to activated carbon adsorption. Not tested at typical siloxane concentrations.	[1,7]
	Membranes	Selective siloxane permeation by solution and diffusion through dense polymeric membranes. Up to 80% removal efficiencies reported. Relatively high investment costs and moderate operating costs.	[8,9]

References: [1] Ajhar *et al.* 2010 [2] Finocchio *et al.* 2009 [3] (Rasi *et al.*, 2008) [4] Schweigkofler and Niessner 2001 [5] (Popat and Deshusses, 2008) [6] (Li *et al.*, 2014) [7] (Urban *et al.*, 2009) [8] (Ajhar and Melin, 2006) [9] (Ajhar *et al.*, 2012)

## 1.4 Adsorption/oxidation technologies

---

### 1.4.1 Adsorption

Adsorption is the result of the unbalanced molecular forces that are present on every solid surface. When a solid surface get in contact with a liquid or a gas, there is an interaction between the force fields of the surface and those of the liquid or gas. The solid surface attracts and retains the molecules of gas or liquid to balance the surface forces, leading to a higher concentration of the gas or liquid in the vicinity of the solid surface.

The physical forces involved may be dipole moment, polarization forces, dispersive forces or short-range repulsive interactions and lead to physical adsorption, where the adsorbate is bound by relatively weak van der Waals interaction, similar to the molecular forces of cohesion. Chemical forces may include valence forces arising out of the redistribution of electrons between the solid surface and the adsorbed atoms leading to chemisorption. Chemical adsorption involves the exchange or sharing of electrons between adsorbate molecules and the surface of the adsorbent, resulting in a chemical bond much stronger than in physisorption. Therefore, while physical adsorption is nonspecific and may occur between any adsorbate-adsorbent systems, chemisorption is specific (Bansal, 2005).

When a solid surface is exposed to a gas, the molecules of the gas strike the solid surface and some of the striking molecules stick to the solid becoming adsorbed. Initially the adsorption rate is large because the whole surface is bare, but the adsorption rate decreases when the solid surface becomes covered by the adsorbate molecules. Then, desorption from the covered surface takes place as the adsorbed molecules rebound, until equilibrium between solid and gas is reached, when the adsorption and desorption rates become equal. Thus, the number of molecules sticking to the surface is equal to the number of molecules rebounding from the surface (Bansal, 2005). Parameters determining the equilibrium are the pressure of the gas and the temperature of the adsorption, thus adsorption equilibrium can be represented as adsorption isotherm, which is the most extensively employed method for representing the adsorption system and modelled by equations such as the Langmuir, the Freundlich or the Brunauer-Emmett-Teller (BET).

### 1.4.2 Activated carbon

Activated carbon includes a wide range of carbonaceous materials with highly developed porosity and surface area. They are prepared by the combustion or thermal decomposition of carbonaceous substances at temperatures below 800 °C in an inert atmosphere and the activation of the carbonized product. The properties of the product depend on the raw material, the activating agent and the carbonization and activation processes undergone. Anthracite, lignite, coal or wood are the most commonly used as precursors, although almost all materials with high carbon content can be used as a for the preparation of activated carbon (Kwiatkowski, 2011).

In the process of carbonization, the pyrolysis of the starting material produces gaseous species such as oxygen, hydrogen and nitrogen. The non-carbon elements, and the residual carbon atoms group themselves randomly into aromatic sheets cross-linked leaving free interstices that give rise to pores. This pore structure is further developed and enhanced during the activation process leading to a number of randomly distributed pores of various sizes and shapes and a high surface area (Marsh and Rodríguez-Reinoso, 2006).

The activation involves the creation of further porosity and the modification of the surfaces by heterogeneous reactions with either carbon dioxide, steam or a mix of these gases, or chemical agents such as  $\text{H}_3\text{PO}_4$ ,  $\text{H}_2\text{SO}_4$ ,  $\text{HNO}_3$ ,  $\text{NaOH}$ ,  $\text{KOH}$  or  $\text{ZnCl}_2$ . Carbon atoms can be removed by gasification at 800-900°C leading to the production of  $\text{CO}$ ,  $\text{CO}_2$  and  $\text{CH}_4$  creating carbons with different porosities and the oxidation of some regions. For the chemical activation, the carbonization and activation of the precursor take place simultaneously. The carbonaceous precursors is treated with the chemical agents by impregnation of physical mixture prior to the carbonization at high temperatures in a controlled atmosphere.

Depending on their size, the pores are divided into three groups: micropores have diameters smaller than 2 nm, mesopores between 2 and 50 nm and macropores, larger than 50 nm. The micropores represent about the 95% of the total surface area of an activated carbon, and mesopores about 5%. The macropores surface area is usually under 0.5 m<sup>2</sup> per gram, and they are not of considerable importance for the adsorption process,

however they act as channels for the adsorbate molecules to access the micro and mesopores (Rodríguez-Reinoso and Linares-Solano, 1989).

The microcrystalline structure is given by the orientation of the aromatic sheets, that contain free radicals and unpaired electrons that interact with oxygen, hydrogen, nitrogen and sulfur heteroatoms giving rise to different types of surface groups (Figure 1.4). The presence of oxygen groups modifies the surface properties of the activated carbons, by adding wettability, polarity and acidity characteristics, and physico-chemical properties like catalytic, electrical and chemical reactivity (Figueiredo *et al.* (1999).

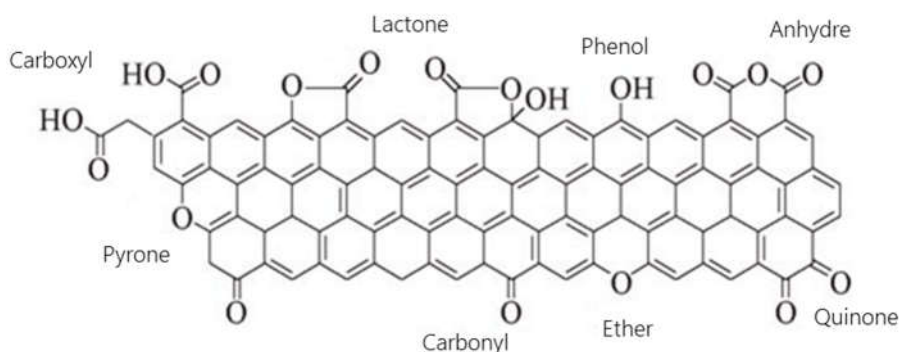


**Figure 1.5** Oxygen functional groups in AC surface.

### 1.4.3 Zeolites

Zeolites are crystalline aluminosilicates with crystalline polymers based on a three-dimensional arrangement of tetrahedral ( $\text{TO}_4$ )  $\text{SiO}_4$  or  $\text{AlO}_4^-$  connected through their oxygen atoms to form subunits and large lattices by repeating identical building unit cells. The general formula  $\text{M}_{x/n}(\text{AlO}_2)_x(\text{SiO}_2)_y$ , where  $n$  is the valence of the  $\text{M}$  cation, and  $x$  and  $y$  the number of tetrahedral per unit cell.  $x/y$  is the  $\text{Si}/\text{Al}$  ratio, varying from a minimal value of 1 to infinite (Kulprathipanja, 2010).

40 different zeolite structures have been discovered in nature, and 130 zeolites have been synthesized, and they have applicability in three main areas: adsorption, catalysis and ion-exchange. Zeolite structures are codified in a 3 capital letter code according to the rules set by the Commission of the International Zeolite Association (IZA).

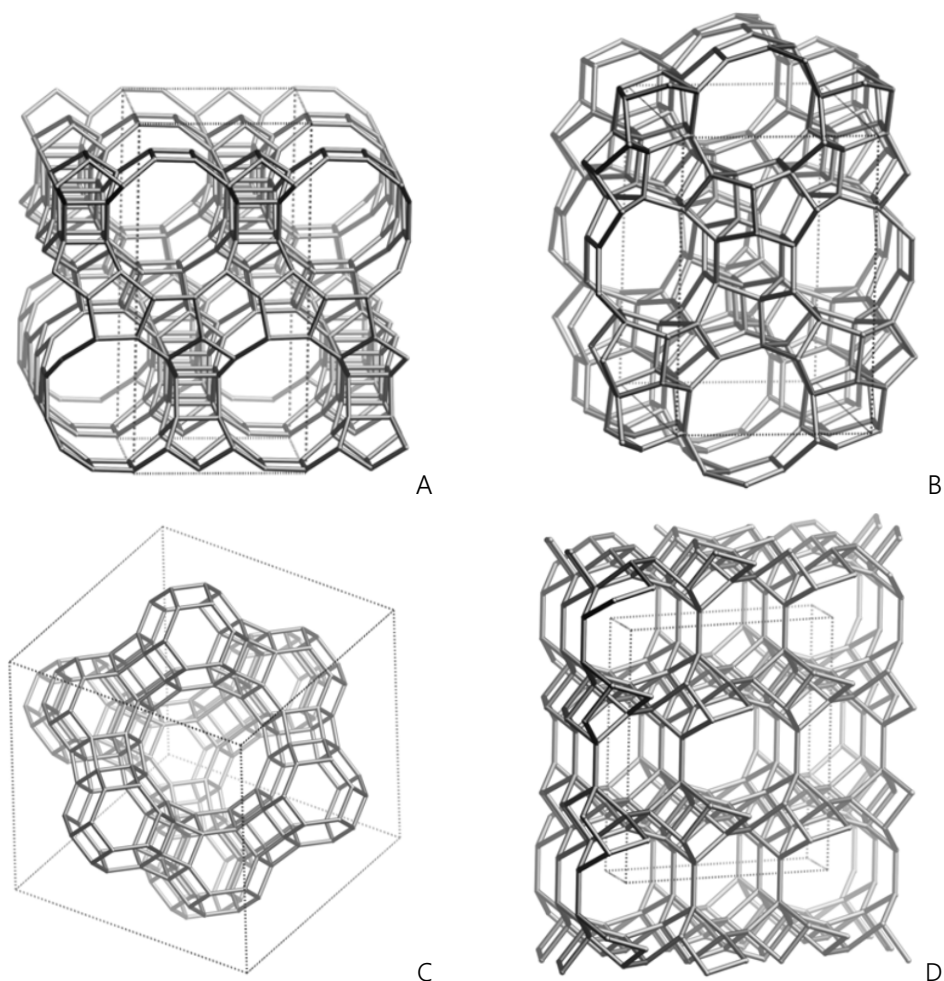


**Figure 1.6** Frameworks types of A) BEA, B) MFI, C) FAU and D) HEU zeolites.

Adsorption and catalytic processes involve the diffusion of molecules in the zeolites pores structure, thus, zeolites can be classified depending on their pore apertures. Large pore zeolites (12 ring apertures between 0.6 and 0.8 nm) include BEA (Beta) (Figure 1.6-A), FAU (Faujasite) (Figure 1.6-B) and MOR (Mordenite). Medium pore zeolites (10 ring aperture between 0.45 and 0.60 nm) include MFI (ZSM5) (Figure 1.6-C) and HEU (Figure 1.6-D) and there are also small pore zeolites (8 ring pore apertures and diameters between 0.30 and 0.45 nm) (Xiao and Meng, 2015).

Protonic sites of the zeolites are responsible for many reactions and catalytic transformations. They are associated with bridging hydroxyl groups attached to framework oxygen linking tetrahedral Si and Al atoms (Al(OH)Si). Thus, the maximum number of protonic sites is equal to the number of framework aluminum atoms. Due to cation exchange, dehydroxylation and dealumination during activation at high temperatures, the number and density of protonic sites can be adjusted. Therefore the maximum number of protonic sites is obtained for a framework with a Si/Al ratio of 1 and corresponds to 8.3 mmol H<sup>+</sup> g<sup>-1</sup> zeolite.

The strength of the protonic sites is related to the T-O-T bond angles. The greater the angles, the stronger the sites. In this sense, the protonic sites of MFI (133-177°) are stronger than those of FAU (138-147°), but the accessibility of the protonic sites depends on the location of the OH in the zeolites and the size of the reactant molecules. Moreover, extraframework aluminum species also increase the catalytic activity of zeolites, as they enhance the acidity through interaction by the creation of Brønsted sites and Lewis sites (Andreyev and Zubkov, 2012).

#### 1.4.4 Regeneration of adsorbents

The regeneration of the exhausted adsorbents assumes essential importance for the use of adsorption techniques from an economical point of view. Classical thermal regeneration of exhausted AC is performed off-site in furnaces, rotary kilns or multiple hearth furnaces. The thermal regeneration process is similar to that used to manufacture the original AC, and about 5-10% of the AC mass is lost. Many regeneration treatments are currently being investigated, including the use of steam, pressure swing, vacuum, microwaves ultrasounds, bioregeneration and chemical and oxidative treatments. The selection of the method depends on whether the adsorbate is recoverable or its destruction is required, but it must ensure the highest degree of desorption of the adsorbed compounds, with the least erosion and destruction of the adsorbents.

AOP-driven regeneration was first proposed by Mourand *et al.* (1995) while looking for innovative techniques for the *in-situ* regeneration of the exhausted adsorbents without the need to remove the adsorbent from the adsorption column. AOPs cause the generation of reactive radicals in aqueous solution, mainly ·OH, which are able to oxidize

the organic compounds present in solution.  $\text{H}_2\text{O}_2$  and  $\text{O}_3$  are the most used substances to generate  $\cdot\text{OH}$  radicals in water. Although the AOPs for the wastewater treatment are prominent industrial technologies and a fertile field for research (Mantzavinos *et al.*, 2009), the sequential application of adsorption/oxidation has received less scholarly attention (Georgi *et al.*, 2010; Anfruns *et al.*, 2013; Gonzalez-Olmos *et al.*, 2013). The overall treatment objective of the sequential adsorption/oxidation process is to transform the contaminants immobilized and concentrated in the adsorbent into byproducts with low affinity for the adsorbent, thus re-establishing its adsorptive capacity.

In the case of AC, contaminants are transformed on or near its surface by reaction with  $\cdot\text{OH}$  radicals. The catalytic production of  $\cdot\text{OH}$  radicals from  $\text{H}_2\text{O}_2$  can be achieved by the AC surface itself (Anfruns *et al.*, 2013), or by adding Fe salts, known as Fenton reagent (Toledo *et al.*, 2003; Huling *et al.*, 2012), and it is reported to be significantly enhanced if Fe-amended ACs are used (Huling *et al.*, 2000; Huling *et al.*, 2007; Huling *et al.*, 2009; Hwang *et al.*, 2010). The use of  $\text{O}_3$  has also been studied for the regeneration of AC exhausted with organic compounds in wastewater treatment plants (Álvarez *et al.*, 2004; Alvarez *et al.*, 2009).

Zeolites can be used as dual functional adsorbents/catalysts, as firstly organic molecules can be adsorbed (and transformed) in their porous structure and secondly they can catalyze the AOP reactions, without being vulnerable to oxidation. Thus, they have the potential to be long-lived reusable catalysts (Gonzalez-Olmos *et al.*, 2013; Shahbazi *et al.*, 2014). In addition, iron can be easily introduced into the structure of zeolites due to their ion-exchange capacity and the resulting Fe-containing zeolites show high catalytic activities in the oxidation of organic compounds with minimal iron leaching (Gonzalez-Olmos *et al.*, 2009; Gonzalez-Olmos *et al.*, 2011). Therefore, the AOP-driven regeneration of exhausted adsorbents/catalyst involves the sequential and synergistic use of two reliable and well-established treatment technologies in a two-step process: dynamic siloxane adsorption, and regeneration using AOPs.

## 1.5 State of the art

---

Table 1.4 resumes the publications concerning siloxane adsorption on porous solids, reporting a wide range of removal efficiencies. ACs are the most common adsorbents used due to their high adsorption capacities, but inorganic materials such as zeolites or silica gel are also applied. D4 and D5 are the most common siloxanes tested in lab-scale adsorption tests. L2, which is found in landfill gases, is also considered in some studies (Schweigkofler and Niessner, 2001; Ortega and Subrenat, 2009) and D3 removal is only reported by Finocchio *et al.* (2009) and Montanari *et al.* (2010). Several studies report the adsorption capacities in dynamic adsorption tests at concentrations much higher than the concentration found in real biogas, leading to high adsorption capacities (Matsui and Imamura, 2010), while other report the adsorption isotherms in batch experiments (Nam *et al.* 2013, Boulinguez and Cloirec, 2009). Most of lab scale adsorption experiments are conducted in dry N<sub>2</sub> matrices, but the use of CH<sub>4</sub>/CO<sub>2</sub> mix is used as synthetic biogas in some studies (Boulinguez and Le Cloirec, 2010; Yu *et al.*, 2013).

The main conclusions drawn so far, were reported by Oshita *et al.* (2010) comparing the D4 and D5 adsorption capacity of several AC with their textural properties, identifying positive relation with the surface area and pore volumes. Thus, the adsorbent textural development determines the accessibility of siloxanes through the pore structure.

On the other hand, an additional issue of particular interest which has been also barely explored is the formation of non-volatile compounds, such as silicon polymers on AC surface. This polymerization of the adsorbed siloxanes on the AC surface limits the regeneration of spent Acs by thermal treatment (Finocchio *et al.*, 2009; Montanari *et al.*, 2010), Therefore, siloxane exhausted AC is not usually regenerated (Ajhar *et al.*, 2010), and the regular replacement of the adsorbent beds constitutes the predominant part of the operational costs for the removal of siloxanes by adsorption. In the same sense, Ajhar *et al.* (2010) indicated that future research trends should be focused on regenerative systems to reduce costs for adsorbent renewal.

Thermal treatment of the AC is one of the most used regeneration techniques. However, in the case of siloxanes, the regeneration efficiency (RE) of the thermal treatment may be hampered by the presence or the formation of non-volatile siloxane polymers of higher

molecular weight in the adsorbent surface (Finocchio *et al.*, 2009; Sigot *et al.*, 2015). (Ortega and Subrenat, 2009) studied the thermal regeneration of hexamethydisiloxane (L2) exhausted-AC at 90°C for three cycles, obtaining about a 40% of RE, while (Gislon *et al.*, 2013) achieved a 70% recovery applying a thermal regeneration at 200 °C. More recently, (Giraudet *et al.*, 2014) studied the electro-thermal desorption of different biogas compounds, and found out that siloxane D4 was only partially desorbed, being one of the most problematic compounds for the AC regeneration. Furthermore, heating at these temperatures requires a high energy consumption, which implies an important economical drawback. Moreover, through this process large amounts of siloxanes are released to the environment. Recently, cyclic siloxanes have been assessed for their human and environmental risks, as well as their atmospheric transport pathways and bioaccumulation (Whelan *et al.*, 2004; McLachlan *et al.*, 2010; Warner *et al.*, 2010; Genualdi *et al.*, 2011; Wang *et al.*, 2013). Siloxane emission is currently under consideration for regulation in Europe and Canada because of the concerns about persistence, toxicity and potential for accumulation in aquatic food chains (Genualdi *et al.*, 2011).

Since thermal regeneration has a limited efficiency for siloxane-exhausted adsorbents, the use of advanced oxidation processes (AOPs) constitutes a promising low energy option. There are several studies in the literature reporting the AOP-driven regeneration of exhausted AC, usually for the removal of polar organic compounds such as, phenol (Ince and Apikyan, 2000), benzene and ethyl acetate (Stavitskaya *et al.*, 2002), organochlorides (Toledo *et al.* 2004), isopropylene and acetone (Hornig and Tseng, 2008) or toluene and limonene (Anfruns *et al.*, 2013). These studies agree that, due to the surface properties, AC acts as heterogeneous catalyst for the generation of ·OH radicals. These radicals are able to oxidase the organic compounds adsorbed in the carbons surface, although the regeneration efficiencies range from 5 to 99%. The research performed by Huling *et al.* (2005, 2007, 2009, 2010, 2012) is prominent on this field, studying the effects and optimization of the iron amendment to the AC in order to enhance the oxidation of MTBE molecules in the AC surface.

**Table 1.4**

Review of the studies concerning siloxane removal by adsorption on different porous materials.

Reference	Siloxane	Gas matrix	Adsorbent Conditions	Results
Lee <i>et al.</i> (2001)	D4	CH <sub>4</sub> /CO <sub>2</sub> mixture Sewage gas 100 ml min <sup>-1</sup>	Alumina Molecular sieve 0.5 g	Relatively flat breakthrough curves for all adsorbents in sewage gas matrix. Adsorbent capacity for alumina highest, molecular sieve lowest. D4 load per kg alumina in gas mixture: 46 g D4 load for kg alumina in real sewage gas: 13 g.
Schweigkifler and Niessner (2001)	L2 and D5 0.08 ppmv	Nitrogen 200 ml min <sup>-1</sup>	Carbopack B Tenax TA XAD-2 Molecular sieve 13X AC Silica gel	Greater affinity to L2 than AC D5 capacity of all adsorbents good. Carbopack B < 0.2wt% L2 0.3 wt% L2 < 0.1 wt% L2 Approx. 0.2 wt% L2 No breakthrough, neither L2 nor D5 below 1wt% loading > 10 wt% D5 desorption efficiency for both L2 and D5 > 95%
Doczyck (2003)	N/A	Landfill gas	AC	AC-consumption correlates with total contaminant load, not with silicon content. AC-consumption in identical gas matrix differs as much as 50%. Minimum AC-consumption varies depending on the landfill.
Rossol <i>et al.</i> (2003)	N/A	Sewage gas	AC	Removal from max. Concentrations of 20 mg m <sup>-3</sup> CH <sub>4</sub> to below 0.1 mg m <sup>-3</sup> . Contaminant loading per kg AC: 100 g Siloxane loading per kg AC: 20-50 g

Wheless and Jeffrey (2004)	D4	Sewage gas	Alumina Coconut AC Graphite AC Silica gel	0.4-1.0 wt% / 0.6-1.5 wt% siloxane adsorption at 4°C dew point, 5-25 bar g 50% increase in siloxane loading compared to AC was observed
Matsui and Imamura (2009)	D4 342 ppmv	Nitrogen 1.5 L min <sup>-1</sup>	AC (22 types) Molec. sieves Silica gel  150 g	ACs with higher surface area have higher adsorption capacity. Maximum D4 load per kg AC: 150-200 g. Maximum D4 load per kg molecular sieve: 10-80 g. Maximum D4 load per kg silica gel: 100 g.
Boulinguez and Le Clorec (2009)	D4 919 ppmv	CO <sub>2</sub> /CH <sub>4</sub> mixture  2L batch reactors	Granulated AC AC fibre-cloth	Type IV isotherm (over entire concentration range) Langmuir Freundlich isotherms (at typical low D4-concentrations in biogas). BET surface and micropores volume influence adsorption capacity greatly. Fibre-cloth has faster kinetics and similar capacity at low D4-concentrations.
Finocchio <i>et al.</i> (2009)	D3 0.51 ppmv	CH <sub>4</sub> /CO <sub>2</sub> mixture Water vapor  60 ml min <sup>-1</sup>	AC Silica gel  1.3 g	Best AC impregnated with CrIV and CuII salts: 88 wt%. Partial polymerization to PDMS occurs upon adsorption. Accumulation of silica on AC in real processes visible. Strong reduction of adsorption capacity after regeneration. Lower adsorption capacity of silica gel than pure AC.
Ortega and Subrenat (2009)	L2 190 ppmv	Air, 70% R.H. 1000 ml min <sup>-1</sup>	AC fibre-cloth  1-1.2 g	7 wt% L2 at breakthrough decreasing to relatively constant 2.5 wt% after repeated desorption-adsorption cycles

Oshita <i>et al.</i> (2010)	D4 and D5  21-46 ppmv	Nitrogen  1 L min <sup>-1</sup>	AC, silica gel, zeolite, synthetic resin  0.5 g	Adsorbents with large BET-specific surface areas, especially those with a high external specific surface area and pores of relatively larger diameters, are desired for the removal of siloxanes.
Nam <i>et al.</i> (2013)	L2, D4, D5 1:1:1 mix	N <sub>2</sub> dry matrix  250 ml batch reactors	AC, silica gel, alumina oxide	Adsorption of siloxanes depends on the molecular size and pore distribution of the adsorbents. L3, L4, L5 and D6 were generated in the reactors with a non-carbon adsorbents as conversion products of siloxane.
Yu <i>et al.</i> (2013)	D4  1440 mg m <sup>-3</sup>	CH <sub>4</sub> /CO <sub>2</sub> mix  200 ml min <sup>-1</sup>	11 AC  1g adsorbent beds	1.7-3 nm diameter pores are the most favourable for D4 adsorption.
Gislon <i>et al.</i> (2013)	L2  20-300 ppmv	N <sub>2</sub>	AC acid and basic, impregnated with KOH, KI, Cu and Cr salts	L2 adsorption into AC is physical and determined by the specific area of the AC. Thermal regeneration degrades the original x/M to 70%.
Sigot <i>et al.</i> (2015)	D4  30 ppmv	N <sub>2</sub>	Silica gel	The retention mechanism suggested is hydrogen bonding, D4 ring-opening and polymerization. 350°C thermodesorption was insufficient due to polymerization occurred.



---

Chapter 2  
OBJECTIVES



## Objectives

---

Aiming to develop a hybrid adsorption/oxidative process for siloxane abatement in biogases, this thesis is focused in the systematic study of activated carbon and inorganic zeolites as adsorbents and  $\text{H}_2\text{O}_2$  and  $\text{O}_3$  as oxidants for regeneration purpose. In this sense, a compromise between the siloxane adsorption capacity and the catalytic activity towards promoting oxidation is pursued. The following specific objectives are defined:

- To define the main parameters determining the adsorption of siloxanes in both activated carbons and zeolites:
  - Finding the correlations between the chemical and physical properties of the adsorbents and their adsorption capacity.
  - Studying the adsorption capacity at different siloxane inflow concentration in a nitrogen matrix.
  - Studying the adsorption using synthetic biogas as gas matrix.
  - Assessing the effect of the competitive adsorption of siloxanes and other volatile organic compounds present in biogas.
  
- To elucidate the polymerization mechanisms of cyclic siloxanes in contact with the different adsorbents:
  - Identifying the siloxane transformation products.
  - Determining the relations between the adsorbents functionalities and the compounds formed.
  
- To tailor adsorbents to both adsorb volatile siloxanes from biogas and act as hydroxyl radical promoters in AOPs:
  - Iron amended activated carbon.
  - Catalytic iron exchanged zeolites.

- To establish cause-effect relationships between the adsorbents/catalysts properties and their performance in sequential adsorption/oxidation processes.
  - Determining the optimal conditions to obtain high regeneration efficiencies with H<sub>2</sub>O<sub>2</sub> and O<sub>3</sub> treatments.
  - Studying the sequential performance of the adsorbents after several cycles of adsorption/oxidation.
  
- To implement the knowledge obtained in real scenario conditions and determine the best materials for siloxane abatement in biogas

The attainment of the previous objectives has led to the following thesis outline:

- **Chapter 4** presents the results of the study of D4 siloxane removal with a full set of 12 commercial activated carbons. The adsorption and polymerization processes are fully described.
- **Chapter 5** details the AOP-driven regeneration of two selected commercial ACs and a tailored iron-amended AC. The regeneration efficiencies of the siloxane exhausted activated carbons with O<sub>3</sub> and H<sub>2</sub>O<sub>2</sub> are assessed.
- **Chapter 6** defines the mechanisms of D4 transformation and uptake in zeolites. A set of 7 zeolites is studied for D4 removal, and oxidation processes were used for the regeneration of an iron-containing zeolite.
- **Chapter 7** explores the siloxane removal in conditions similar to real biogas, including parameters such as concentration, gas matrix, humidity and the competition of VOCs. The performance of conventional AC is compared to chemically AC.

---

## Chapter 3

# MATERIALS & METHODS



## 3.1 Adsorbents

---

### 3.1.1 Activated carbons

12 commercial granular activated carbons (AC) supplied by *MeadWestvaco* (MWV) (USA), *Jacobi* (JCB) (Sweden), *Desotec* (DST) (Belgium), *Chemviron Carbon* (CMV) (Belgium), *Calgon* (CLG) (USA) and *Norit* (NRT) (USA) were tested for D4 removal (Chapter 4). Pellets were grounded and sieved in order to obtain a particle size between 212 and 425  $\mu\text{m}$ . In Table 3.1 commercial name, origin and the activation method of the ACs used in this work are shown.

**Table 3.1**

Commercial name, origin and activation process undergone for the ACs.

AC	Commercial name	Origin	Activation
CLG-1	Filtrisorb	Coal	n/a
CLG-2	Centaur	Coal	Steam
CMV-1	F100	Coal	Steam
CMV-2	F300	Coal	Steam
DST-1	Organosorb 10AA	Lignite	Steam
DST-2	Airpel 10	Anthracite	Steam
JCB-1	Aquasorb	Coconut	Other chemical
MWV-1	Nuchar A1100	Wood	H <sub>3</sub> PO <sub>4</sub>
MWV-2	Nuchar BAX150	Wood	H <sub>3</sub> PO <sub>4</sub>
NRT-1	Row 0.8 Supra	n/a	Steam
NRT-2	RB3	Peat	Steam
NRT-3	1240	Coal	Steam

(n/a) not available

### 3.1.2 Zeolites

Six synthetic zeolites and one natural zeolite (Clinoptilolite) were studied for D4 removal (Chapter 6). Their properties are summarized in Table 3.2. Fe-BEA, Fe-MFI, DAY and USY were obtained as pellets, BEA-38 and BEA-300 in powder form and the natural Clinoptilolite as a sand. Pellet and sand form zeolites were grinded and sieved in order to obtain a particle size of 212 - 425  $\mu\text{m}$ .

**Table 3.2**

Properties of commercial zeolites considered.

Zeolite	Framework code	Supplier	Max. diameter (Å)	SiO <sub>2</sub> /Al <sub>2</sub> O <sub>3</sub> molar ratio	Cation form	Fe (%wt)
Fe-BEA	BEA	Sued-Chemie	7.5	25	H <sup>+</sup>	3.1
BEA-38	BEA	Zeolyst	7.5	38	NH <sub>4</sub> <sup>+</sup>	-
BEA-300	BEA	Zeolyst	7.5	300	H <sup>+</sup>	-
Fe-MFI	MFI	Sued-Chemie	5.6	26	H <sup>+</sup>	2.2
USY	FAU	Zeochem	7.4	55	n.a.	-
DAY	FAU	Degussa	7.4	>200	n.a.	-
Clinoptilolite	HEU	Zeocat	n.a.	5.5	n.a.	-

n.a. not available

## 3.2 Adsorbents characterization

Adsorbents used in this thesis were exhaustively characterized. The applied techniques and their purpose are summarized in Table 3.3 and described in the following sections.

**Table 3.3**

AC characterization techniques and their purpose.

Technique	Purpose	Section
N <sub>2</sub> and CO <sub>2</sub> adsorption-desorption isotherms	Determination of BET specific area ( $S_{BET}$ ), total pore volume ( $V_t$ ), micropore volume ( $VDR_{N_2}$ ) and narrow micropore volume ( $VDR_{CO_2}$ ).	3.2.1
Thermal programmed desorption (TPD)	Determination of oxygen functional groups on the activated carbon surface.	3.2.2
X-ray Photoelectron Spectroscopy (XPS)	Determination of the chemical composition of the first 5-10 layers of the sample.	3.2.3
Elemental analysis (EA)	Determination of the C, H and N content of the ACs.	3.2.4
Energy-dispersive X-ray spectroscopy (EDX) and Scanning electron microscopy (SEM)	Determination of the differences on the chemical composition of fresh and exhausted AC.	3.2.5
Fourier transform infrared spectroscopy (FT-IR)	Detection of siloxane polymers in exhausted samples of adsorbents, determination of adsorbed pyridine molecules in acidity determination.	3.2.6
pH slurry	Determination of the pH of the adsorbents.	3.2.7

### 3.2.1 Textural characterization

The surface areas and pore volumes of the ACs and zeolites were calculated from the N<sub>2</sub> and CO<sub>2</sub> adsorption-desorption isotherms, performed at -196 °C in a Micromeritics ASAP 2420 volumetric adsorption system and at 0 °C in a Quantachrome Nova Station A, respectively. Prior to measurement, samples were outgassed overnight by heating at 250°C under vacuum. Specific surface areas ( $S_{\text{BET}}$ ) were calculated using the Brunauer-Emmett-Teller (BET) method, taking 16.2 nm<sup>2</sup> for the cross-sectional area of the nitrogen-adsorbed molecule. Total micropore (diameter 0.7-2 nm) volumes ( $V_{\text{DR}_{\text{N}_2}}$ ) were assessed by applying the Dubinin-Radushkevich (DR) equation to the suitable adsorption data. Total pore volumes ( $V_t$ ) were determined by the amount of N<sub>2</sub> adsorbed at  $P/P^0 = 0.99$ . Mesopore volumes ( $V_{\text{meso}}$ ) were calculated by subtracting the  $V_{\text{DR}_{\text{N}_2}}$  micropore volumes from the total pore volumes. Narrow micropore (diameter <0.7 nm) volumes ( $V_{\text{DR}_{\text{CO}_2}}$ ) were obtained from the CO<sub>2</sub> isotherms by using the DR method.

### 3.2.2 Thermal programmed desorption (TPD)

AC samples were heated at 10°C min<sup>-1</sup> under a He flow of 50 ml min<sup>-1</sup> in the quartz reactor of an Autochem II apparatus (Micromeritics). Desorbed gases were analyzed with an Omnistar (Pfeiffer Vacuum) mass spectrometer. TPD curves were obtained by plotting the desorbed CO and CO<sub>2</sub> (μmol g<sup>-1</sup>) vs. the temperature (°C). TPD curves were deconvoluted using the OriginPro software, following the criteria reported in previous studies (Figueiredo *et al.*, 1999). The relationships between the deconvoluted peaks and functional groups are shown in Table 3.4.

**Table 3.4**

Groups decomposed at each temperature by TPD analysis (Figueiredo *et al.*, 1999).

Temperature (°C)	Groups decomposed
CO <sub>2</sub>	
100-400	Carboxylic
200-400	Lactone
400-600	Anhydride
CO	
600-700	Phenolic
700-900	Carbonyl
>800	Ether

### 3.2.3 X-ray Photoelectron Spectroscopy (XPS)

The AC spectra of C (1s) and O (1s) were obtained with a VG ESCALAB 220i-XL spectrometer, using an unmonochromatized AlK $\alpha$ X-ray source (1486.6 eV). The vacuum in the analysis chamber was under 4·10<sup>-9</sup> mbar. The survey scan spectra were collected with a pass energy of 50 eV, whereas the high-energy resolution spectra were performed with the pass energy of 25 eV. Peaks were deconvoluted adjusting Gaussian functions using OriginPro software. Peaks were assigned according to previous studies (Moreno-Castilla, 2004; Rey *et al.*, 2008; Figueiredo and Pereira, 2010) as reported in Table 3.5.

**Table 3.5**

Assignment of peaks corresponding to each binding energy on XPS analysis.

Binding energy (eV)	Assignment
C (1s)	
284.4	C=C
285.2	C (aliphatic defects)
286.0	C-OH; C-O-C
287.1	C=O
288.5	COOH; COOC
291.0	$\pi \rightarrow \pi^*$
O (1s)	
531.1	C=O
532.2	C-OH; C-O-C
533.3	COOCO
534.2	COOH
535.9	Adsorbed H <sub>2</sub> O

### 3.2.4 Elemental Analysis (EA)

In order to determine the carbon, hydrogen and nitrogen composition of the activated carbon and zeolites, elemental analysis was carried out with a 2400 Series II CHNS/O System (Perkin Elmer).

### 3.2.5 Energy-dispersive X-ray spectroscopy and SEM analysis (EDX/SEM)

The chemical composition of the samples surfaces of both fresh and D4-saturated adsorbents was studied by EDX. Dry AC samples were fixed and recovered with carbon and analyzed (Quantax EDS, Bruker). Samples for SEM analysis (DSM 960, Zeiss) were sputtered with a 22.5 nm gold layer using a current of 30 mA, with a deposition time of 2

minutes (sputter coater K550, Emitech). Digital images were collected and processed by Esprit 1.9 Bruker software.

### 3.2.6 Fourier transform infrared spectroscopy (FT-IR)

FT-IR analysis of both fresh and D4 saturated activated carbons and zeolites was accomplished by means of an Alpha FT-IR spectrometer (Bruker) equipped with the sampling module Platinum-ATR.

### 3.2.7 $\text{pH}_{\text{slurry}}$ of the ACs

0.50 g of activated carbon were suspended in 25 ml of MilliQ water and left stirring for 24 hours. The pH was then measured with a Crison micro pH 2000 pHmeter.

### 3.2.8 Zeolites acidity determination

The Lewis acidic sites (LAS) and Brønsted acidic sites (BAS) were determined by FT-IR using pyridine as probe molecule. The pyridine adsorption/desorption was performed at 150°C. 5 mg of zeolite were introduced in 120 ml vials with a septum cap. A volume of 0.5 ml of liquid anhydrous pyridine (99.8%, Sigma-Aldrich, Missouri, USA) were injected and the bottles were heated to 150 °C to completely volatilize the pyridine. After 2 h the gas was vented and 0.5 ml more of pyridine were injected through the septum and maintained at 150 °C. After 24 h the bottles were opened and heated again to 150 °C to desorb the physisorbed pyridine.

The FT-IR spectrum was obtained by means of a Cary 630 FT-IR spectrometer (Agilent Technologies, CA, USA). The band around 1540  $\text{cm}^{-1}$  is characteristic of pyridinium ions, corresponding to BAS, while bands at 1440  $\text{cm}^{-1}$  are attributed to coordinately adsorbed pyridine on LAS (Lercher *et al.*, 1996). Quantitation of the number of acid sites present was obtained from the integral intensity of the corresponding IR bands after adsorption of pyridine and the molar extinction coefficients: 1,67 and 2.22  $\text{cm}^2/\mu\text{mol}$  for BAS and LAS sites respectively (Flanigen *et al.*, 1991).

## 3.3 Adsorption tests

---

### 3.3.1 Static adsorption tests

Static adsorption tests were carried out at room temperature ( $20 \pm 2$  °C), using 50 mg of AC in 120 ml glass bottles. The bottles were closed with a septum cup and connected to a syringe pump (Model 33, Harvard Apparatus, USA). Syringes were load with liquid D4 (Aldrich Chemistry) and the injection rate was adjusted to  $20 \mu\text{l h}^{-1}$ . After different periods of injection time, depending on the adsorption capacity of the AC, the D4 concentration in the bottle gas phase was analysed by a gas chromatograph equipped with a flame ionization detector (GC-FID, CP3800 Varian), with a capillary column FactorFour CP8860 (Varian) operated in manual injection. Adsorption isotherms were obtained by plotting the equilibrium concentration in the bottle gas phase vs the AC uptake.

### 3.3.2 Dynamic adsorption tests

Dynamic adsorption tests were carried out at room temperature ( $20 \pm 2$  °C), using 250 mg of AC or zeolite packed in a small fixed-bed column with an internal diameter of 7 mm. The adsorbents were ground and sieved to obtain a particle size between 212 and 425  $\mu\text{m}$ . Bed heights ranged from 5 to 11 mm depending on the tested adsorbent. The carrier gas flow was set to  $200 \text{ ml min}^{-1}$  using a mass flow controller (Alicat Scientific). The siloxanes selected for this study were D4, D5 and L2. The mono-component adsorption system was set up as shown in Figure 3.1. Carrier gases used in this study were nitrogen, synthetic biogas ( $\text{CH}_4/\text{CO}_2$ , 55/45 v/v) or air with 20% relative humidity. Relative humidity of 80% was obtained by bubbling the carrier through water. The humidity content of the carrier gas was measured with an appropriate sensor (Testo 635). The adsorption capacities were tested at different adsorbate concentrations by means of two different experimental set-ups.

#### *D4 mono-component adsorption tests*

A gas wash bottle with a known amount of liquid D4 (Aldrich Chemistry) was used to prepare gas streams with high D4 concentration (1000 ppm v/v). In order to obtain

streams with lower concentration, i.e. 40, 120 or 180 ppm v/v, the 1000 ppm v/v flow gas was diluted by means of a gas mixing and dilution system (Enviroincs Inc., Series 4020). For very low concentration tests, i.e. 1.45 ppm v/v, a permeation device (Dynacalibrator 150, Vici Metronics Inc.) with a D4 permeation tube (Vici Metronics Inc.) was used. The Dynacalibrator equipment is a constant temperature system designed to generate precise ppm v/v or ppb v/v concentrations of chemical compounds in a gas stream. All the experiments were carried out at room temperature ( $\approx 20$  °C). D4 concentration in the column outlet was measured with the GC-FID (CP3800 Varian), by a 1 ml loop automatic injection system to sample and analyze the column outlet every 10 minutes.

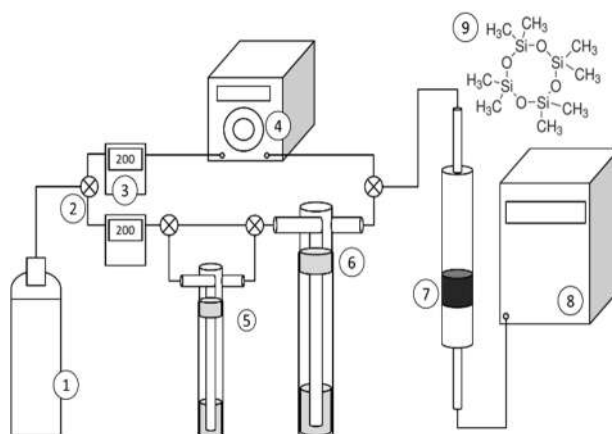


**Figure 3.1** Schematic of the dynamic adsorption experiment: (1) carrier gas, (2) valves; (3) mass flow controller; (4) Permeation chamber; (5) gas wash bottle filled of water; (6) gas wash bottle filled of D4; (7) fixed bed adsorbent; (8) GC-FID, (9) Chemical structure of D4.

### *Multicomponent adsorption test*

The generation of a multicomponent test-gas was achieved by the mix of 5 different streams of siloxanes (L2, D4, D5 supplied by Sigma-Aldrich) and VOCs (Toluene and Limonene, supplied by Sigma-Aldrich). Each stream was obtained by bubbling dry  $\text{N}_2$  in a gas wash bottle filled with each compound. By means of five mass flow controllers (Alicat Scientific) and  $\text{N}_2$  dilution, the flow of each stream was adjusted to obtain the desired concentration of each compound in the test gas. The concentration of each compound in the outlet flow was continuously measured by GC-FID (CP3800, Varian) in the same condition than monocomponent tests.

### Adsorption capacity determination

For each adsorption experiment, the adsorption column was operated until the adsorbates outlet concentration matched the inlet concentration (i.e., bed exhaustion). Breakthrough curves were thus obtained by plotting the  $c(t)/c_0$  vs. time where  $c_0$  is the adsorbate inlet concentration (ppm v/v) and  $c(t)$  is the adsorbate outlet concentration (ppm v/v) at a given time. The adsorption capacity ( $x/M$ , mg of adsorbate  $g^{-1}$  of adsorbent) was calculated as follows:

$$\frac{x}{M} = \frac{QM_w}{\omega V_M} \left( c_0 t_s + \int_0^{t_s} c(t) dt \right) \quad \text{Eq. 1}$$

where  $Q$  is the inlet flow ( $m^3 s^{-1}$ ),  $\omega$  is the adsorbent weight (g),  $M_w$  is the adsorbate molecular weight ( $mg mmol^{-1}$ ),  $V_M$  is the ideal gas molar volume ( $ml mmol^{-1}$ ) and  $t_s$  is the bed exhaustion time (s). Average adsorption capacities values and standard deviations were calculated from triplicates.

The fractional capacity ( $\Phi$ ) measures the efficiency of the carbon within the mass transfer zone. Values of  $\Phi$  vary between 0 and 1 and were obtained from equation 2,

$$\Phi = \frac{\int_{V_{0.02}}^{V_{0.95}} (C_0 - C) dV}{(V_{0.95} - V_{0.02})C_0} \quad \text{Eq. 2}$$

where  $V_{0.95}$  and  $V_{0.02}$  are the volume of gas treated up to a relative outlet concentration of 0.95 and 0.02 respectively.

The height of the mass transfer zone ( $H_{MTZ}$ ) indicates the rate of siloxane removal by the adsorbent, calculated as equation 3

$$H_{MTZ} = h \left( \frac{V_{0.95} - V_{0.02}}{V_{0.02} + (V_{0.95} - V_{0.02})\Phi} \right) \quad \text{Eq. 3}$$

where  $h$  is the bed depth. A lower  $H_{MTZ}$  reflects a faster adsorption rate (Fairén-Jiménez *et al.*, 2007).

### 3.3.3 Analysis of exhausted AC

250 mg of the spent ACs were recovered after the dynamic adsorption tests, mixed with 25 ml of hexane (Aldrich Chemistry) and stirred overnight at room temperature in order to extract the adsorbed organic compounds from the AC. The extract was analyzed using gas chromatography with a mass spectrometry detector (5977E Series GC/MSD System, Agilent Technologies, USA) equipped with a capillary column HP-5ms Ultra Inert (Agilent Technologies). Calibration was carried out using standards of cyclic siloxanes (D4, D5 and D6) (Aldrich Chemistry), and lineal siloxanes (octamethyltrisiloxane (L3), decamethyltetrasiloxane (L4) and dodecamethylpentasiloxane (L5)) (Aldrich Chemistry).

### 3.3.4 Analysis of exhausted zeolites

Exhausted and regenerated zeolite samples were treated with anhydrous tetrahydrofuran (THF) (Sigma-Aldrich, USA) maintained in a solvent system (MBraun MB-SPS-800) in order to extract adsorbed siloxanes and potential transformation products. Samples of 250 mg of exhausted zeolites were suspended in 4 ml of anhydrous THF and mixed for 10 minutes in an orbital mixer. Then, suspensions were centrifuged and liquid phases were analyzed by gas chromatography with a mass spectrometry detector (5977E series GC/MSD system, Agilent Technologies).

Cyclic siloxanes and siloxane diols were identified following the procedure indicated by Varaprath and Lehmann (1997). The gas chromatograph was operated at 60 °C for 3 minutes, followed by a heating ramp of 20 °C min<sup>-1</sup> from 60 to 120 °C and 40 °C min<sup>-1</sup> until 250 °C.

Additionally, elemental analyses (EA) were carried out using a PerkinElmer 2400 series II CHNS/O system in order to determine the carbon content that remains after zeolite regeneration and can be related to remaining D4 and products formed.

## 3.4 Regeneration tests

---

### 3.4.1 Regeneration with H<sub>2</sub>O<sub>2</sub>

Regeneration of the D4-exhausted adsorbents using H<sub>2</sub>O<sub>2</sub> was carried out in glass reactors filled with 100 ml of solutions containing different concentrations of H<sub>2</sub>O<sub>2</sub> (Scharlau chemicals, Spain). The solution pH was not adjusted. Reactors were placed on an orbital mixer for 24 hours at room temperature 22 ± 1 °C.

After the oxidation step, the suspended adsorbents samples were filtered and dried in a glass column with an air flow of 200 ml min<sup>-1</sup>. The column outlet flow was analyzed by GC-FID in order to prove that no desorption of D4 took place during the drying. Humidity at the column outlet was analyzed using a humidity sensor (Test 635). When humidity was no longer detected, new dynamic adsorption tests were carried out. The regeneration efficiency (RE) was calculated as the percentage of D4 uptake after the oxidation over the original D4 uptake obtained in the first use. In order to determine the D4 desorption into water, the same process was carried out without H<sub>2</sub>O<sub>2</sub> as blank treatment.

#### *H<sub>2</sub>O<sub>2</sub> decomposition tests*

The H<sub>2</sub>O<sub>2</sub> decomposition in the presence of adsorbents/catalysts was determined. 250 mg samples were suspended in 100 ml H<sub>2</sub>O<sub>2</sub> solutions and were left in agitation. The H<sub>2</sub>O<sub>2</sub> concentration was periodically determined by spectrophotometry measurements (Genesys 10S, Thermo Scientific) at 405 nm using a commercial solution of titanium (IV) oxysulfate (TiOSO<sub>4</sub>, Fluka Analytical).

#### *Iron amendment*

Fe amendment into AC was carried out by suspending 2 g of Nuchar in 10 ml of iron solution (0.4-4.0 g Fe L<sup>-1</sup>) obtained from ferrous sulfate (FeSO<sub>4</sub>·7H<sub>2</sub>O). The process was carried out at acidic conditions (pH 2.5) by adding H<sub>2</sub>SO<sub>4</sub> in order to maintain soluble Fe in the AC suspension (Gonzalez-Olmos *et al.*, 2013). The suspension was agitated during 4 days to facilitate the diffusion of the Fe into the porous structure of the AC. After this

period, the pH was raised to 4.0 using NaOH. The AC was decanted and rediluted in 10 ml of DI water, agitated for 2 hours in order to clean the residues, and dried at 105 °C overnight. To determinate the iron content in carbon after the described process, samples were digested with HNO<sub>3</sub>, HCl and HF at 180 °C for 180 minutes, and neutralized with HF and H<sub>3</sub>BO<sub>3</sub> at 160 °C for 15 minutes. Then iron concentration was determined by inductively coupled plasma atomic emission spectroscopy (ICP-AES) (Liberty SeriesII, Varian).

#### *Iron leaching analysis*

After each experiment, the amount of iron that was leached into the liquid phase was determined by spectrophotometry using the commercial Reactive Iron Test Spectroquant (Merck Millipore, Darmstadt, Germany).

#### 3.4.2 Ozonation in batch experiments

Ozone regeneration of exhausted adsorbents was performed in batch experiments in aqueous suspension. For that, 250 mg of D4-exhausted zeolites were suspended in a glass reactor containing 500 ml of deionized water at room temperature (22 ±1 °C). A continuous ozone mass flow of 70 mg O<sub>3</sub> min<sup>-1</sup> obtained from pure oxygen using an ozone generator (Anseros, COM-AD-01) was bubbled into the reactor. The O<sub>3</sub> concentration was measured by means of the Ozone Gas Analyzer Anseros GM-TRI (Anseros, Germany). Experiments were carried out for different reaction times (5-30 minutes). The same process was carried out using a nitrogen flow in order to assess the effect of D4 desorption into water.

After the oxidation step, suspended zeolite samples were filtered and dried in glass columns following the same procedure explained in section 3.4.1. New dynamic adsorption tests were carried out and regeneration efficiencies were calculated.



---

# RESULTS



---

# Chapter 4

## RESULTS I

### Octamethylcyclotetrasiloxane adsorption into activated carbon

Redrafted from:

Biogas upgrading: Optimal activated carbon properties for siloxane removal  
Alba Cabrera-Codony, Miguel A. Montes-Morán, Manuel Sanchez-Polo, Maria J. Martin, Rafael Gonzalez-Olmos  
*Environmental Science & Technology*, 48 (2014) 7187-719



## 4.1 Overview

---

The most widely used technology to reduce siloxanes concentration in biogas is adsorption in activated carbons. However, despite some scarce publications (Matsui and Imamura, 2010; Oshita *et al.*, 2010; Gislou *et al.*, 2013), little is known about the influence of the AC surface properties (i.e., porosity and surface chemistry) on the removal of these compounds. On the other hand, an additional issue of particular interest which has been also barely explored in this chapter is the formation of non-volatile compounds, such as silicon polymers, on the AC surface. This polymerization of the adsorbed siloxanes on the AC limits the regeneration of spent ACs by thermal treatment (Finocchio *et al.*, 2009; Montanari *et al.*, 2010), hence increasing the price of biogas pre-treatment.

For these reasons, the objectives of this chapter are to investigate the effect of the textural properties and surface chemistry of ACs in the adsorption of D4, as well as the polymerization phenomena.

Twelve commercial activated carbons (ACs) were tested in D4 dynamic adsorption experiments using dry N<sub>2</sub> with 1000 ppm v/v of D4. Characterization of the ACs included several physical and chemical techniques. The D4 adsorption capacities were strongly related with the textural development of the ACs. Results showed that the optimum adsorbent for D4 are wood-based chemically activated carbons.

The polymerization of D4 over the surface of all ACs was found to be relevant after prolonged contact times. The extent of this phenomenon, which affects negatively the thermal regeneration of the AC, correlated reasonably well with the presence of phenolic and carboxylic groups on the carbon surfaces.

## 4.2 Methodology

---

The materials used in this chapter are the commercial activated carbons listed in Table 3.1. All ACs were characterized by the analytical techniques considered in section 3.2: Textural characterization, Thermal programmed desorption (TPD) and X-ray Photoelectron spectrometry (XPS).

The D4 adsorption capacity of all the ACs considered was tested in high concentration dynamic adsorption tests following the experimental set up described in section 3.3.1. The siloxane adsorbed in the exhausted ACs was extracted following the methodology described in section 3.3.2 both in short and long term using hexane as dissolvent.

## 4.3 Results and Discussion

---

### 4.3.1 D4 adsorption on commercial ACs.

D4 adsorption capacity of a set of 12 commercial ACs was evaluated in dynamic adsorption experiments using  $200 \text{ ml min}^{-1}$  of dry  $\text{N}_2$  with 1000 ppm v/v of D4. This concentration is at least 100 times higher than the typical concentration found in sewage biogas. The reason to carry out experiments with such a high D4 concentration was to allow us performing one-day experiments, since low D4 concentration tests took several weeks (40 days) for completion. Also, this high concentration inlet would render the maximum capacities of the ACs. The D4 adsorption breakthrough curves obtained for each tested adsorbent are shown in Figure 4.1. Breakthrough times, defined as  $c(t)/c_0=0.05$ , range from 5-160 min. The adsorption capacities for the tested ACs were calculated according to equation 1. Results, collected in Table 4.1, indicate that the tested materials have adsorption capacities ranging between  $249 - 1732 \text{ mg g}^{-1}$ , similar to those reported in the literature (Matsui and Imamura, 2010; Oshita *et al.*, 2010). Previous works published into the literature about siloxane adsorption with ACs are listed as a table-review in Table 4.1, which includes a wide set of ACs with diverse origin, activation and textural properties.

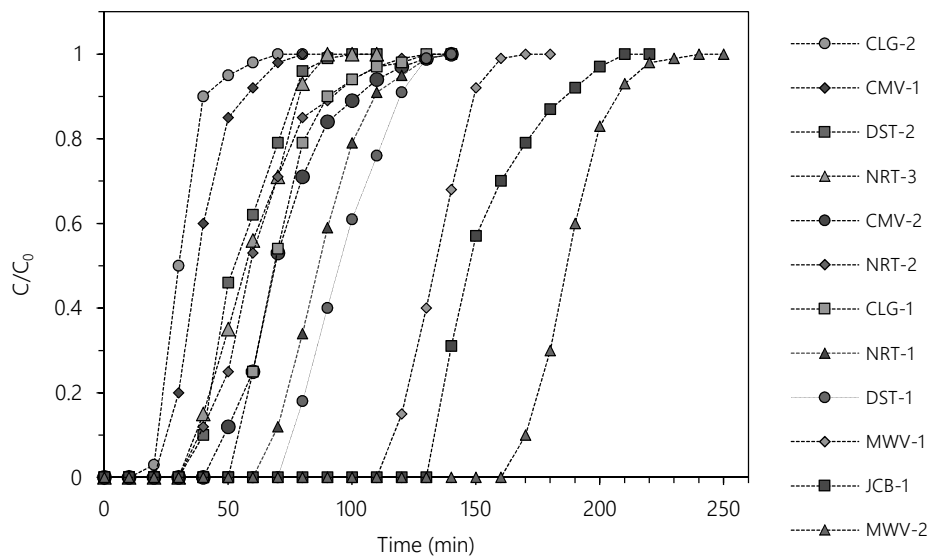


**Figure 4.1** Dynamic adsorption breakthrough curves for D4 onto different commercial activated carbons.

**Table 4.1**

D4 adsorption capacity, textural properties of the activated carbons considered and  $H_{MTZ}$ .

AC	D4 x/M (mg g <sup>-1</sup> )	$S_{BET}$ (m <sup>2</sup> g <sup>-1</sup> )	$V_t$ (cm <sup>3</sup> g <sup>-1</sup> )	$VDR_{N_2}$ (cm <sup>3</sup> g <sup>-1</sup> )	$VDR_{CO_2}$ (cm <sup>3</sup> g <sup>-1</sup> )	$V_{meso}$ (cm <sup>3</sup> g <sup>-1</sup> )	$H_{MTZ}$ (cm)
CLG-1	523 ± 33	1276	0.75	0.48	0.13	0.27	0.39
CLG-2	249 ± 8	851	0.45	0.44	0.20	0.01	0.51
CMV-1	305 ± 22	850	0.52	0.38	0.22	0.14	0.46
CMV-2	476 ± 47	950	0.71	0.41	0.15	0.29	0.50
DST-1	697 ± 75	1158	0.76	0.44	0.16	0.32	0.43
DST-2	322 ± 23	933	0.46	0.38	0.09	0.08	0.36
JCB-1	1108 ± 20	1487	1.09	0.53	0.18	0.56	0.30
MWV-1	989 ± 76	1757	1.19	0.67	0.15	0.52	0.27
MWV-2	1732 ± 93	2142	1.52	0.76	0.16	0.76	0.10
NRT-1	674 ± 64	1212	0.89	0.47	0.21	0.42	0.57
NRT-2	480 ± 4	1183	0.53	0.45	0.24	0.08	0.45
NRT-3	468 ± 46	1141	0.65	0.43	0.20	0.22	0.49

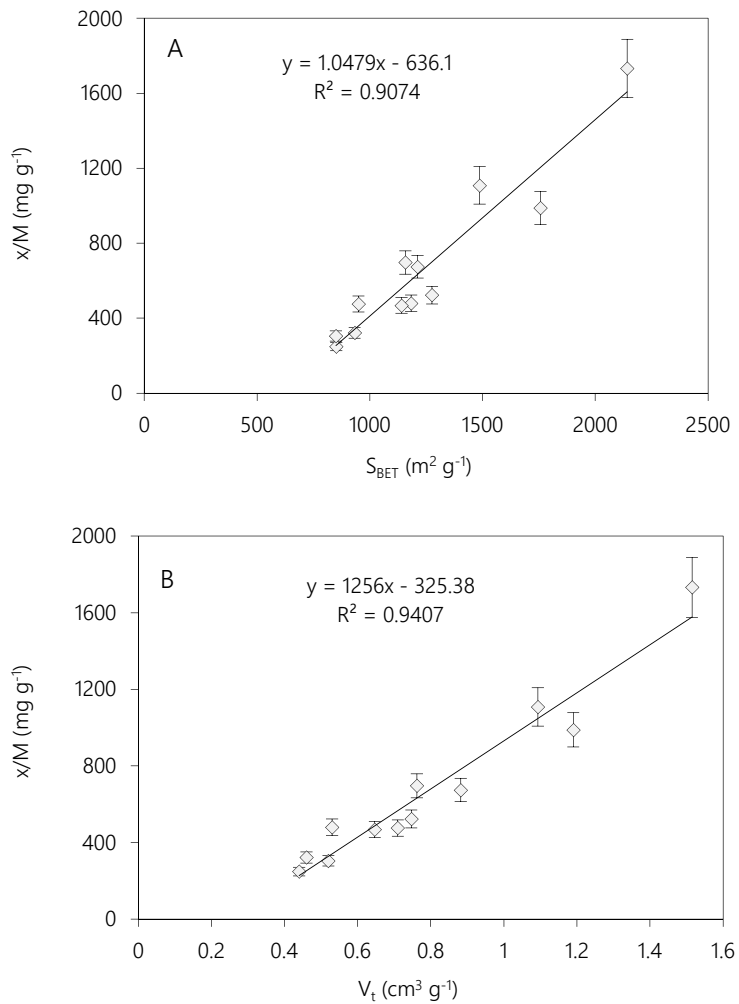
### 4.3.2 Influence of the AC textural properties on D4 adsorption

Table 4.1 shows selected textural parameters obtained from the N<sub>2</sub> and CO<sub>2</sub> isotherms of the ACs, including BET surface area ( $S_{\text{BET}}$ ) ( $\text{m}^2 \text{g}^{-1}$ ), total pore volume ( $V_t$ ) ( $\text{cm}^3 \text{g}^{-1}$ ), total micropore volume ( $V_{\text{DR}_{\text{N}_2}}$ ) ( $\text{cm}^3 \text{g}^{-1}$ ), narrow micropore volume ( $V_{\text{DR}_{\text{CO}_2}}$ ) ( $\text{cm}^3 \text{g}^{-1}$ ), and mesopore volume ( $V_{\text{meso}}$ ) ( $\text{cm}^3 \text{g}^{-1}$ ). Figure 4.2 shows the correlation of these textural parameters with the D4 adsorption capacities of the ACs obtained in experiments carried out at 1000 ppm v/v of D4 in dry nitrogen.

Generally speaking, there is a good correlation between all textural parameters of the ACs and the D4 adsorption capacities, except the  $V_{\text{DR}_{\text{CO}_2}}$ .  $S_{\text{BET}}$  is a good parameter for estimating the D4 adsorption capacity of ACs (Figure 4.2-A), as reported before (Matsui and Imamura, 2010; Oshita *et al.*, 2010; Yu *et al.*, 2013). However, the best data regression is obtained with the  $V_t$  values, i.e., there is a direct relationship between the total pore volume of the ACs and their D4 x/M values (Figure 4.2-B). A more detailed analysis reveals that mesopore volumes are more related with D4 adsorption capacities than micropores (Figure 4.2 C-E). Oshita *et al.* (2010), suggested that D4 should be more likely adsorbed onto mesopores, whose diameter is larger than 2 nm. Surprisingly, though, there is an acceptable correlation between the adsorption capacities of the ACs and their  $V_{\text{DR}_{\text{N}_2}}$  values, which account for the total micropore volume (Figure 4.2-D). Narrow micropore (<0.7 nm) volumes do not correlate at all with the ACs capacities, which was somehow expected taking into account that the D4 molecular cross-sectional size is 1.08 x 1.03 nm (Hamelink *et al.*, 1996). In other words, only large micropores on ACs are expected to be relevant for D4 adsorption and a direct relationship between  $V_{\text{DR}_{\text{N}_2}}$  and x/M values (as that observed in Figure 4.2-D) could be anticipated as far as large micropores are the main contributors to the total micropore volume, which is the case for the tested ACs (Table 4.1).

Nevertheless, the relevance of mesoporosity on the adsorption of D4 on ACs is exemplified with the results obtained for the more adsorbing carbons JCB-1, MWV-1 and MWV-2, which are also the ACs with the higher mesopore volumes. The beneficial role of mesopores should not be limited to the possibility of allocating quantities of D4 but also to favor the diffusion of D4 into the (large) micropore network.

The height of the mass transfer zone ( $H_{MTZ}$ ) indicates the rate of adsorbate removal by the adsorbent.  $H_{MTZ}$  was determined (Table 4.1) following a previous description (Fairén-Jiménez *et al.*, 2007). A lower  $H_{MTZ}$  reflects a faster adsorption rate. Activated carbons with the highest  $S_{BET}$  and  $V_t$  present the fastest adsorption rate as these parameters can be linearly correlated with the  $H_{MTZ}$ . Correlations are depicted in Figure 4.3. MWV-2 presented the lowest  $H_{MTZ}$  and it increases for carbons with lower pore volume and  $S_{BET}$ , which means that the adsorption rate decreases in the same sense.



**Figure 4.2** (Continued)

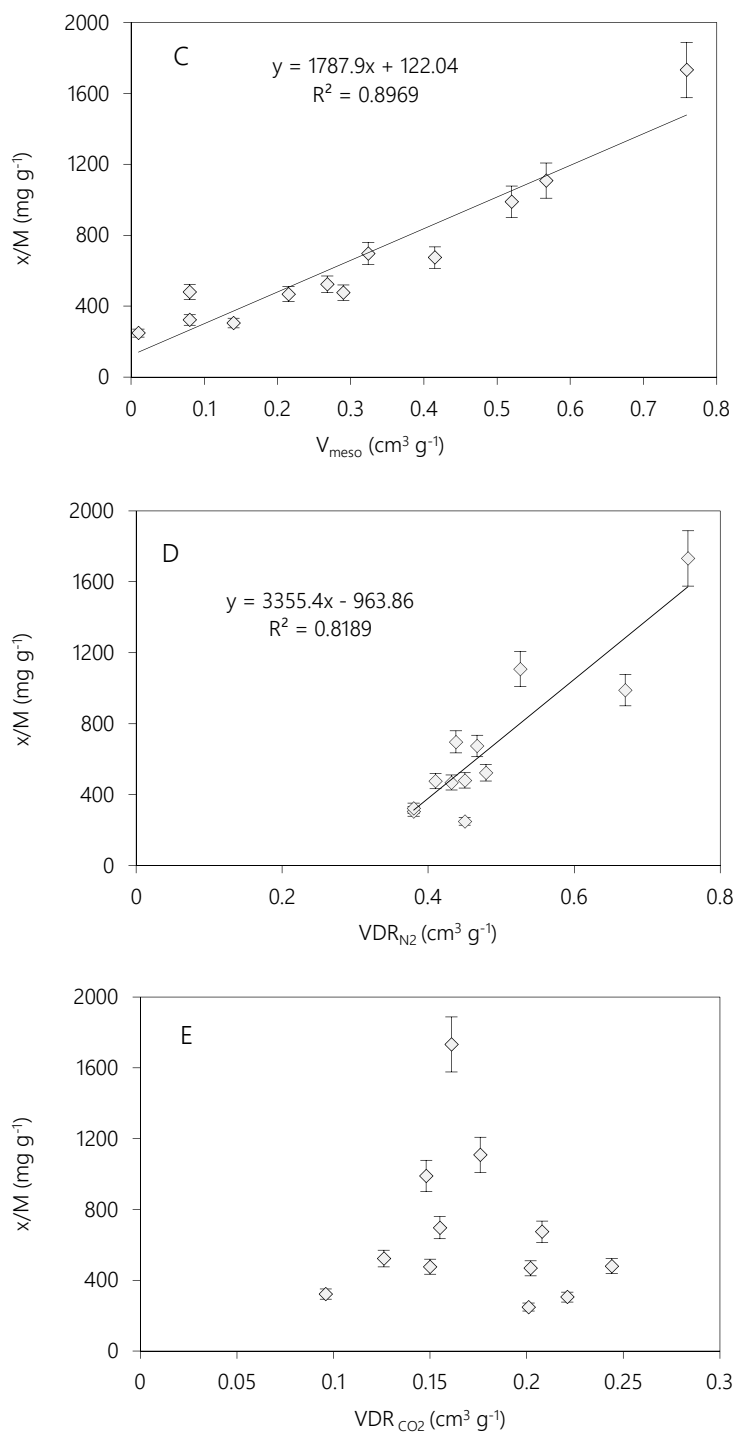


**Figure 4.2** Correlation between D4 adsorption capacity ( $x/M$ ) of the tested AC vs A)  $S_{\text{BET}}$  surface area; B) Total pore volume; C) Mesopore volume; D) Total micropore volume; E) Narrow micropore volume.

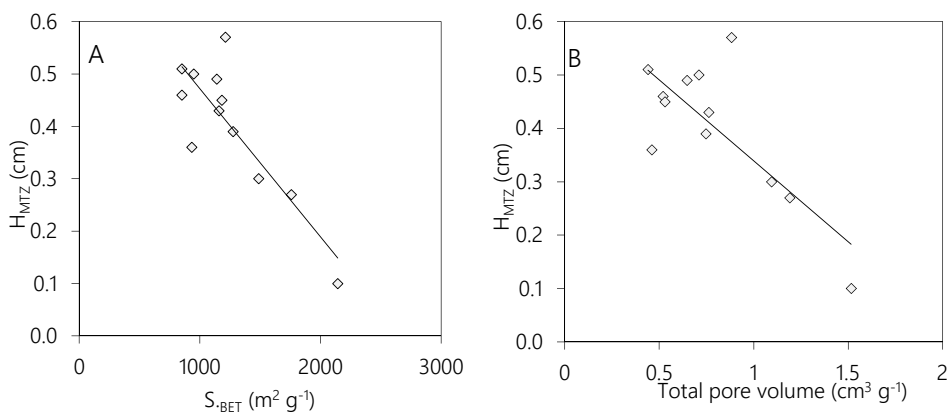


**Figure 4.3** Correlation between A)  $S_{BET}$  and B) Total pore volume and the  $H_{MTZ}$ .

Fresh and D4-saturated samples of MWV-2 were analysed by SEM/EDX. A silicon increase was revealed in the EDX spectra, while SEM analysis of saturated MWV-2 (Table 4.2, Figure 11.13, 11.14) does not show any visual evidence of D4 deposits or agglomerates on the external surface, even working with such a high concentration of D4 (1000 ppm v/v). Considering that the apparent density of D4 in liquid phase is  $0.956 \text{ g cm}^{-3}$ , the volume of D4 adsorbed on each carbon ( $x/M$ ) is closely related to its total pore volume (as measured by  $N_2$  adsorption) in most cases, confirming again that one of the main factors determining the D4 adsorption capacity is the AC textural development.

**Table 4.2**

EDX elemental composition of the AC samples analyzed by SEM.

Element	Carbon [wt%]	Oxygen [wt%]	Silicon [wt%]
MWV-2	85.58	10.18	1.15
D4-MWV-2	74.87	11.01	13.02

#### 4.3.3 Influence of the AC surface chemistry on D4 adsorption

The influence of the surface chemistry on the adsorption of hydrogen sulphide and other biogas impurities on ACs is well-known (Seredych and Bandosz, 2008; Boulinguez and Le Cloirec, 2010). Nevertheless, there is a lack of studies about the influence of the AC surface chemistry on the adsorption of siloxanes. Oxygen functional groups are the most common moieties that may influence the adsorption of different adsorbates on ACs (Moreno-

Castilla, 2004; Yu *et al.*, 2007; Vega *et al.*, 2013). Surface oxygen complexes affect the electronic density of the carbon layers. This might affect the dispersive interactions between the carbon surfaces and the adsorbate molecules. For instance, carboxyl groups fixed at the carbon surface have the ability to withdraw electrons, whereas phenolic groups release electrons. The Si-O-Si group in siloxanes could act as electron donor and possible hydrogen bonds could be formed between this group and hydroxyl moieties on the carbon surface.

In order to assess the chemistry of the outermost layers, the ACs under this study were analyzed by XPS and the O (1s) and C (1s) spectra were obtained (Figure 11.15, 11.16). The O/C ratio of the outermost carbon layers are shown in Table 4.3. MWV-2 and CLG-2 are the ACs with the highest percentage of oxygen while CMV-2 and CLG-1 have the lowest. Results pointed out that there is no evident relation between D4 adsorption capacity and the O/C ratio in the outermost layers (Figure 4.4). The O (1s) and C (1s) spectra were deconvoluted according to the experimental procedure mentioned above in order to quantify the contribution of each functional group (Table 4.3). No relation could be found between the relative abundance of any group and the adsorption capacity.

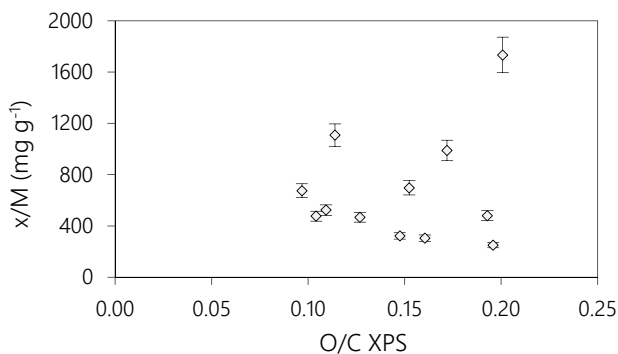


**Figure 4.4** Relation between O/C ratio obtained by XPS and the D4 adsorption capacity of the ACs studied.

TPD analyses were carried out in order to quantify the total oxygen functional groups present in the ACs (Figure 11.17, 11.18). From the oxygen content obtained by TPD and the carbon content determined by elemental analysis, the O/C ratio of each carbon was calculated (Table 4.4). In this case, MWV-1 and MWV-2 are the carbons with the highest O/C ratio, while CLG-1 and NRT-3 are the ACs showing the lowest. No apparent relation was found between D4 adsorption capacity and the individual contribution of TPD results

(Figure 4.5), i.e., the quantity of oxygen functional groups present in the ACs is not related with the D4 adsorption capacity. Therefore, from the XPS and TPD data of this study, modifications on activated carbon for the incorporation of any specific oxygen functional group would not be relevant for enhancing the adsorption of D4 on ACs. Textural properties (i.e., total pore volumes) are determinant in the AC adsorption capacity for siloxanes.

**Table 4.3**

Results of  $\text{pH}_{\text{slurry}}$  and XPS analysis of the ACs considered.

AC	$\text{pH}_{\text{slurry}}$	XPS (%)				XPS O/C
		C=O	COH COC	COOCO	COOH	
CLG-1	7.75	17.0	17.6	20.6	26.1	0.109
CLG-2	4.10	34.3	27.3	16.9	11.9	0.196
CMV-1	7.10	31.1	24.6	14.3	14.5	0.160
CMV-2	7.10	25.3	28.2	19.9	14.8	0.104
DST-1	8.53	18.6	35.0	18.1	19.8	0.152
DST-2	8.24	23.7	24.1	16.3	24.8	0.148
JCB-1	7.44	40.1	23.5	13.1	7.1	0.114
MWV-1	7.33	17.1	32.2	6.5	37.7	0.172
MWV-2	4.75	29.8	8.2	28.6	8.6	0.201
NRT-1	8.81	26.8	19.5	18.1	23.1	0.097
NRT-2	8.10	20.3	39.3	9.2	23.4	0.193
NRT-3	8.10	18.2	19.6	12.5	45.5	0.127

**Table 4.4**

Results of the TPD analysis of the ACs considered.

AC	TPD ( $\mu\text{mol g}^{-1}$ )						TPD O/C
	Carboxylic	Lactone	Anhydride	Phenolic	Carbonyl	Ether	
CLG-1	44.4	9.0	77.8	163.9	148.5	118.9	0.0133
CLG-2	140.1	27.3	201.1	1016.0	350.8	115.2	0.0466
CMV-1	109.4	19.8	243.9	831.4	362.7	98.1	0.0447
CMV-2	59.4	17.5	70.1	147.5	432.3	118.6	0.0203
DST-1	51.9	26.2	73.7	138.6	457.5	15.7	0.0183
DST-2	61.1	26.0	64.5	296.1	543.8	10.3	0.0256
JCB-1	73.8	16.3	244.2	234.3	319.7	24.6	0.0249
MWV-1	208.3	33.1	192.5	1386.5	443.5	374.8	0.0688
MWV-2	180.0	15.9	242.6	1866.1	221.9	117.8	0.0752
NRT-1	84.4	18.3	100.7	215.8	882.1	188.2	0.0352
NRT-2	120.0	16.7	129.9	536.5	671.8	18.1	0.0340
NRT-3	62.4	2.1	76.8	165.9	147.3	39.5	0.0136

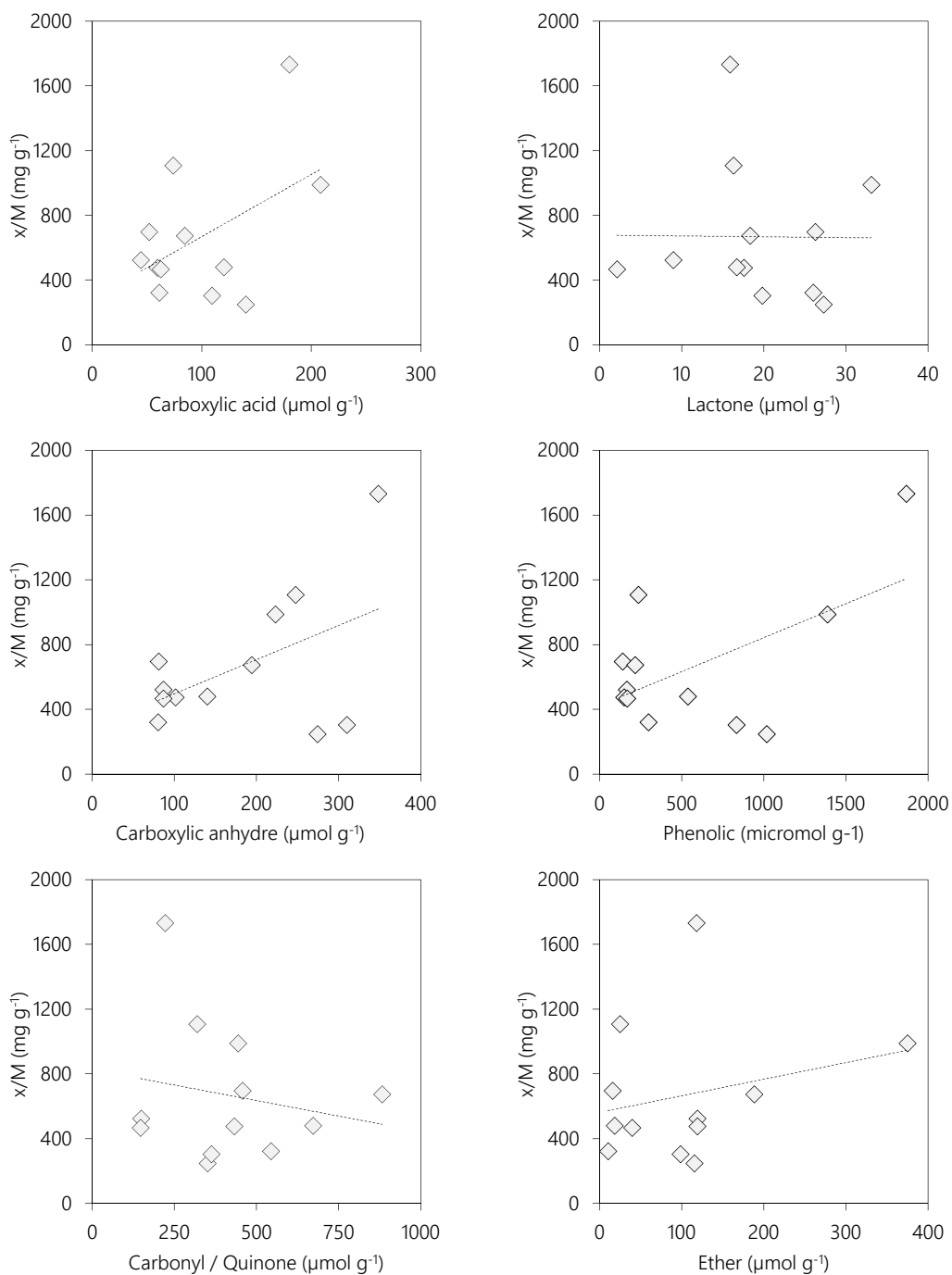


**Figure 4.5** Concentrations of A) Carboxylic acid, B) Lactone, C) Carboxylic anhydride, D) Phenolic, E) Carbonyl / Quinone and F) Ether groups obtained by TPD related with adsorption capacity of each AC.

#### 4.3.4 Polymerization of the adsorbed D4 on ACs

It has been previously reported (Finocchio *et al.*, 2009; Montanari *et al.*, 2010) that hexamethylcyclotrisiloxane (D3) polymerizes to larger siloxane molecules during the AC adsorption process. Due to the formation of these high molecular weight polymers, thermal regeneration of ACs is ineffective. The FT-IR spectra of fresh MVW-2, MVW-2 spent during the D4 dynamic adsorption tests already discussed and liquid D4 were compared in order to detect the presence of polymerization (Figure 4.6). A double band at  $1100\text{ cm}^{-1}$  can be observed for the D4-saturated MVW-2, which indicates the existence of siloxane polymers formed as a result of the D4 ring-opening and further polymerization (Finocchio *et al.*, 2009).

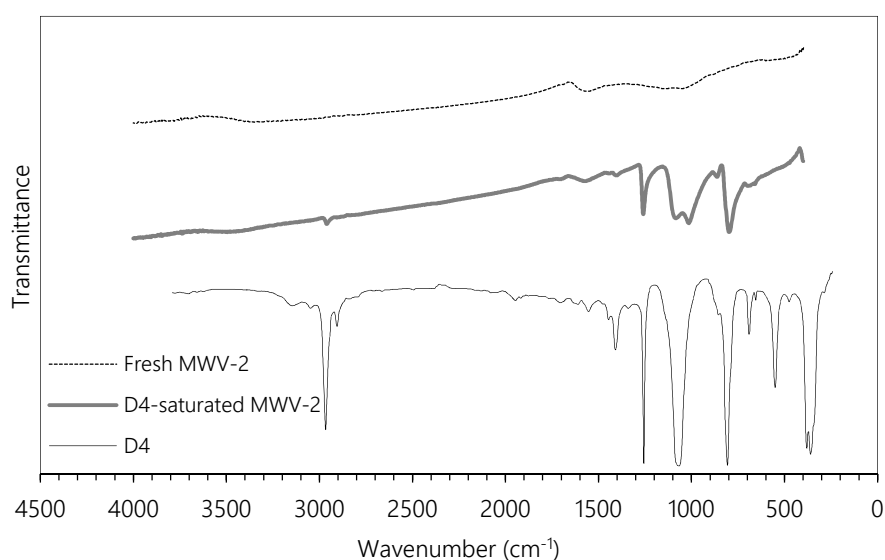


**Figure 4.6** FT-IR spectra of fresh and D4-saturated MVW-2 compared to the spectrum of pure D4 in liquid phase.

In order to study this phenomenon, compounds adsorbed in exhausted MVW-2 were extracted with hexane as explained in the experimental section. By GC analysis of the extracts, mainly D5 but also other larger cyclic siloxanes like D6 and tetradecamethylcycloheptasiloxane (D7) were detected in addition to D4. The polymerization ratio was defined and calculated as the fraction of D5, D6 and D7 extracted polymers over the amount of extracted D4 (Equation 4),

$$PR = \frac{[D5] + [D6] + [D7]}{[D4]} \times 100 \quad (\text{Eq. 4})$$

where [D4], [D5], [D6] and [D7] correspond to the concentration of each compound as measured by GC analysis of the extracted samples. Table 4.5 shows the contribution of each compound on the long-term PR.

The evolution of the polymerization ratio with time has been also considered. Accordingly, two different extracts were analyzed after different contact times of D4 on the ACs surface. An extract was thus obtained just after the dynamic adsorption tests, and the corresponding relative concentration of polymeric species (equation 4) is called "short term polymerization ratio". On the other hand, spent ACs were kept under refrigeration and dark conditions for 30 days before extraction. The corresponding ratio is called "long term polymerization ratio". Results of both polymerization ratios for the studied ACs are shown in Figure 4.7. The first conclusion that can be drawn from results of Figure 4.7 is that there is no evidence of a direct relationship between the amount of D4 adsorbed (i.e., x/M values, Table 4.1) and either the short or long term polymerization ratios. Accordingly, textural properties of the ACs have little effect on the D4 polymerization.

**Table 4.5**

Contribution of D5, D6 and D7 on the long-term polymerization of each AC.

AC	D5 (%)	D6 (%)	D7 (%)
CLG-1	83.6	13.1	3.3
CLG-2	53.1	39.2	7.8
CMV-1	73.7	19.9	6.4
CMV-2	75.2	18.7	6.1
DST-1	72.1	21.9	5.9
DST-2	85.6	10.5	3.9
JCB-1	75.8	18.2	6.0
MWV-1	69.3	23.5	7.2
MWV-2	70.7	23.0	6.3
NRT-1	81.9	13.1	5.0
NRT-2	73.9	18.7	7.4
NRT-3	82.0	14.9	3.1

On the short term, only the wood-based carbons activated by H<sub>3</sub>PO<sub>4</sub>, MWV-1 and MWV-2 present a significant percentage of polymerization (17% and 47% respectively, Figure

4.7). On the other hand, long term polymerization takes place in all the studied samples, which indicates that this phenomenon is clearly time-dependent. Long term polymerization ratios are very different from one AC to another, with values ranging from 15% for DST-1 to 79% for MWV-1.

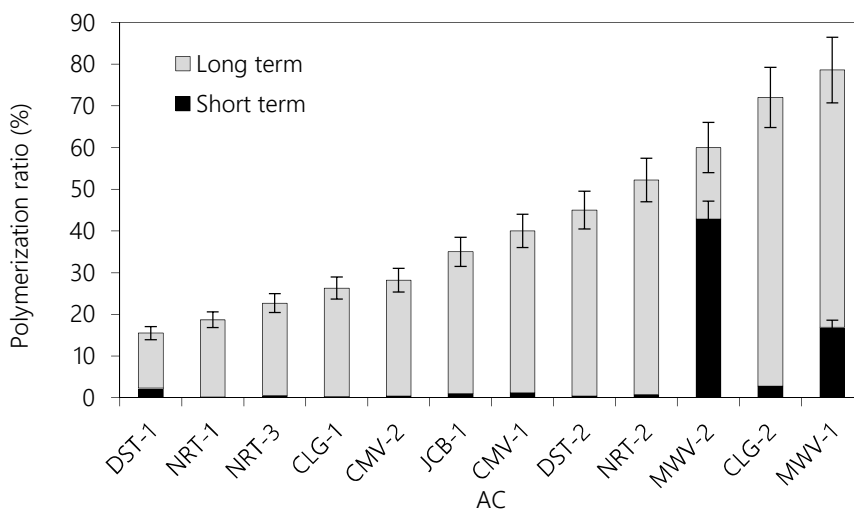
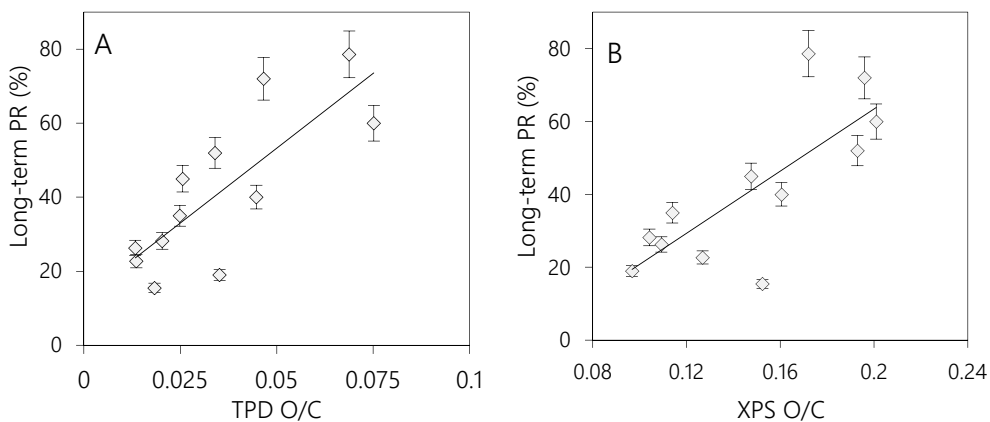


**Figure 4.7.** Short and long term polymerization ratio of D4 adsorbed on ACs.

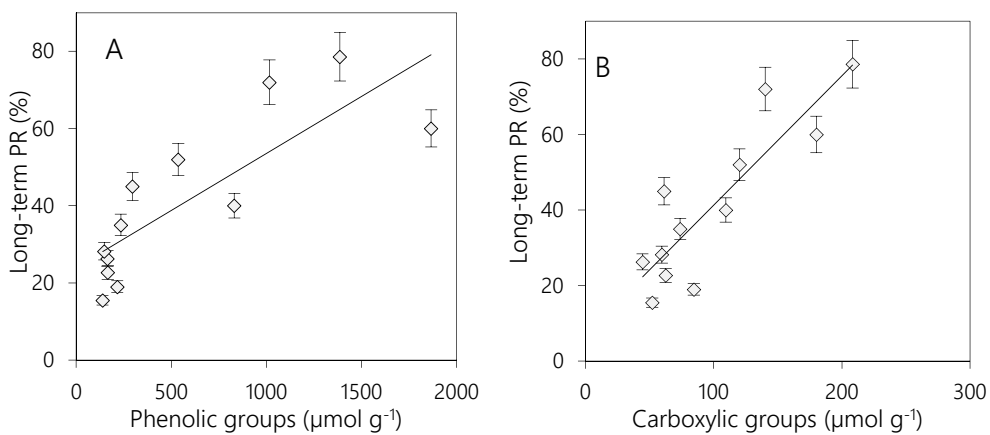
Figure 4.8 and and Figure 4.9 show an outstanding outcome of this Chapter. The polymerization of the adsorbed D4 seems related to the oxygen content of the carbons. Specifically, long term polymerization ratios are higher for ACs having relatively high concentration of surface oxygen, and there is a good correlation between the O/C ratio obtained both by the XPS and, especially the TPD analyses (4.14). Furthermore, the long-term polymerization ratio was also compared to the relative amount of each specific functional group as calculated from the TPD measurements (see Table 4.4). As shown in Figure 4.9, the content of phenolic and carboxylic groups correlates with the polymerization ratio.

Although a detailed mechanistic study is beyond the scope of the present work, these proton donating groups present on the carbon surfaces are proposed here to act as catalytic active centers for cyclosiloxane ring-opening polymerization and further propagation reactions (Figure 4.10) (Jiang *et al.*, 2010; Yashiro *et al.*, 2010). It is also worth to notice that there exists little correlation between the long term polymerization values

and the overall acidity of the ACs (Figure 4.10), as measured by their  $\text{pH}_{\text{slurry}}$  values (Table 4.3), thus stressing the amphoteric character of carbon surfaces.



**Figure 4.8** Correlation between chemical surface properties A) O/C ratio obtained by XPS ratio, B) O/C ratio obtained by TPD



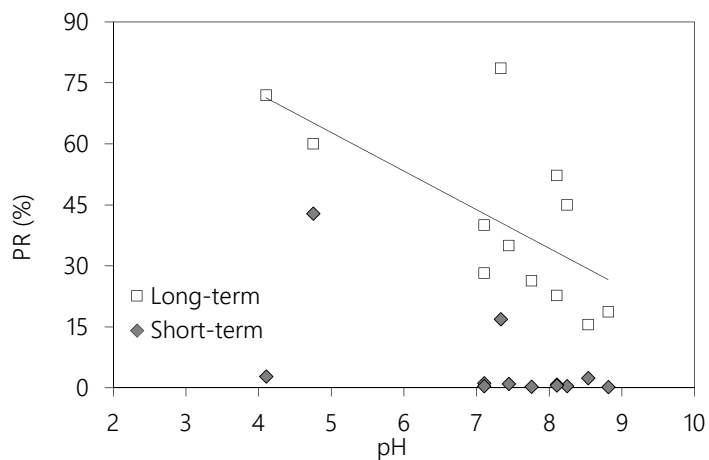


Figure 4.10 Influence of the  $\text{pH}_{\text{slurry}}$  of the AC in the short and long term polymerization ratio.

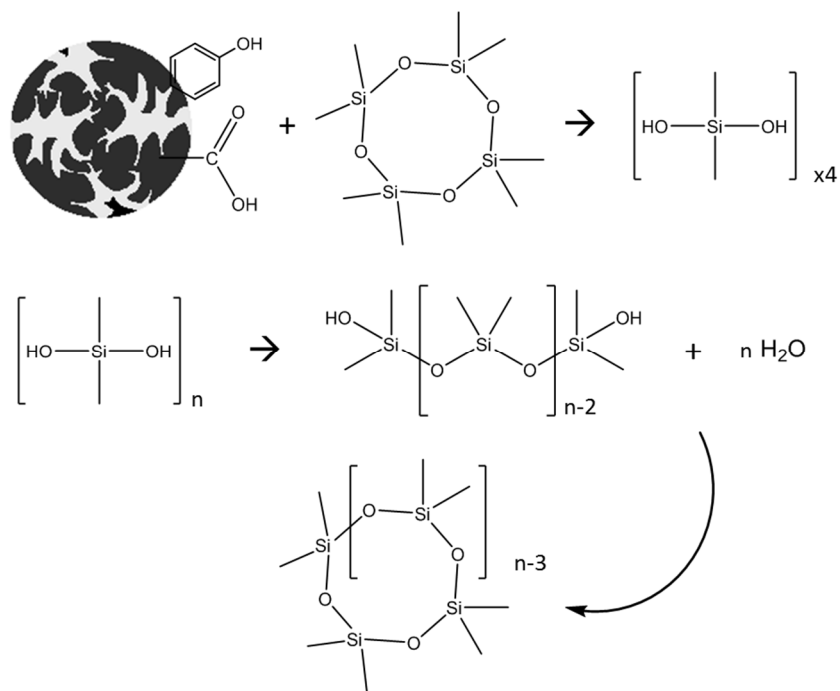


Figure 4.11. Proposed mechanism for the polymerization of cyclosiloxanes adsorbed on carbon surfaces.

## 4.4 Final remarks

---

The findings of this Chapter confirm that the main parameter determining the D4 adsorption capacity is the total pore volume of the ACs. Knowing the total pore volume of an AC, its performance on the siloxane removal could be predicted since the regression between these parameters is high. On one hand, the high porosity development obtained in the wood based ACs by the  $H_3PO_4$  activation enhances the siloxane adsorption capacity.

On the other hand, these wood based ACs have the highest concentration of oxygen functional groups, especially phenolic and carboxylic groups which play a key role in promoting the siloxane polymerization reactions on the carbon surface. Polymerization is an undesired phenomenon since it may hamper the thermal regeneration of the saturated ACs. High pore volumes and low oxygen content based ACs, specifically low carboxylic and phenolic groups' contents, are recommended for siloxane removal, in order to attain high removal capacities and to facilitate the thermal regeneration of the adsorbent, respectively.

---

# Chapter 5

## RESULTS II

### Regeneration of D4-exhausted AC by AOPs

Redrafted from:  
Regeneration of siloxane-exhausted activated carbon by advanced oxidation processes,  
Alba Cabrera-Codony, Rafael Gonzalez-Olmos, Maria J. Martin  
Journal of Hazardous Materials, 285 (2015) 501-508



## 5.1 Overview

---

In the context of the biogas upgrading, siloxane exhausted ACs need to be regenerated in order to avoid them becoming a residue. In this Chapter, two commercial activate carbons which were proved to be efficient in the removal of D4 from biogas, have been regenerated through AOPs using both  $O_3$  and  $H_2O_2$ . AOP-driven regeneration consists on the generation of reactive radicals in aqueous solution, mainly  $\cdot OH$  radicals, which are able to oxidize the organic compounds adsorbed or present in solution.  $H_2O_2$  and  $O_3$  are the most used substances to generate  $\cdot OH$  in water. Although the AOPs for the wastewater treatment are prominent industrial technologies and a fertile field for research (Coelho *et al.*, 2006), the sequential application of adsorption/oxidation has received less scholarly attention (Mourand *et al.*, 1995; Liu *et al.*, 2007; Anfruns *et al.*, 2013). The overall treatment objective of the sequential adsorption/oxidation process is to transform the contaminants immobilized and concentrated in the adsorbent into byproducts with low affinity for the adsorbent, thus re-establishing its adsorptive capacity.

In the case of AC, contaminants are transformed on or near its surface by reaction with  $\cdot OH$  radicals. The catalytic production of  $\cdot OH$  radicals from  $H_2O_2$  can be achieved by the AC surface itself (Anfruns *et al.* (2013), or by adding Fe salts, known as Fenton reagent (Mantzavinos *et al.*, 2009; Georgi *et al.*, 2010), and it is reported to be significantly enhanced if Fe-amended ACs are used (Toledo *et al.*, 2003; Huling *et al.*, 2005; Gonzalez-Olmos *et al.*, 2013). The use of  $O_3$  has also been studied for the regeneration of AC exhausted with organic compounds in wastewater treatment plants (Huling *et al.*, 2007; Huling and Hwang, 2010; Hwang *et al.*, 2010). In the case of siloxanes, a partial oxidation may lead to the generation of silanols which is desirable due to their high water solubility. Therefore, the AOP-driven regeneration of siloxane-exhausted ACs proposed in this Chapter involves the sequential and synergistic use of two reliable and well-established treatment technologies in a two-step process: dynamic siloxane adsorption onto AC, and regeneration using AOPs. After the treatment with  $O_3$ , the activated carbon recovered up to 40% of the original adsorption capacity while by the oxidation with  $H_2O_2$  the regeneration efficiency achieved was up to 45%. In order to enhance the  $H_2O_2$  oxidation, activated carbon was amended with iron. In this case, the regeneration efficiency increased up to 92%.

## 5.2 Methodology

---

Two commercial ACs were tested: Organosorb (*Desotec*, Belgium) and Nuchar (*MeadWestVaco*, United States). Their performance on the D4 removal, as well as the textural and chemical characterization have been previously reported in Chapter 4, and are summarized in Table 5.1. Organosorb is a steam-activated carbon obtained from lignite, which has a high concentration of ashes. Meanwhile, Nuchar is a wood-based carbon, chemically activated, which presents a high  $S_{\text{BET}}$  surface area and pore volume. Due to the greater porosity development of Nuchar, it has higher adsorption capacity ( $x/M$ ) than Organosorb. Nuchar also presents a higher content of oxygen functional groups (higher O/C ratios) than Organosorb, as it is corroborated by the more acidic  $\text{pH}_{\text{slurry}}$  of Nuchar than Organosorb. As reported in the previous Chapter, these chemical properties lead to a higher polymerization ratio, meaning that D4 polymerizes forming higher molecular weight siloxanes in contact with the carbon.

Wet regeneration tests with  $\text{H}_2\text{O}_2$  and  $\text{O}_3$  were carried out following the experimental procedures described in section 3.4.1 and 3.4.2 with both activated carbon. Nuchar was also amendment with iron as described in section 3.2.1.4. The  $\text{H}_2\text{O}_2$  decomposition was analyzed (see section 3.4.1.1) and the iron leaching determined (see section 3.4.1.3).

**Table 5.1**  
Physico-chemical properties of the AC tested in this work.

AC	Nuchar	Organosorb
Origin	Wood	Lignite
Activation	$\text{H}_3\text{PO}_4$	Steam
$S_{\text{BET}}$ ( $\text{m}^2 \text{g}^{-1}$ )	2142	1158
Pore volume ( $\text{cm}^3 \text{g}^{-1}$ )	1.52	0.76
D4 $x/M$ ( $\text{mg g}^{-1}$ )	1732	697
O/C $_{\text{XPS}}$	0.201	0.152
O/C $_{\text{TPD}}$	0.075	0.018
Polymerization ratio (%)	60.0	15.5
Ashes (%)	3.5	14.0
$\text{pH}_{\text{slurry}}$	4.75	8.53

## 5.3 Results and Discussion

### 5.3.1 Regeneration of D4-exhausted AC by O<sub>3</sub>

The use of O<sub>3</sub> and AC has been investigated as an effective process to remove toxic and/or low biodegradable compounds (Rivera-Utrilla *et al.*, 2013). The catalytic ozonation process not only takes advantage of the high adsorption capacity of AC and the high oxidant power of the O<sub>3</sub>, but AC may also transform the O<sub>3</sub> into secondary oxidants, such as hydroxyl radicals, which can degrade and mineralize faster the adsorbed organic compounds (Faria *et al.*, 2005; Sánchez-Polo *et al.*, 2008; Alvarez *et al.*, 2009).

Both D4-exhausted Nuchar and Organosorb were treated with aqueous O<sub>3</sub> solutions for different reaction times, between 5 and 60 minutes. The results of these tests, presented in Figure 5.1, show that the regeneration efficiencies obtained for Nuchar were between 20% and 27% while those for Organosorb were between 31% and 40%. When the treatment is applied longer than 5 minutes, the results obtained hardly improved in both cases. In all the O<sub>3</sub> treatments, the performance of Organosorb is higher than Nuchar.

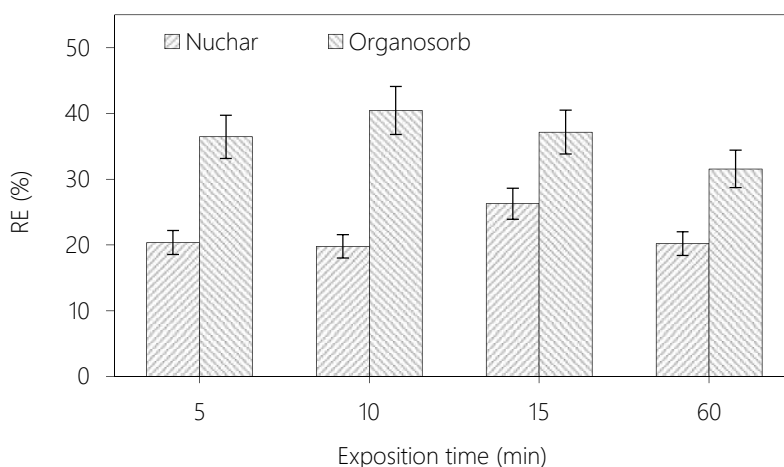


**Figure 5.1** Nuchar and Organosorb regeneration efficiency (RE) obtained with the O<sub>3</sub> treatment at different exposition times. Experiments were conducted with 0.250 g of AC, in 500 ml solution, O<sub>3</sub> flow of 70 mg min<sup>-1</sup>, room temperature, and free pH.

As investigated by (Valdés and Zaror, 2006a; Valdés and Zaror, 2006b), the aqueous O<sub>3</sub> decomposition in the presence of AC is governed by the presence of oxygenated surface groups and mineral matter among other parameters. As seen in Table 5.1, Organosorb presents a higher content of ashes, which may lead to a higher production of radicals, increasing slightly the regeneration efficiency (RE).

Obtained RE values reveal that the process was not completely successful in recovering the adsorption capacity of the AC, which may be attributed to the: (i) Failure of ozonation to oxidize the adsorbed D4 in the AC, (ii) deposition of insoluble by-products from D4 oxidation, such as SiO<sub>2</sub>, plugging up the pores and/or (iii) surface modification and destruction of adsorptive sites leading to the drop of the adsorption capacity.

Further investigation with the IR spectra of fresh, D4-exhausted and regenerated Nuchar (Figure 5.2) shed more light on the efficiency of the regeneration process with O<sub>3</sub>. The spectrum of D4-exhausted Nuchar (Figure 5.2-6) presents the characteristic peaks of the D4 (Figure 5.2-7). The widening and splitting of the Si-O-Si band at 1100 cm<sup>-1</sup> reflects the presence of cyclic siloxanes higher than D5, formed due to ring opening polymerization (see Chapter 4). After the O<sub>3</sub> regeneration (Figure 5.2-2), the IR spectrum does not reveal the characteristic band corresponding to amorphous silica at 1000-1200 cm<sup>-1</sup> (Figure 5.2-8), meaning that the deposition of insoluble compounds is unlikely. Moreover, the low intensity of the characteristic siloxane bands after regeneration confirms the ability of O<sub>3</sub> to oxidize the adsorbed compounds.

In spite of this, both the intensity of the IR bands (Figure 5.2-4) and the RE obtained (Figure 5.1) clearly indicate that the adsorption capacity of the pristine sample was far from being restored. Thus, induced changes in the AC surface properties are likely to cause the decrease of the adsorption capacity. Although no further tests were deemed necessary due to the low efficiency of the O<sub>3</sub> treatment for siloxane, there are enough evidences that substantiate this assessment.

It is well known that the exposure of activated carbon to O<sub>3</sub> or other oxidative treatments such as HNO<sub>3</sub> or H<sub>2</sub>O<sub>2</sub> modifies the chemical composition of the carbon surface: basic sites are transformed into acid sites because of oxidation, and new acid sites are generated, because of the addition of O<sub>3</sub> to the double bond of the carbon structure (Valdés and Zaror, 2006b). In addition, the BET surface area and micropore volumes are

reduced, due to pore widening (micropore destruction) and/or micropore obstruction due to the formation of surface oxygen groups at the entrance of the pores (Jaramillo *et al.*, 2009; Vega *et al.*, 2013).

With RB3 (commercial AC supplied by Norit), the D4-adsorption capacity was tested for both the pristine and the HNO<sub>3</sub>-oxidized carbon, resulting in 480 and 295 mg g<sup>-1</sup> respectively. Thus, the oxidation of activated carbon negatively affects the performance for D4 adsorption, decreasing the adsorption capacity by 40%.

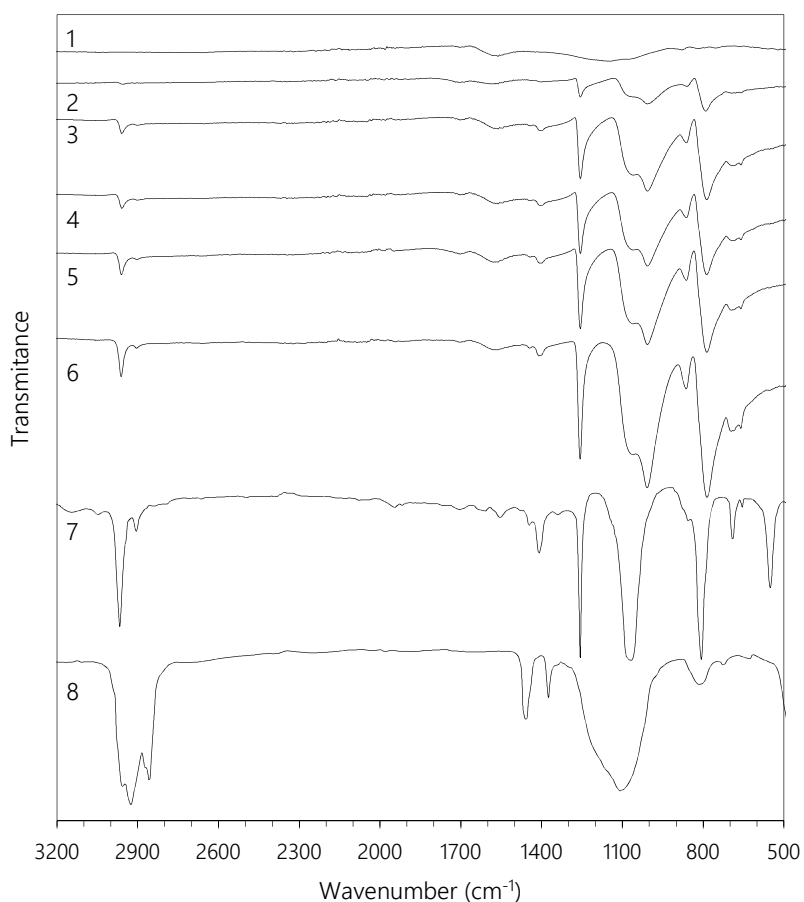


**Figure 5.2** IR spectra of NuChar 1) Fresh, 2) after O<sub>3</sub> regeneration (15 minutes), 3) after H<sub>2</sub>O<sub>2</sub> regeneration (1% w/v), 4) D4-exhausted after O<sub>3</sub> regeneration, 5) D4-exhausted after H<sub>2</sub>O<sub>2</sub> regeneration, 6) D4-exhausted first cycle, and spectrum of 7) D4 and 8) SiO<sub>2</sub>.

### 5.3.2 Regeneration of D4-exhausted AC by H<sub>2</sub>O<sub>2</sub>

It is well known that AC catalyzes the decomposition of H<sub>2</sub>O<sub>2</sub> to generate oxidant species (Anfruns *et al.*, 2014). Although the reaction mechanism is not completely established, some recent results have shown that AC is active in the degradation of some dissolved organic pollutants in the presence of H<sub>2</sub>O<sub>2</sub>, providing some evidences that AC can promote the H<sub>2</sub>O<sub>2</sub> decomposition through the formation of hydroxyl radicals (OH) (Serp and Figueiredo, 2008; Rey *et al.*, 2011). These free radical species have been postulated as intermediates in the reaction mechanism (Georgi and Kopinke, 2005), whose formation would take place through an electron-transfer with AC and AC<sup>+</sup> as the reduced and oxidized catalyst states (Domínguez *et al.*, 2013). In addition to AC surface itself, the presence of metals also influences the kinetics of H<sub>2</sub>O<sub>2</sub> decomposition with carbon materials (Rey *et al.* 2008).

H<sub>2</sub>O<sub>2</sub> decomposition kinetics was studied for both Nuchar and Organosorb. Figure 5.3-A shows the H<sub>2</sub>O<sub>2</sub> decomposition vs. time catalyzed by both fresh ACs. It can be observed that the behavior of the ACs is completely the opposite. While Organosorb had decomposed all the H<sub>2</sub>O<sub>2</sub> after two hours, after the same time Nuchar had only decomposed up to 20%. These results are in agreement with the findings of (Ribeiro *et al.*, 2013) who concluded that carbons with low oxygen content promote better decomposition of H<sub>2</sub>O<sub>2</sub>. As reported in Table 5.1, Organosorb presents a lower concentration of oxygen-containing functionalities which gives it a markedly basic character and enhances the yield of the OH formation (Ribeiro *et al.*, 2013). Moreover, Organosorb presents a higher content of ashes (i.e., higher content of metals) which also promote the H<sub>2</sub>O<sub>2</sub> decomposition.

Figure 5.4 shows the RE obtained for both ACs at different H<sub>2</sub>O<sub>2</sub> concentrations. The best RE obtained for Organosorb was 45% when the treatment with the 0.3% w/v solution was applied. Beyond this value, higher doses of H<sub>2</sub>O<sub>2</sub> did not show a better upshot on RE in any of the cases. Meanwhile, the best RE obtained for Nuchar was 38%, achieved with the 1% w/v solution.

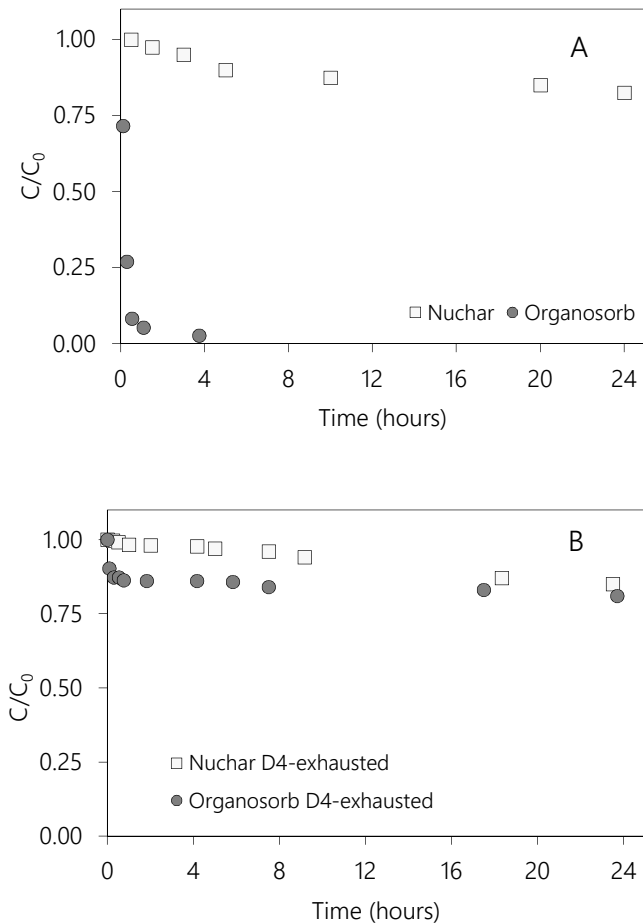


**Figure 5.3** H<sub>2</sub>O<sub>2</sub> decomposition of A) fresh and B) D4-exhausted Nuchar and Organosorb. Experiments were conducted with C<sub>AC</sub> = 2.5 g l<sup>-1</sup>, C<sub>H<sub>2</sub>O<sub>2</sub></sub> = 1% w/v, room temperature, free pH.

Although the RE of Nuchar and Organosorb were expected to be different due to their different properties and H<sub>2</sub>O<sub>2</sub> decomposition kinetics, similar RE were obtained. In order to explain this outcome, H<sub>2</sub>O<sub>2</sub> decomposition kinetics of the exhausted carbons were studied. As shown in Figure 5.3-A, Organosorb H<sub>2</sub>O<sub>2</sub> decomposition rate is fast when the carbon is fresh, but once it is D4-exhausted, the decomposition rate decreases (Figure 5.3-B). As pointed by (Zazo *et al.*, 2006) and (Bach and Semiat, 2011), the H<sub>2</sub>O<sub>2</sub> decomposition decreases with the presence of adsorbed compounds. Thus, the adsorbed D4 blocks the catalytic surface of Organosorb affecting the catalytic activity of the AC toward the H<sub>2</sub>O<sub>2</sub> decomposition rate. Accordingly, the residual H<sub>2</sub>O<sub>2</sub> concentration was

also determined at the end of all the oxidation tests and it was similar for both AC, being higher than 80% in all cases. Thus, when the ACs are D4-exhausted, the efficiency of the H<sub>2</sub>O<sub>2</sub> regeneration is similar in spite of the different textural and chemical properties of the ACs.

After the oxidation process, the liquid phase was analyzed through GC-MS. In spite of the partial regeneration achieved, dimethylsilanediol (C<sub>2</sub>H<sub>8</sub>O<sub>2</sub>Si) was detected by the GC-MS analysis as a by-product of the D4 oxidation (Figure 5.5). The presence of this by-product proves the partial oxidation of the D4 to more soluble compounds, which were transferred from the carbon surface to the liquid phase regenerating partially the AC.

Furthermore, as seen in the IR spectra in Figure 5.2-3, H<sub>2</sub>O<sub>2</sub> is less efficient oxidizing the preadsorbed siloxane than O<sub>3</sub> (Figure 5.2-2). Thus, although the effect of any AC surface modification brought about by the regeneration process cannot be ruled out (Anfruns *et al.*, 2013), the remaining adsorbed D4 seems to play an important role in the overall performance.

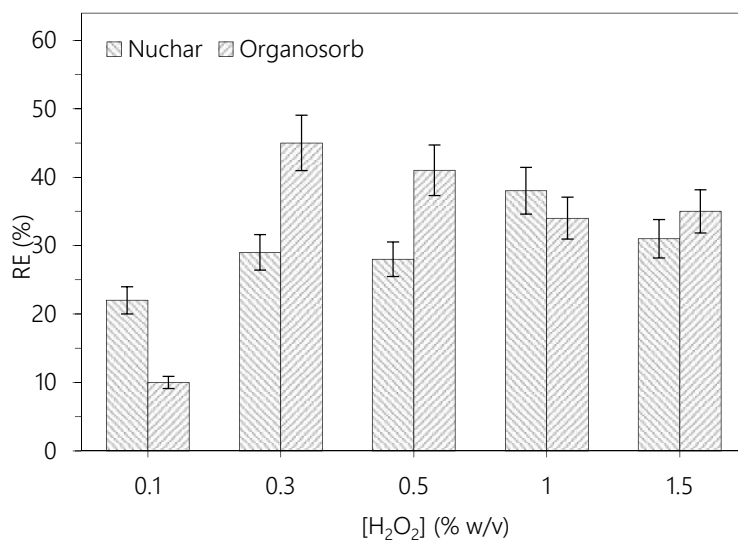


**Figure 5.4** Nuchar and Organosorb regeneration efficiency (RE) obtained with different H<sub>2</sub>O<sub>2</sub> concentrations. Experiments were conducted with C<sub>AC</sub> = 2.5 g l<sup>-1</sup>, for 24 h of reaction time, room temperature, free pH.

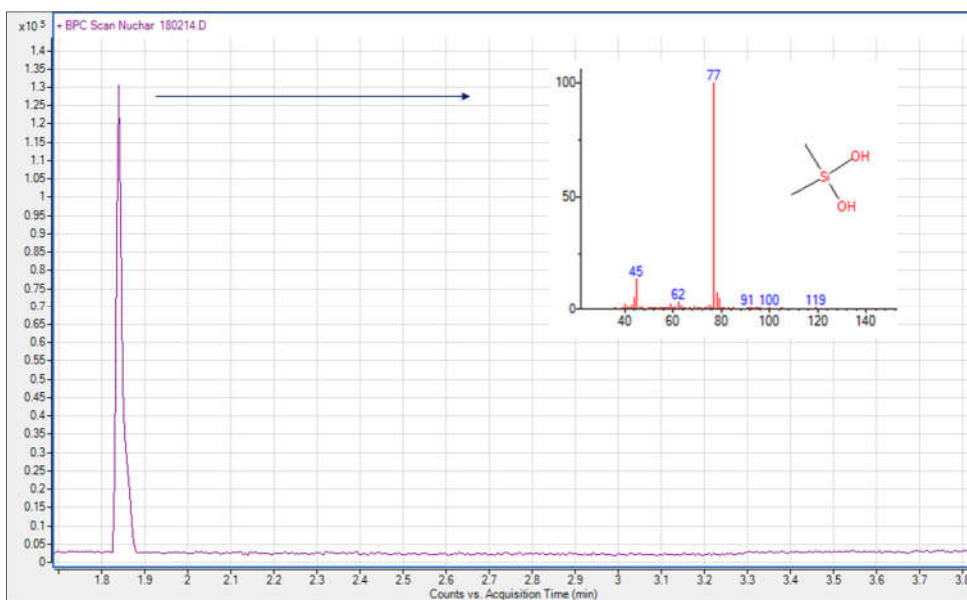


**Figure 5.5** Chromatogram obtained by GC-MS analysis of the liquid phase of the H<sub>2</sub>O<sub>2</sub> (1% w/v) oxidation of D4-exhausted Nuchar. According to NIST library, the peak had 97.9% of similarity to dimethyl silanediol.

### 5.3.3 Regeneration of Fe-AC with H<sub>2</sub>O<sub>2</sub>

Aiming at increasing the regeneration rates achieved with H<sub>2</sub>O<sub>2</sub>, iron deposition on the AC was tested. It is well known that iron has a high catalytic activity for the production of radicals from H<sub>2</sub>O<sub>2</sub>. Fenton-driven regeneration of spent AC involves the combination of H<sub>2</sub>O<sub>2</sub> with Fe-species. In this case, H<sub>2</sub>O<sub>2</sub> reacts with the ferrous irons (Fe<sup>2+</sup>) deposited on the AC or in solution increasing the production of hydroxyl radicals. Organic compounds immobilized in the AC are transformed on or near the AC surface by the reaction with ·OH and other reactive species generated during the reaction between H<sub>2</sub>O<sub>2</sub> and Fe (Toledo *et al.* 2003).

Nuchar, the AC which showed the highest D4 adsorption capacity of those reported in Chapter 4, was selected to prepare Fe-modified AC in order to promote its regeneration with H<sub>2</sub>O<sub>2</sub>. Different concentrations of iron solutions were used in order to determine the maximum iron uptake. The iron fixation achieved with different iron solutions is presented in Table 5.2, where the fraction retained is calculated as the percentage of the initial

aqueous iron that is incorporated into the carbon. As seen in Table 5.2, a maximum incorporation of 11.5 mg Fe g<sup>-1</sup> was achieved, nevertheless, for aqueous iron concentrations higher than 3 mg Fe l<sup>-1</sup> the achieved Fe-fixation was not remarkably higher.

**Table 5.2**

Iron concentration in each sample of Nuchar ([Fe]<sub>AC</sub>) depending on the iron concentration of the solution ([Fe]<sub>aq</sub>) of ferrous sulfate applied and Fe fraction retained in the AC.

[Fe] <sub>aq</sub> (mg l <sup>-1</sup> )	[Fe] <sub>AC</sub> (mg g <sup>-1</sup> )	Fe Fraction retained (%)
4.0	11.5 ± 0.14	57 ± 1
3.0	11.4 ± 0.14	76 ± 1
2.0	10.3 ± 0.26	100 ± 1
1.0	2.2 ± 0.01	45 ± 2
0.4	0.2 ± 0.04	11 ± 1

H<sub>2</sub>O<sub>2</sub> decomposition tests with the different Fe-amended Nuchar were done in order to evaluate the effect of the iron concentration in the carbon. Experiments were carried out at free pH, which was between 5.0 and 5.8. Figure 5.6 shows how H<sub>2</sub>O<sub>2</sub> decomposition increases with the iron content in the AC, what clearly proves that the iron promotes the H<sub>2</sub>O<sub>2</sub> decomposition. After 24 hours, the experiment with the AC with the highest Fe content (11.5 mg Fe g<sup>-1</sup>) had decomposed 75% of the initial H<sub>2</sub>O<sub>2</sub>. This carbon was selected for further experiments and it was named Fe-Nuchar. In this case, the decomposition kinetics of the D4-exhausted Fe-Nuchar was also studied in order to see if the adsorbed D4 was also blocking the catalytic effect of the iron incorporated on the AC. As seen in Figure 5.6, the H<sub>2</sub>O<sub>2</sub> decomposition decays with the presence of D4, but it is still higher than the original Nuchar. Nonetheless, it is important to highlight that iron deposition on the AC causes a decrease on its surface area and pore volume (Huling *et al.*, 2005). Since D4 adsorption is mainly governed by the porous structures (see Chapter 4), a reduction on the adsorption capacity of the Fe-Nuchar was observed from 1732 mg g<sup>-1</sup> to 1136 mg g<sup>-1</sup>.

Regeneration of D4-exhausted Fe-Nuchar with H<sub>2</sub>O<sub>2</sub> was carried out at different H<sub>2</sub>O<sub>2</sub> concentrations, 0.5% w/v, 1% w/v and 1.5% w/v. Results, presented in Figure 5.7, show that high efficiencies were obtained, ranging from 51.8 to 92.1% depending on the H<sub>2</sub>O<sub>2</sub> concentration. Thus, the enhancement of the H<sub>2</sub>O<sub>2</sub> decomposition promoted by the iron

incorporation seems to be effective for the D4 oxidation, leading to the higher RE of the Fe-Nuchar compared to the  $\text{H}_2\text{O}_2$  regeneration of Nuchar.

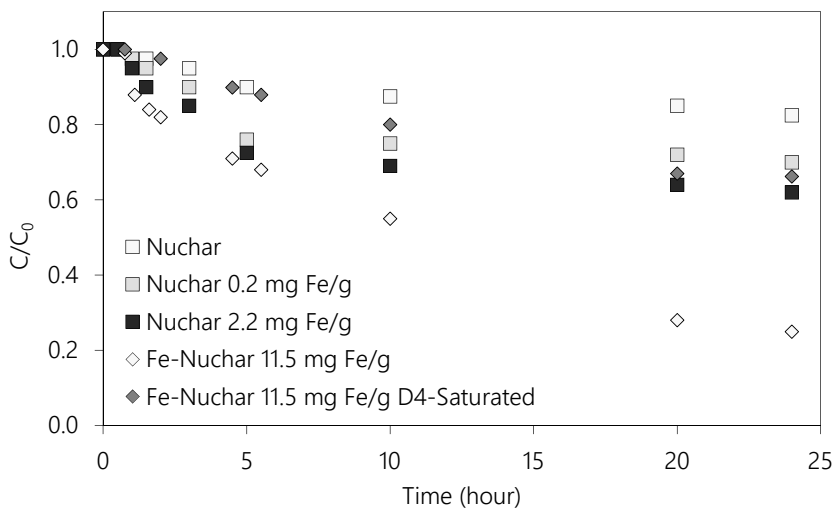


**Figure 5.6**  $\text{H}_2\text{O}_2$  decomposition for fresh Nuchar, fresh Fe-amended Nuchar with different iron content, and fresh and D4-exhausted Fe-Nuchar. Experiments were conducted with  $C_{AC} = 2.5 \text{ g l}^{-1}$ ,  $C_{\text{H}_2\text{O}_2} = 1\% \text{ w/v}$ , room temperature, free pH.

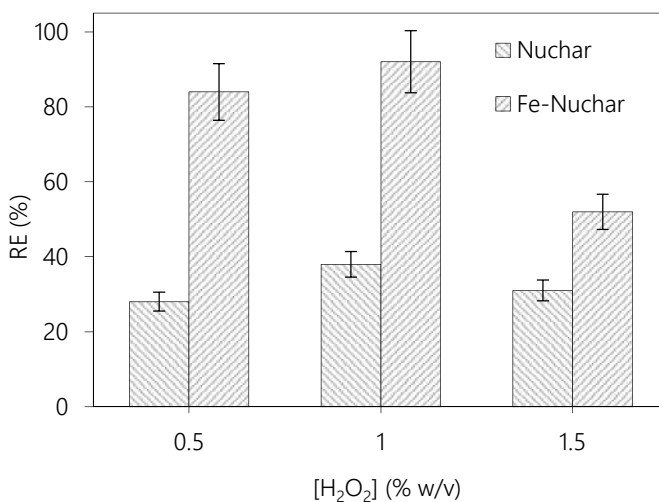


**Figure 5.7** Nuchar and Fe-Nuchar regeneration efficiency (RE) obtained with different  $\text{H}_2\text{O}_2$  concentrations. Experiments were conducted with  $C_{AC} = 2.5 \text{ g l}^{-1}$ , for 24 hours of reaction time, room temperature, free pH.

In the tests with 1% w/v of H<sub>2</sub>O<sub>2</sub> an almost complete regeneration was obtained, achieving 92.1% of recovery. The treatment with lower H<sub>2</sub>O<sub>2</sub> concentration, 0.5% w/v, led to a lower RE of 84.2%, nevertheless, at higher H<sub>2</sub>O<sub>2</sub> concentrations, 1.5% w/v, the efficiency of the process reduced up to 52.3%. On one hand, quenching reactions may be responsible for this decrease in the efficiency, since H<sub>2</sub>O<sub>2</sub> is a potential scavenger of ·OH. Thus, high concentrations of H<sub>2</sub>O<sub>2</sub> favor the reaction between ·OH and H<sub>2</sub>O<sub>2</sub> at expense of the oxidation efficiency (Hwang *et al.*, 2010). On the other hand, at higher H<sub>2</sub>O<sub>2</sub> concentration, the complete oxidation of D4 may take place, leading to the formation of insoluble by-products, such as silica (SiO<sub>2</sub>), which may be deposited onto the AC blocking the adsorption sites.

In order to assess the yield of the iron incorporation on the D4 oxidation, the IR spectra of Fe-Nuchar before and after the H<sub>2</sub>O<sub>2</sub> regeneration are shown in Figure 5.8. The transmittance of the D4 peaks on the Fe-Nuchar spectrum after the oxidation treatment (Figure 5.8-2) decays considerably comparing it to the spectrum of the D4-exhausted Fe-Nuchar (Figure 8-4). After the second run (Figure 5.8-3) it increases reaching similar transmittance values to the first run, as the adsorption capacity was restored (RE = 92.1%).

In order to evaluate the performance of the sequential adsorption/oxidation in successive cycles, two more regeneration stages were applied using 1% w/v of H<sub>2</sub>O<sub>2</sub>. Results, in Table 5.3, show how in the second and third cycle the RE decays progressively, until 77.2% and 46.3% respectively. It should be noted that, in spite of the decrease, regeneration efficiency obtained in the third cycle is still higher than the obtained with Nuchar without the iron incorporation in the first. After four uses, Fe-Nuchar maintains an adsorption capacity of 526 mg g<sup>-1</sup>, which is within the range of most activated carbons tested in Chapter 4.

Iron leaching was studied after each regeneration cycle (Table 5.3) because it may have a significant effect in the sequential decrease of the performance. In the first regeneration cycle the iron leaching was 12.4%, 5.9% in the second and 1.5% in the third, which constitutes an important loss. This progressive loss of iron decreases the decomposition of H<sub>2</sub>O<sub>2</sub> into ·OH radicals, leading to an important decrease in the performance of the regeneration. In fact, the incorporation of iron reduces the amount of the remaining adsorbed siloxane (Figure 5.8-2) as compared with the IR spectra of the H<sub>2</sub>O<sub>2</sub>-

regenerated Nuchar (Figure 5.2-3). In successive cycles, with the progressive loss of iron, the remaining D4 may be increasingly being accumulated in the pores, declining the performance of Fe-Nuchar.

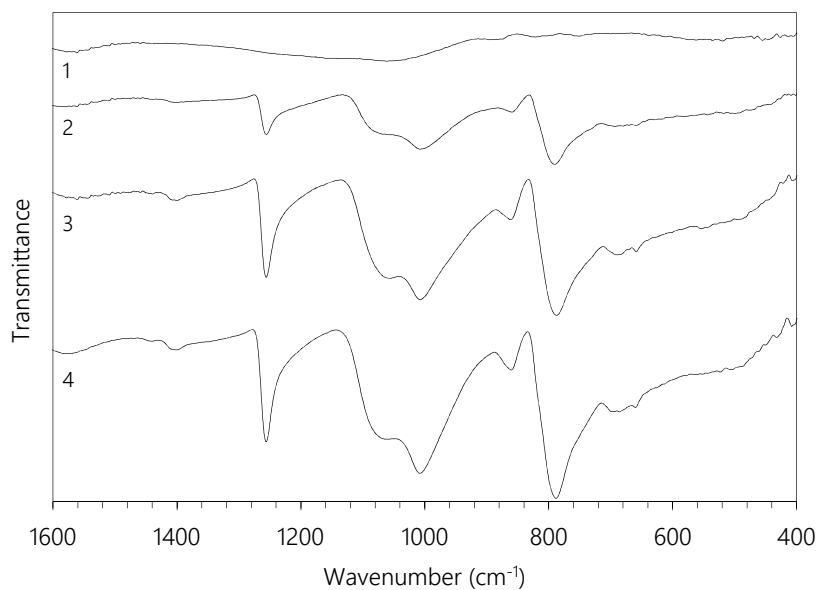


**Figure 5.8** FT-IR spectra of 1) Fresh Fe-Nuchar, 2) Fe-Nuchar after  $H_2O_2$  oxidation treatment ( $C_{H_2O_2} = 10 \text{ g l}^{-1}$ ), 3) D4-exhausted Fe-Nuchar after  $H_2O_2$  oxidation treatment ( $C_{H_2O_2} = 10 \text{ g l}^{-1}$ ), and 4) D4-exhausted Fe-Nuchar after first use.

**Table 5.3**

Regeneration efficiency (RE) and Fe leached determined after each regeneration cycle of Fe-Nuchar ( $C_{H_2O_2}=1\% \text{ w/v}$ ).

	1 <sup>st</sup> cycle	2 <sup>nd</sup> cycle	3 <sup>rd</sup> cycle
RE (%)	$92.1 \pm 7.3$	$77.2 \pm 15.2$	$46.3 \pm 10.1$
Fe leached (%)	$12.4 \pm 1.2$	$5.9 \pm 0.4$	$1.5 \pm 0.2$

## 5.4 Final remarks

---

The research performed in this study concludes that the chemical regeneration of D4-exhausted AC by advanced oxidation processes can be achieved with Fe-amended AC. Without the iron incorporation,  $O_3$  has a limited efficiency, recovering 31-40% of the adsorption capacity due to the  $O_3$ -induced modifications of the textural and chemical properties of the AC. Concerning the regeneration with  $H_2O_2$ , slightly higher efficiencies were obtained, restoring 40-45% of the original D4 adsorption capacity. The different textural and chemical properties of the AC did not show differences on the RE either by  $O_3$  or  $H_2O_2$ .

The iron deposition on the AC increased the overall performance of the adsorption/oxidation process using  $H_2O_2$  since an almost complete recovery of the D4 adsorption capacity could be achieved after the first regeneration step. The catalytic activity of the iron plausibly promoted the  $\cdot OH$  formation and a higher ratio of D4 oxidation, so that, the regeneration efficiency was up to 92.1%. Two more regeneration steps were applied to the same carbon, so it was used for four times with high adsorption capacities. In these successive cycles, the iron leaching from the carbon, the induced changes in the carbon material itself and/or the increasing accumulation of non-reacted D4 contributed to the decrease in the regeneration performance. Therefore, future research should be focused on the improvement of the iron fixation or on alternative adsorbent materials, more resistant to  $O_3$  oxidation than AC.

---

# Chapter 6

## RESULTS III

### Zeolites as recyclable adsorbents/catalysts for D4 removal

Redrafted from:  
Zeolites as recyclable adsorbents/catalysts for biogas purification: removal of octamethylcyclotetrasiloxane  
Alba Cabrera-Codony, Anett Georgi, Rafael Gonzalez-Olmos, Héctor Valdés María J. Martín

*Submitted for publication*



## 6.1 Overview

---

Natural and synthetic zeolites with different properties (pore structure,  $\text{SiO}_2/\text{Al}_2\text{O}_3$  ratio, acidity and Fe-loading) were evaluated as adsorbents/catalysts for siloxane removal in biogas purification. Zeolites can be used as dual functional catalysts. Firstly, siloxanes can be adsorbed (and transformed) in their porous structure and secondly, zeolites can promote AOP reactions, without being vulnerable to oxidation. Thus, zeolites have the potential to be long-lived reusable catalysts (Gonzalez-Olmos *et al.*, 2013; Shahbazi *et al.*, 2014). In addition, iron can be easily introduced into the structure of zeolites due to their ion-exchange capacity and the resulting Fe-containing zeolites showed high catalytic activities in the Fenton-like oxidation of organic compounds with hydrogen peroxide with minimal iron leaching (Gonzalez-Olmos *et al.*, 2009; Gonzalez-Olmos *et al.*, 2011).

In this Chapter, a sequential siloxane uptake/wet oxidation process is applied in order to transform immobilized and concentrated siloxanes on zeolite surfaces into water-soluble products with low affinity toward zeolite, thus re-establishing its adsorption capacity. The use of this type of treatment has been applied for the regeneration of siloxane-exhausted ACs in adsorption/oxidation cyclic processes in Chapter 5. It was concluded that, although AC is an optimal adsorbent due to its high textural development, the use of AOPs was not completely successful in the recovery of AC adsorption capacity toward siloxane. Adsorbed siloxane could be oxidized to soluble by-products by heterogeneous Fenton processes, as well as by ozonation, without silica ( $\text{SiO}_2$ ) deposition in the pores. Nevertheless, AC itself remains too prone to oxidation and cannot be reused at long term because of porosity loss (Alvarez *et al.*, 2009; Vega *et al.*, 2013).

Therefore, the first objective of this Chapter was to select the most effective zeolite for siloxane catalytic removal from the gas phase. Subsequently, selected zeolites were evaluated as catalyst for the oxidation of the adsorbed/transformed siloxane, whereby regeneration by a heterogeneous Fenton-like reaction or by ozone in aqueous suspension was carried out. Zeolites with acid properties promote the catalytic formation of smaller  $\alpha$ - $\omega$ -silanediols and their uptake into the channel system. BEA zeolites resulted to be the best zeolite for D4 removal due to both, high content of Lewis and Brønsted sites and channel size, which is large enough to accommodate the formed silanediols. In a dynamic

adsorption test with a D4 inflow gas concentration of  $3000 \text{ mg m}^{-3}$ , D4 uptake on the best performing BEA zeolite was 14 wt% before breakthrough was observed.

Wet oxidation processes were used for the regeneration of the spent zeolites, including ozonation and Fenton-like treatment. Both treatments were optimized to recover almost completely the D4 uptake of the iron-exchanged Fe-BEA in the first use. Thus, its feasibility to be reused was evaluated in successive adsorption/oxidation cycles, recovering up to 80% in at least three subsequent steps. However, in further cycles the accumulation of D4 and/or by-products led to a successive decline in the catalytic activity of the zeolites, hampering not only the capacity to transform D4 into lineal silanediols, thus reducing the adsorption capacity, but also the catalytic activity towards promoting Fenton-like reactions during regeneration.

## 6.2 Methodology

---

Six synthetic zeolites and one natural zeolite (Clinoptilolite) were studied for D4 removal. Their properties are summarized in Table 3.2. Fe-BEA, Fe-MFI, DAY and USY were obtained as pellets, BEA-38 and BEA-300 in powder form and the natural Clinoptilolite as a sand. Pellet and sand form zeolites were grinded and sieved in order to obtain a particle fraction in the range of  $212 - 425 \mu\text{m}$ . In order to determine the humidity content of the zeolites, 250 mg samples were dried by means of infrared moisture analyzer (Sartorius MA150) operated in a heating rate of  $20 \text{ }^\circ\text{C min}^{-1}$  until  $105 \text{ }^\circ\text{C}$ . The Brønsted and Lewis acidic sites of the zeolites were determined by the procedures detailed in section 3.2.8.

The D4 adsorption capacity of all the zeolites considered was tested at  $3000 \text{ mg m}^{-3}$  concentration dynamic adsorption tests following the experimental set up described in section 3.3.1. The siloxane adsorbed in the exhausted zeolites was extracted following the methodology described in section 3.3.3 using anhydrous THF as dissolvent.

Regeneration experiments were carried out with the best performing zeolite, including  $\text{H}_2\text{O}_2$  in Fenton-like reactions (section 3.4.1) and ozone (section 3.4.2).

## 6.3 Results and Discussion

### 6.3.1 D4 uptake by zeolites

All zeolites considered in this work (see Table 3.2) were tested for their D4 removal performances. Dynamic adsorption breakthrough curves are shown in Figure 6.1. Adsorption tests were carried out using a high inlet concentration of D4 ( $3000 \text{ mg D4 m}^{-3}$ ), in order to reach the breakthrough in one day experiments and reach high D4 loading, which represents severe exhaustion conditions used for testing the effectiveness of regeneration. Under such experimental conditions, zeolite D4 equilibrium uptake ranged from  $11.2$  to  $143 \text{ mg g}^{-1}$  (see Table 6.1). BEA type zeolites showed the highest D4 removal. Their breakthrough times ( $c(t)/c_0=0.05$ ) were around up to  $40 \text{ min}$ , with adsorption capacities similar to some activated carbons that have been tested under the same experimental conditions (Matsui and Imamura, 2010). The least effective zeolite was the natural Clinoptilolite, which presented the lowest BET surface area and hardly adsorbed D4, with a breakthrough time below  $5 \text{ min}$ .

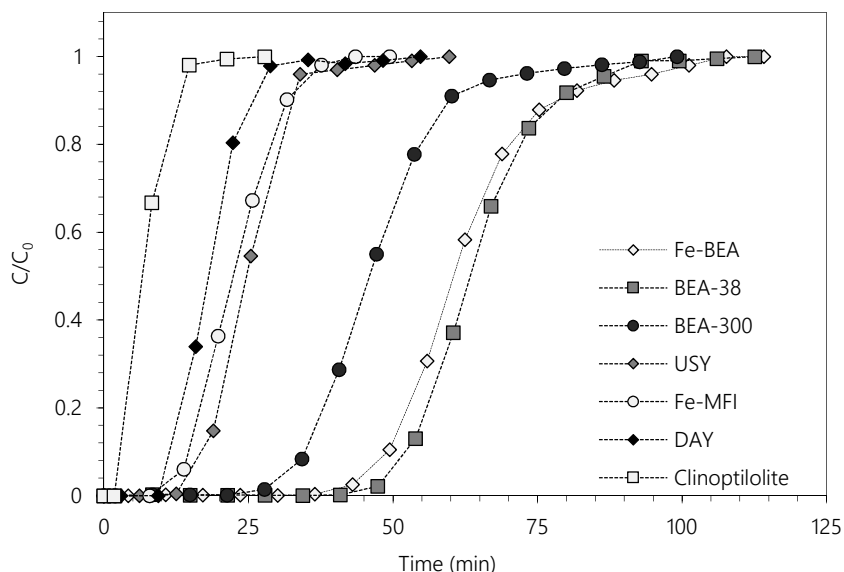


**Figure 6.1** Dynamic adsorption breakthrough curves obtained for all tested zeolites in this study. Experimental conditions:  $250 \text{ mg}$  of zeolite,  $200 \text{ mL min}^{-1}$  of dry  $\text{N}_2$  containing  $3000 \text{ mg D4 m}^{-3}$ .

**Table 6.1**

Physico-chemical properties of the tested zeolites and D4 uptake

Zeolite	$S_{\text{BET}}$ ( $\text{m}^2 \text{g}^{-1}$ )	D4 uptake* ( $\text{mg g}^{-1}$ )	Total BAS ( $\text{mmol g}^{-1}$ )	Total LAS ( $\text{mmol g}^{-1}$ )	Humidity (wt%)
Fe-BEA	600	143	0.75	2.23	8.0
BEA-38	710	135	0.48	3.07	9.5
BEA-300	620	104	0.12	4.04	9.5
Fe-MFI	370	30.6	0.80	1.63	5.0
USY	900	36.2	0.51	2.27	3.8
DAY	910	27.8	0.17	2.42	3.0
Clinoptilolite	36	11.2	n.d.	n.d.	4.5

n.d. not determined

\*tested in dynamic adsorption tests, inflow concentration of D4:  $3000 \text{ mg m}^{-3}$ .

In the case of activated carbons, textural development is claimed as the main parameter determining the adsorption capacity toward D4, as proved in Chapter 4. Nevertheless, in the case of zeolites, adsorption capacities clearly do not depend solely on their specific surface area of the samples (Figure 6.2). It was found that BEA type zeolites performed the best for D4 removal. It has to be highlighted that the zeolites used in this work differ markedly in their channel structure. MFI has two types of channels formed by 10 T-atoms ( $T = \text{Si}$  or  $\text{Al}$ ) with minor and major axis dimensions of  $5.1 \times 5.5 \text{ \AA}$  and  $5.4 \times 5.6 \text{ \AA}$  for the sinusoidal and straight channels, respectively (C.M. Baerlocher, 2007). HEU has 10- and 8-ring channels, whereby the 10-ring channels have an ellipsoid cross-section with approximate dimensions of  $7.5 \times 3.1 \text{ \AA}$  (variable due to considerable flexibility of framework) (C.M. Baerlocher, 2007). BEA and FAU belong to the zeolites with the largest pore dimensions, since they have 12-ring channels with dimensions of  $6.5 \times 5.6$  and  $7.5 \times 5.7 \text{ \AA}$  for the two channel types of BEA and  $7.4 \times 7.4 \text{ \AA}$  in case of FAU zeolites (C.M. Baerlocher, 2007). In addition, FAU zeolite has the so called supercages at the channel crossings that can accommodate a sphere with  $11.24 \text{ \AA}$  diameter. However, the access of a molecule to these larger cages is limited by the ability to pass through the narrow channel system. Taking into account that the molecular cross-sectional size of the D4 is  $10.8 \times 10.3 \text{ \AA}$  (Hamelink *et al.*, 1996), D4 molecules should not be able to diffuse into zeolite pores in spite of the zeolite type used.

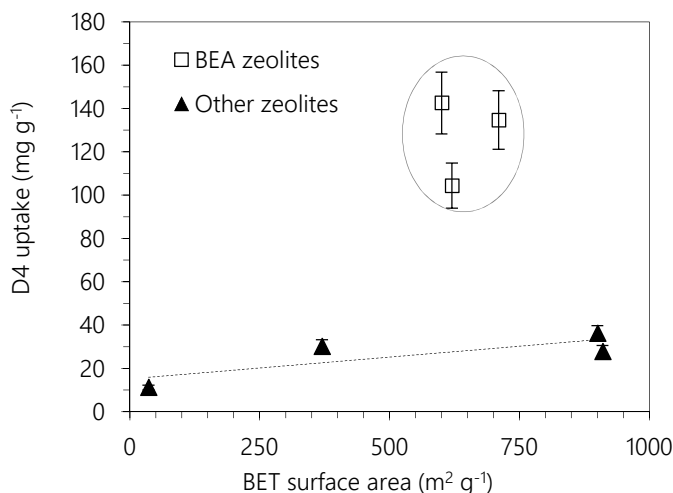


**Figure 6.2** Relation between BET surface area and D4 uptake at bed exhaustion of the zeolites considered at D4 inflow concentration of 3000 mg m<sup>-3</sup>.

### 6.3.2 D4 uptake mechanisms

Taking into account steric limitations, the high capacities of BEA zeolites can hardly be understood unless catalytic transformations take place, leading to the formation of linear by-products, narrow enough to fit inside the channel system. Indeed, when investigating the silylation of zeolite BEA by chemical liquid deposition of D4, Parker and co-workers (Parker Jr *et al.*, 2010) found that this cyclic siloxane, even though it is much bulkier than the tetraalkoxysilanes traditionally used for the same purpose, was able to enter into the framework and modify the internal surface of a BEA zeolite. It was proposed that the impaired modifications were only compatible if the formation of the ring-opened linear tetramer took place: narrow enough (ca. 6 Å) to fit inside the linear channel system of BEA and long enough (ca. 12 Å) to reach some internal sites.

Moreover, the characterization of D4-exhausted adsorbent materials by hexane extraction followed by GC/MS analysis of the extracts allowed identifying the presence of cyclic siloxanes other than D4. Although linear  $\alpha$ - $\omega$ -silanediols were not detected in the extracts, they have been proposed as intermediates in hydrolysis/condensation reactions promoted by activated carbons (see Chapter 4) or mesoporous aluminosilicates (Sigot *et al.*, 2015; Jiang *et al.*, 2016) used for biogas upgrading.

In this study, the first evidence of the presence of –OH functionalities in the conversion products of D4 was found in the differential mid-IR spectra of the Fe-BEA exhausted zeolite. The curves shown in Figure 6.3 were obtained by subtracting the spectrum of the zeolite before adsorption from the spectrum of zeolite exhausted with the adsorbate. Upon D4 adsorption, the exhausted materials showed a net increase in the intensity of a broad and intense band at  $1065\text{ cm}^{-1}$  and a weak (broad) shoulder centered near  $1215\text{ cm}^{-1}$ , that are attributed to asymmetric stretching of the Si-O-Si groups. The band at  $805\text{ cm}^{-1}$  is a strong methyl rocking mode band that is characteristic of a silicon atom linked to two methyl groups (the symmetric bend appearing at  $1265\text{ cm}^{-1}$ ). A band at  $955\text{ cm}^{-1}$  in the spectrum of the Fe-BEA zeolite, which is not present in the DAY counterpart, could be compatible with the presence of siloxanes with -OH functionalities.

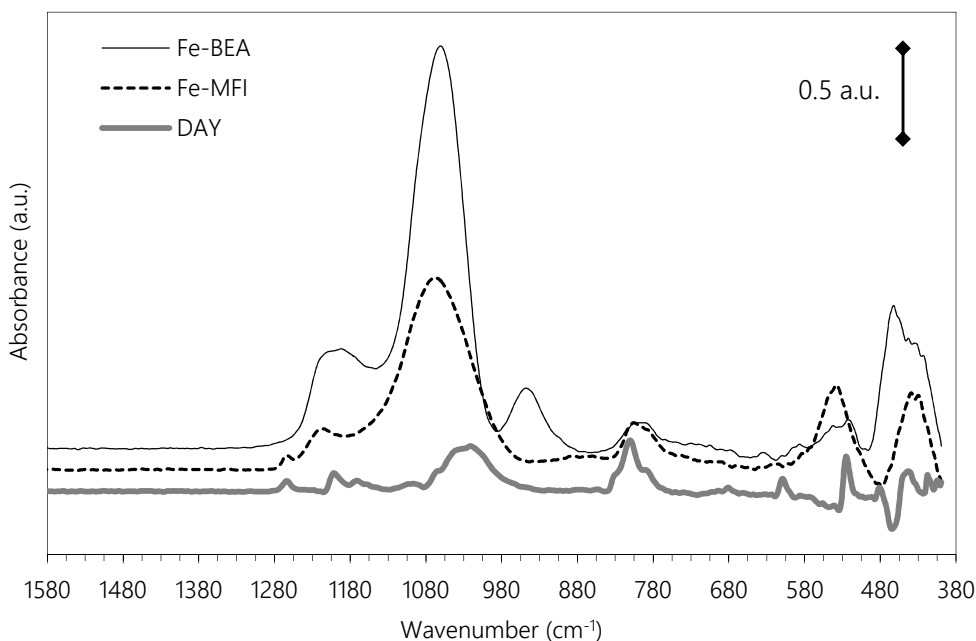


**Figure 6.3** Differential FT-IR spectra of D4-exhausted zeolites

To get a further insight into the mechanism responsible for the removal of D4, exhausted zeolites were treated with anhydrous THF, which is suitable for extraction of polar and non-polar by-products (Varaprath and Lehmann, 1997), and the extracts were analyzed by GC/MS. As it can be seen in Figure 6.4, each zeolite responds differently to THF extraction. GC-MS analysis showed that, although the pristine compound was the main

component of the extracts, several by-products are formed including cyclic siloxanes, mainly D3 and D5, and higher quantities of  $\alpha$ - $\omega$ -silanediols: from the longest chain identified with nine silicon atoms down to the monomeric dimethylsilanediol (see Table 6.2).

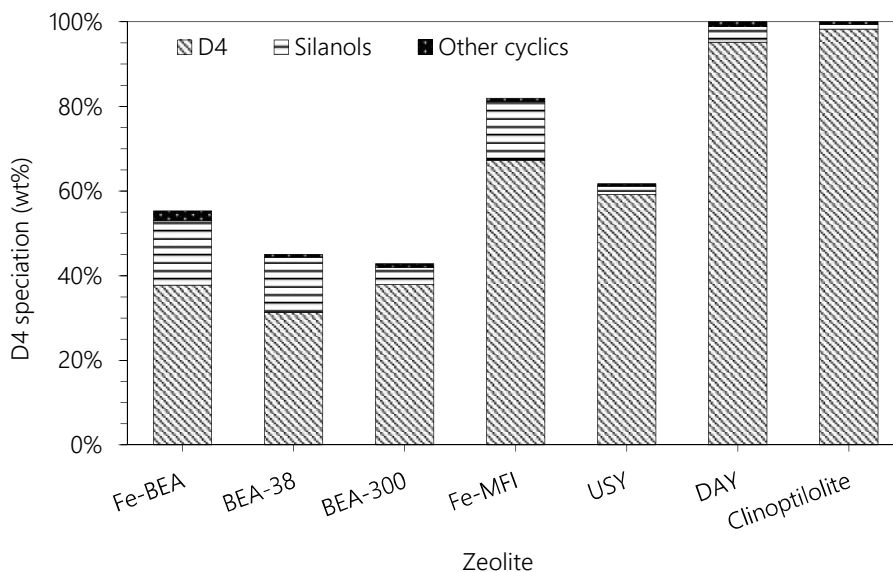


**Figure 6.4** Percentage of D4 recovered or transformed to other cyclic siloxanes and  $\alpha$ - $\omega$ -silanediols from THF extracts of exhausted zeolites.

**Table 6.2**

List of identified compounds by GC-MS analysis after THF extraction of D4-exhausted zeolites.

Compounds	MW (g mol <sup>-1</sup> )	Retention time (min)	Analytical ions ( <i>m/z</i> )
<b>Cyclic siloxanes</b>			
Hexamethylcyclotrisiloxane (D3)	222.5	4.1	207/191
Octamethylcyclotetrasiloxane (D4)	296.6	6.4	281/265
Decamethylcyclopentasiloxane (D5)	370.8	7.7	355/267
Dodecamethylcyclohexasiloxane (D6)	444.9	9.1	429/341
Tetradecamethylcycloheptasiloxane (D7)	519.1	10.2	503/415
<b><math>\alpha</math>-<math>\omega</math>-silanediols</b>			
Dimethylsilanediol	92.2	2.2	77/45
Tetramethyl-1,3-disiloxanediol (Dimerdiol)	166.3	5.2	133/151
Hexamethyl-1,5-trisiloxanediol (Trimerdiol)	240.5	7.1	207/191
Octamethyl-1,7-tetrasiloxanediol (Tetramerdiol)	314.4	8.4	281/265
Decamethyl-1,9-pentasiloxanediol (Pentamerdiol)	388.7	9.5	355/267

The observed product distribution indicates that both condensation and hydrolysis reactions coexist. For both reaction pathways, the first necessary step, i.e. the cleavage of one of the Si-O bonds, can be catalyzed by either proton or Lewis acids (Noll (1968) present in different amounts in the tested zeolites (Table 6.1).

As expected, zeolites with lower  $\text{SiO}_2/\text{Al}_2\text{O}_3$  ratios (Fe-BEA (25), BEA-38 and Fe-MFI (27)) have a higher content of Brønsted acidic sites (Si-OH-Al) than high-silica zeolites (Table 6.1). Indeed, within BEA zeolites the number of BAS is a key factor that clearly ranks their removal efficiency for D4 (Figure 6.5). In Fe-loaded zeolites a part of the Brønsted acid sites is occupied by Fe(II/III) ions. According to the  $\text{SiO}_2/\text{Al}_2\text{O}_3$  ratio of Fe-BEA, the maximum content of Brønsted sites caused by the Al content is estimated as  $1.25 \text{ mmol g}^{-1}$ . Based on the Fe loading of 3.1 wt% for this Fe-zeolite, a portion of Brønsted sites of  $0.6 \text{ mmol g}^{-1}$  is expected to be occupied, if we assume a binding ratio of Fe:Al of 1. Thus, about  $0.65 \text{ mmol g}^{-1}$  free Brønsted acid sites are expected to be remaining in Fe-BEA, which is close to the experimentally determined content of  $0.75 \text{ mmol g}^{-1}$  as the highest content among all the BEA tested zeolites.

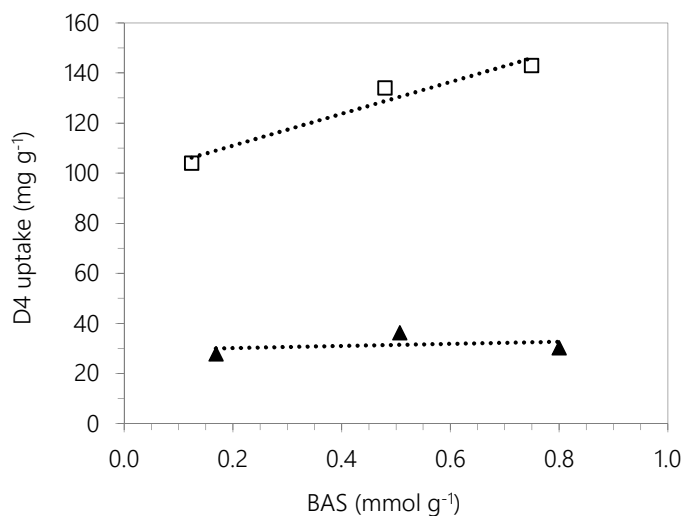


**Figure 6.5** Correlation between content of Brønsted acidic sites and D4 uptake for BEA zeolites (□) and other zeolites (▲).

Moreover, BEA zeolites have many local defects due to the fact that building units of their structure can be connected in different ways, so that it consists of two interconnected polymorphs (Newsam *et al.*, 1988). Because of this faulting, BEA zeolites have a high number of Lewis acid sites (partially coordinated alumina), besides their Brønsted site content (Jansen *et al.*, 1997). Their location either inside the channels or on the outer surface of zeolite crystallites is certainly relevant for the transformation of the large D4 molecules. BEA zeolites are known to have generally small crystallite sizes (20 – 50 nm) and thus a high external surface area, which explains that specifically BEA zeolites have been successfully applied for catalytic conversions involving bulky molecules (Simon-Masseron *et al.*, 2007).

Whether bond cleavage is promoted by Lewis or Brønsted acid sites, the formation and detachment of the  $\alpha$ - $\omega$ -silanediols requires water. Since zeolites were used as-received, they have a humidity content between 3 and 9.5 wt% (Table 6.1), which may participate in the formation and detachment of silanediols. The free  $\alpha$ - $\omega$ -silanediols formed could be able to diffuse inside the zeolite channels, since they are chain-like molecules with some degree of rotational freedom of the Si-O single bonds. As estimated by computational calculation based on the B3LYP/6-31G(d,p) method (Frisch *et al.*, 1984; Becke, 1993) using the Gaussian 09 software (Frisch *et al.*(2009), the molecular cross-sectional diameters of the different conformers are between 4.5 and 7 Å. Thus,  $\alpha$ - $\omega$ -silanediols would even be able to enter the narrower Fe-MFI pore framework.

As shown in Figure 6.4, the analysis of exhausted zeolites does not account for the total amount of D4 initially present. Higher molecular weight compounds, either not detectable by the analytical procedure or not extractable, i.e. remaining bound to the zeolite surface, can contribute to the observed unbalance. Indeed, silica-alumina (amorphous and crystalline) materials have been investigated as acid heterogeneous catalysts for cyclic siloxanes polymerization. The mechanistic investigation suggested that the cyclic monomer (i.e. D4) is first converted into a silanol-terminated monomer/oligomer which in turn polycondenses (Vaidya and Kumar, 1998). Product distribution and reaction yield were significantly affected by the catalyst acidity.

The % conversion factor of D4 to silanol-terminated monomers/oligomers in the tested zeolites is indeed related to the content of Brønsted acid sites except for the USY zeolite

(Figure 6.6). The lower amount of  $\alpha$ - $\omega$ -silanediols in the USY sample as compared to the non-accounted fraction of D4 suggests that, besides the number of catalytic acid sites, their nature/strength may also play a significant role promoting further condensation reactions. The USY zeolite has wider distribution of LAS strength, as shown by the asymmetric band in the FT-IR spectrum (Figure 6.7) which points out the presence of both weak Lewis acceptors (absorbance band at around  $1440\text{ cm}^{-1}$ ) and stronger extra framework Al acceptors ( $1450\text{ cm}^{-1}$ ) (Katada and Niwa, 2004; Kulprathipanja, 2010).

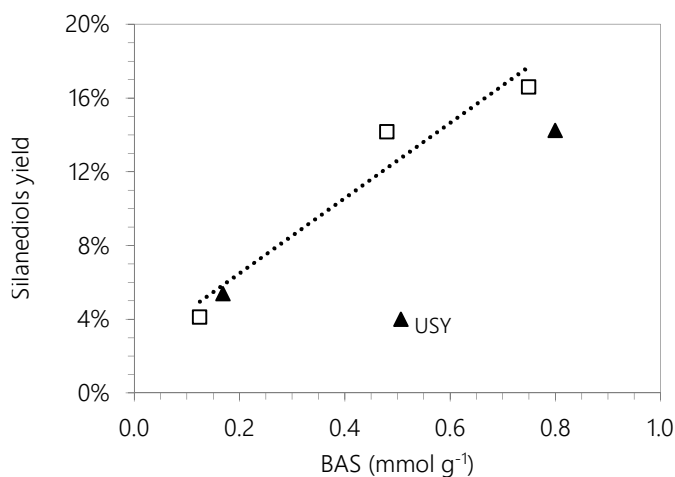


**Figure 6.6** Correlation between content of Brønsted acidic sites and A% yield of D4 into extractable  $\alpha$ - $\omega$ -silanediols for BEA zeolites (□) and other zeolites (▲).

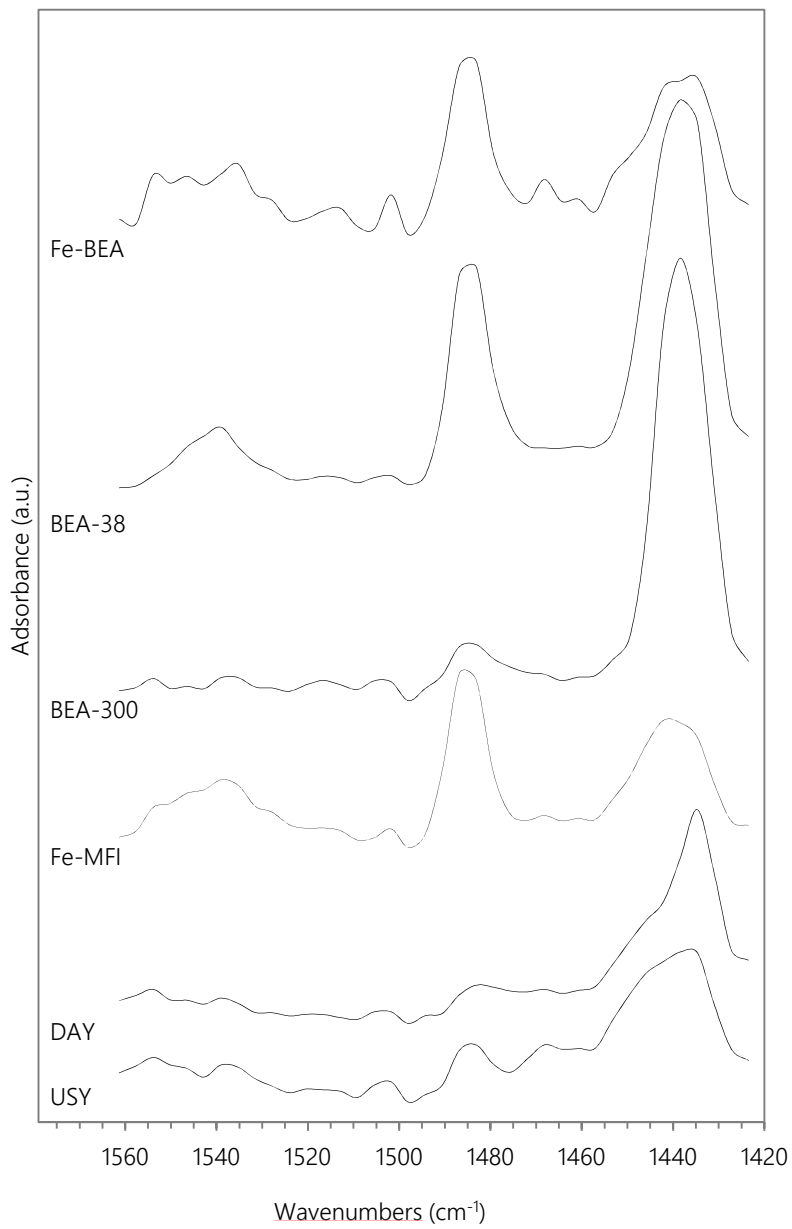


**Figure 6.7** FT-IR spectra of zeolites considered using pyridine as probe molecule for the determination of BAS and LAS.

### 6.3.3 Regeneration of D4-exhausted zeolites by wet procedures

As a results of the study detailed in the previous section, Fe-BEA was the zeolite selected in order to determine the efficiency of wet procedures for the regeneration of siloxane-exhausted zeolites, taking advantage of its proved ability to promote the formation of soluble compounds. In addition, Fe-zeolites have been reported to catalyze organic pollutant oxidation with  $\text{H}_2\text{O}_2$  and several studies have used Fe-loaded BEA zeolites in adsorption/oxidation sequential processes for the removal of refractory contaminants from water (Gonzalez-Olmos *et al.*, 2009; Gonzalez-Olmos *et al.*, 2013; Shahbazi *et al.*, 2014).

Wet regeneration tests of D4-exhausted Fe-BEA zeolite with only water and with different  $\text{H}_2\text{O}_2$  concentrations (1, 3 and 5  $\text{g L}^{-1}$ ) were carried out. Different Fe-BEA regeneration efficiencies in four successive adsorption/regeneration cycles were obtained, as it is shown in Figure 6.8.

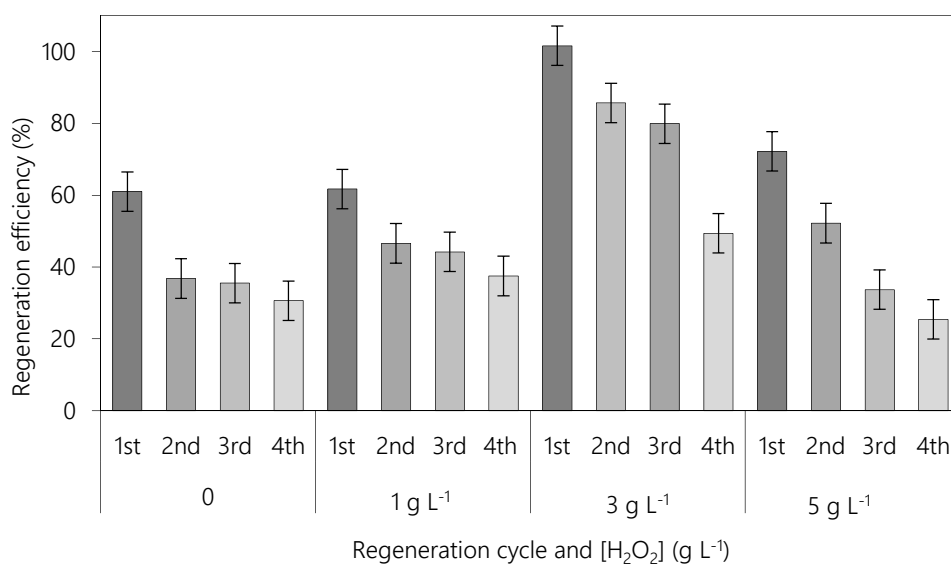


**Figure 6.8** Regeneration efficiencies obtained for Fe-BEA in four adsorption/regeneration cycles at different  $\text{H}_2\text{O}_2$  concentrations. Experimental conditions: 100 mL of solution, 250 mg of D4-exhausted Fe-BEA, and 24 hours of reaction time. Free pH ( $5.5 \pm 0.3$ ) at room temperature ( $22 \pm 1^\circ\text{C}$ ).

When only water was applied, 60% of the original adsorption capacity is restored in the first reuse cycle. As compared with the exhausted Fe-BEA zeolite, in the differential FT-IR spectrum of the water-regenerated sample, the band at  $955\text{ cm}^{-1}$  disappears (Figure 6.9). Therefore, during the regeneration of the exhausted Fe-BEA zeolite using  $\text{H}_2\text{O}$ , silanediols are released into the aqueous phase as expected according to their aqueous solubility. However, the differential FT-IR spectrum also shows an increase in the bands at  $805\text{ cm}^{-1}$  and  $1260\text{ cm}^{-1}$ , characteristic of methyl groups attached to silicon atoms, thus suggesting that after the regeneration with water either D4 or D4 by-products remain bound to the zeolite surface. The presence of residual carbonaceous material in the zeolite after the regeneration with water is further confirmed by the elemental analysis. The amount of C in the exhausted zeolite is 4.79 wt%, in agreement with the experimentally determined removal capacity of the Fe-BEA zeolite for D4 (Figure 6.1). After the first step of regeneration with water, the total carbon remains at 2.98 wt%. Thus, oxidation must lead to products with higher water solubility in order to achieve regeneration of the zeolite. On the other hand, the deposition of D4 or its transformation products may at least partially account for the observed progressive reduction in the adsorption capacity in successive adsorption/regeneration cycles, since they are obviously not easily washed out by water.

When using  $3\text{ g L}^{-1}$  of  $\text{H}_2\text{O}_2$ , the adsorption capacity was almost completely recovered after the first regeneration cycle. For comparison, the total concentration of zeolite-adsorbed siloxanes added into the suspension is  $350\text{ mg L}^{-1}$ . Higher concentrations of  $\text{H}_2\text{O}_2$  did not improve regeneration efficiencies, likely due to quenching of hydroxyl radicals by  $\text{H}_2\text{O}_2$  itself (Kwan and Voelker, 2003).

As evidenced by the reduction of the bands at  $805\text{ cm}^{-1}$  and  $1260\text{ cm}^{-1}$  in the differential FT-IR spectrum, after the first regeneration cycle with  $3\text{ g L}^{-1}$  of  $\text{H}_2\text{O}_2$  (Figure 6.9), the oxidant addition was able to reduce the amount of D4 and/or D4 by-products which remain bounded to the zeolite compared to the results obtained in the absence of oxidant. The reduction of the carbon fraction determined by EA (from 4.79 to 2.08 wt%) in the  $\text{H}_2\text{O}_2$  regenerated sample is also in accordance with the FT-IR spectrum. Therefore the organic carbon is reduced a 60% but the uptake capacity is completely restored in the first cycle, meaning that the adsorbed compounds are transformed into other molecules which are not acting as efficient competitors in the next adsorption step. However, the

high efficiency observed when using  $\text{H}_2\text{O}_2$  was not maintained in successive adsorption/regeneration steps. From this cycle on, the RE decreased down to  $50\% \pm 6\%$  in the fourth cycle (see Figure 6.8), accompanied by a progressive accumulation of C-containing products (3.05 wt%, Figure 6.9).

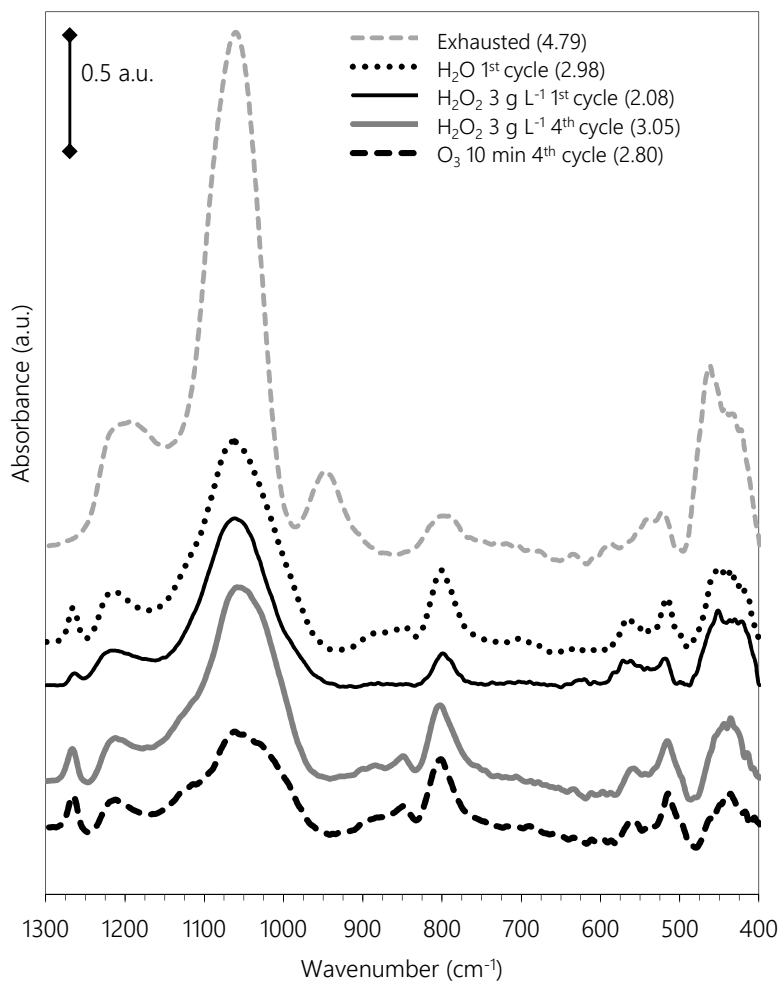


**Figure 6.9** Differential FT-IR spectra of Fe-BEA zeolite after various regeneration cycles. Values between brackets refer to the carbon content (wt%) in the exhausted or regenerated materials determined by EA.

H<sub>2</sub>O<sub>2</sub> decomposition in the suspension of fresh Fe-BEA and D4-exhausted Fe-BEA were tested in five discontinued runs of 24 h in order to evaluate zeolite catalytic performances (Figure 6.10). During the first H<sub>2</sub>O<sub>2</sub> regeneration cycle of fresh Fe-BEA, 42% of the initial amount was decomposed within 24 h. It was also determined that only 1.1% of the total content of iron was leached, representing the most labile fraction of iron in Fe-BEA zeolite. During successive runs, no further iron leaching was detected, and the H<sub>2</sub>O<sub>2</sub> decomposition within 24 h was only slightly reduced to 33% when the catalyst was reused five times. Interestingly, the Fe-zeolite loaded for the first time with D4 and its transformation products showed almost the same activity for H<sub>2</sub>O<sub>2</sub> decomposition (38% conversion in 24 h) as the fresh Fe-zeolite (42%). Nevertheless, when the zeolite was loaded with D4 repeatedly after each H<sub>2</sub>O<sub>2</sub> treatment, the H<sub>2</sub>O<sub>2</sub> decomposition rate dropped significantly, reaching finally a conversion degree of only 8% in 24 h in the fifth use. This finding points out that unreacted D4 and/or D4 by-products are being accumulated and block access to the catalytically active sites for the H<sub>2</sub>O<sub>2</sub> decomposition, thus reducing the oxidation efficiency of the treatment and increasing the unreacted D4 and products on the zeolite surface.

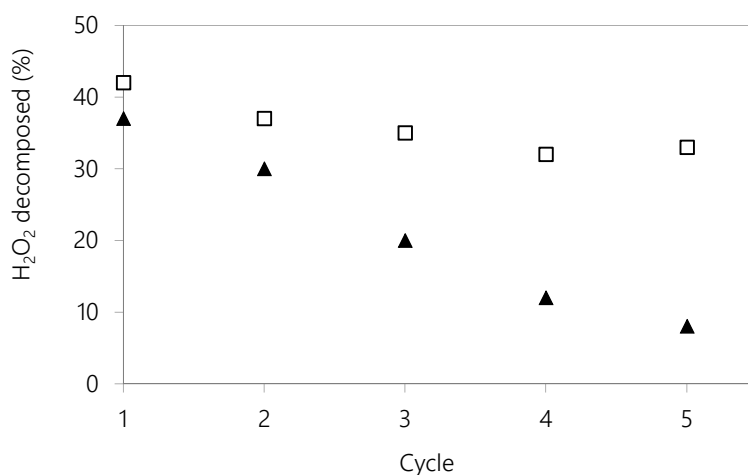


**Figure 6.10** H<sub>2</sub>O<sub>2</sub> decomposed after 24 hours ( $C_{0,H_2O_2} = 3 \text{ g L}^{-1}$ ) in catalyst suspension of fresh Fe-BEA (□) and D4-exhausted Fe-BEA (▲) during 5 treatment cycles

Besides the reduction on the catalytic activity towards  $\text{H}_2\text{O}_2$ , there are several aspects related to the adsorption step itself that are worth discussing. The analysis of the THF extracts of the Fe-BEA zeolite after the fourth exhaustion cycle revealed that the conversion of D4 to oligodimethylsiloxane- $\alpha$ - $\omega$ -diols dropped to 3.8% as compared with the results achieved in the first cycle (17% for Fe-BEA, Figure 3B). This lack of D4 transformation could be due to the reduction in the content of accessible acidic sites, both Brønsted and Lewis. The acidity analysis performed after the fourth cycle of regeneration (Figure 6.11) showed a pronounced reduction on the bands at 1440 and 1540  $\text{cm}^{-1}$  as compared to the pristine sample. Thus, in the successive adsorption/oxidation cycles, the Fe-BEA zeolite lost part of its catalytic ability to promote the ring-opening of D4, the first necessary step for the formation of linear oligomers able to enter the zeolite porous structure.

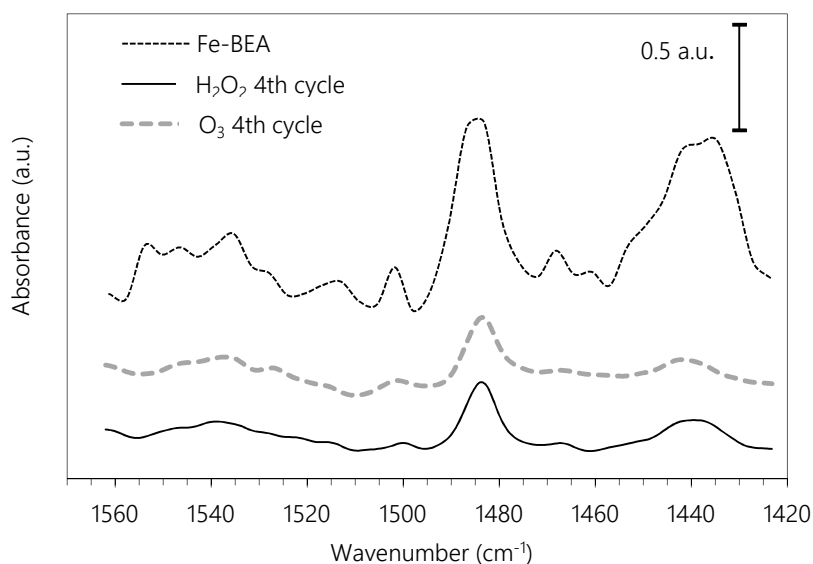


**Figure 6.11** FT-IR spectra of Fe-BEA zeolite using pyridine as probe molecule for the determination of BAS after 4 adsorption/regeneration cycles by  $\text{H}_2\text{O}_2$  or  $\text{O}_3$  as compared to fresh Fe-BEA

#### 6.3.4 Regeneration with aqueous ozone

In the light of the results discussed in the previous section, ozone was considered since it has been reported to be a powerful oxidant for the degradation of various organic pollutants (Von Gunten, 2003). D4-exhausted Fe-BEA samples were exposed to aqueous ozone ( $70 \text{ mg min}^{-1}$ ) in a suspension with  $\text{pH } 6.2 \pm 0.3$  for different time periods ranging from 5 to 30 min. After regeneration with aqueous  $\text{O}_3$ , new dynamic adsorption tests were carried out, and regeneration efficiencies were obtained (Figure 6.12). As it can be seen, 5 min of ozonation treatment were not enough to completely restore the adsorption capacity of Fe-BEA zeolite, with a RE of  $63 \pm 6\%$ . Nevertheless, increasing the reaction time up to 10 min leads on a RE of  $93 \pm 8\%$ . At higher reaction times, 20 and 30 min, treatment performances did not improve, giving REs around 85%. In order to assess the potential effect of water desorption and gas flow stripping of D4 and/or its by-products on the RE, the same process was carried out with an air flow without  $\text{O}_3$  during 10 min, obtaining a D4 adsorption recovery of 39%.

Further four adsorption/oxidation cycles were applied in order to assess cycle sequential performance with the optimal ozonation time of 10 min. REs obtained after each ozone regeneration step are shown in Figure 6. After the first and second cycle, adsorption capacity of Fe-BEA zeolite was almost completely restored, meaning that the zeolite can be reused for three times, still having the maximum performance. After the third cycle (fourth zeolite use), Fe-BEA zeolite performance decreases to  $\text{RE} = 73 \pm 5\%$ , whereas after the fourth cycle Fe-BEA zeolite reached around 40% of its original adsorption capacity. After four cycles of D4 adsorption/ $\text{O}_3$  oxidation, EA and FT-IR analyses of Fe-BEA zeolite were carried out. As it is shown in Figure 6.9, total carbon remains at 2.80 wt% after the regeneration treatment with  $\text{O}_3$  compared to the original 4.79 wt%, indicating that non oxidized forms of siloxanes were successively being accumulated in the zeolite. Like in the  $\text{H}_2\text{O}_2$  regeneration (section 6.3.3), accumulated products blocked the adsorptive sites and the acidic sites responsible for D4 ring-opening (Figure 6.11) leading to a successive decrease on D4 uptake. Therefore, ozonation did not provide any advantage over the Fenton-like regeneration, since the main drawbacks that hinder zeolite regeneration are not overcome.

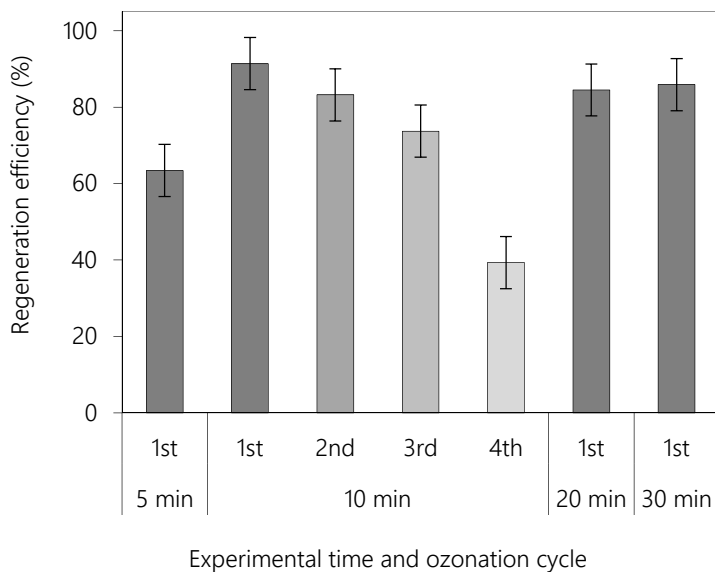


**Figure 6.12** Regeneration efficiencies obtained after various adsorption/oxidation cycles with different ozonation times for D4-exhausted Fe-BEA zeolite. Ozone mass flow of  $70 \text{ mg O}_3 \text{ min}^{-1}$ , free pH ( $6.2 \pm 0.3$ ), room temperature ( $22 \pm 1^\circ\text{C}$ ).

## 6.4 Finals remarks

---

The experimental results on the uptake of gaseous D4 by various zeolites lead to the conclusion that BEA zeolites, due to their high content of Brønsted and Lewis acidic sites, show the greatest catalytic activity for the siloxane ring-opening and the formation of  $\alpha$ - $\omega$ -silanediols. Silanediols formed on the BEA surface can be detached from the acidic sites when water is available, e.g. due to the humidity content of the zeolite, and are narrow enough to diffuse into the channels, enhancing the removal efficiency for D4, thus detached silanediols and other cyclic siloxanes formed as their condensation products were identified in the THF extract.

Soluble silanediols formed by the catalytic activity of a Fe-BEA during D4 adsorption are easily removed in wet regeneration treatments with only water; however, the regeneration is incomplete. Adding  $H_2O_2$  in a heterogeneous Fenton-like regeneration treatment leads to a complete regeneration of zeolite in the first cycle. The regeneration efficiency obtained with oxidation by 10 min ozonation is similar. However, the recyclability of the zeolite in successive cycles is hampered by the accumulation of carbonaceous material that cause a loss of catalytic activity, affecting both the adsorption and the regeneration stages. The block of LAS and BAS reduces the D4 transformation into silanediols, the fundamental step that rules D4 uptake. At the same time, the reduction on the catalytic activity towards promoting Fenton-like reactions during regeneration leads to a higher accumulation of unreacted D4 and insoluble by-products.



---

Chapter 7

TOWARDS REAL SCENARIO  
IMPLEMENTATION



## 7.1 Overview

In order to correctly assess the technical implications of the fundamental knowledge reported in Chapter 4, 5 and 6, the results should be discussed in a context that is as realistic as possible. To achieve this, our findings were contextualized in a study case of a Catalan WWTP. The Catalan Water Agency (ACA), on its current Sludge Program, plans to incorporate the anaerobic digestion with energy cogeneration in the Catalan WWTP treating more than 15000 equivalent inhabitants. The benefits of the sludge digestion in the reduction of the biowaste volume and stabilization, together with the electric power generated, can potentially compensate the economic investment in a few year's time. Currently, already 17 Catalan WWTP are using their biogas mix to obtain energy.

We studied the siloxane removal process in a WWTP located in Barcelona area. This WWTP, corresponding to a population of 135000 equivalent inhabitants, treats 27000 m<sup>3</sup> per day and produces almost 60000 Nm<sup>3</sup> of biogas every month. In 2007 three 60 kW CR65 Capstone micro-turbines were installed for the energy recovery of biogas, which generates 100000 kWh, corresponding to the 44% of the WWTP electric consume. Previous to the micro-turbines, there is a biogas treatment unit, depicted in Figure 7.1, in order to remove humidity, VOCs and siloxanes.

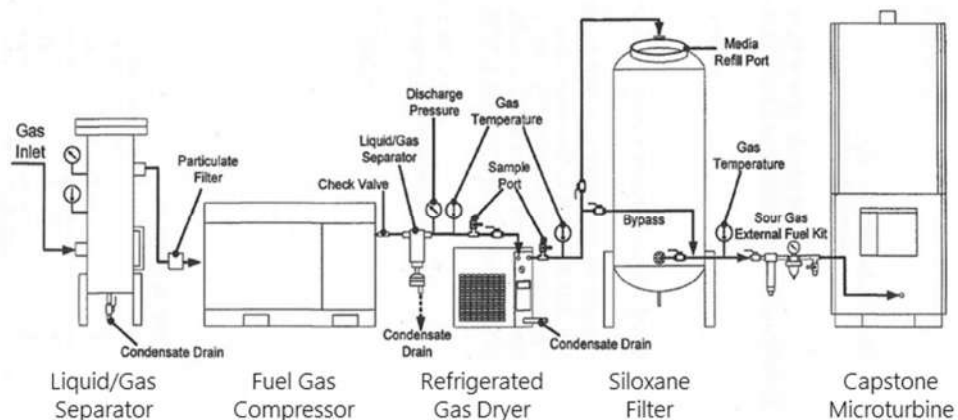


Figure 7.1 Scheme of a Capstone biogas treatment unit.

During the liquid/gas separator and the compression and refrigeration steps, a great part of the volatile compounds are removed. Nevertheless, the concentration of siloxanes after these treatments is still too high, thus two sequential AC filters are used, currently operated with the AC Airpel 10 (Table 3.1). Because of a high concentration of siloxanes in the biogas used at the micro-turbines, in 2010 a severe SiO<sub>2</sub> accumulation forced the stop of the machines in order to clean the internal components. After that episode, the AC filters are checked every five days of operation, and the AC beds are replaced every 4000 hours of use.

## 7.2 Methodology

---

During June and July 2015, we collected biogas samples at different points of the siloxanes filters using Tedlar bags, as well as samples of exhausted Airpel 10 to analyze the compounds adsorbed when the adsorbent bed is replaced. Thus, the siloxane concentration in the biogas produced in the WWTP and in the AC used for their abatement were determined.

In order to explore the best materials to prolong the life of the adsorbent beds, several tests were performed in more realistic conditions which allow the discussion of the best cost-efficient technologies based in the knowledge reported in Chapters 4, 5 and 6 of this dissertation. The approaches considered to assess the siloxane removal in real conditions included the study of the siloxane adsorption at low concentration, use of different gas matrix conditions and the competitive siloxane adsorption in the presence of other VOCs to ascertain the influence of the adsorption conditions.

The experiments were carried out with the AC used in the WWTP siloxane removal treatment and with the best performing AC proven in Chapter 4 (Airpel and Nuchar, respectively, see Table 3.1 and Tabla 4.1.).

## 7.3 Problem statement in a case of study

---

### 7.3.1 Biogas sampling and analysis

Biogas samples were analyzed by GC-MS in order to determine the concentration of siloxanes and VOCs at the different stages of the siloxane removal system. D4, D5 and D6 were the only siloxanes detected at quantifiable concentrations ( $>0.5 \text{ mg m}^{-3}$ ) at two different points: before the first and between the first and second AC vessels.

The average D4 concentration at the first AC vessel was  $45 \pm 3 \text{ mg m}^{-3}$ , which is higher than the values reported in the state of the art literature on siloxane analysis from biogases (see Chapter 1), however, the total cyclic siloxanes concentration was  $62 \pm 8 \text{ mg m}^{-3}$ , considered within the range reported by (Raich-Montiu, 2014).

Moreover, large amounts of a variety of HC were detected in the biogas samples, including toluene, limonene, xylene, ethylbenzene among many others. The concentration of most compounds is reduced after the first AC filter, however the D4 concentration at the outlet of the first AC bed is higher, probably due to roll up phenomena.

### 7.3.2 Exhausted AC analysis

The exhausted Airpel AC samples collected were treated with THF in order to extract the compounds adsorbed, which are concentrated in the carbon surface. Thus, by this procedure, compounds not detected in the gas samples can be identified. In Chapter 4, we report on the extraction of D4-exhausted activated carbons that was carried out with hexane, which did not allow to detect the silanediols proposed as intermediate products of ring-opening polymerization. Further, we used anhydrous THF to extract the molecules adsorbed, since it is a suitable solvent for both polar and non-polar compounds (Chapter 6).

Airpel 10 is an anthracite based carbon activated by steam process, so that, it has a moderate quantity of oxygen functional groups (Table 4.3 and Table 4.4) which promote the ring-opening polymerization of siloxanes (Figure 4.13). As discussed in section 4.3.4, Airpel long-term polymerization ratio is notable, therefore polymerization of the siloxanes

adsorbed leading to the formation of higher molecular weight siloxanes through hydrolysis and condensation reactions are expected to occur in an intermediate extend.

Figure 7.2 shows a chromatogram corresponding to the GC-MS analysis of THF extraction of exhausted Airpel samples. The GC-MS was operated in Scan mode in order to detect all the compounds present in the sample. However, given the large amount of HC species in the sample, the extracted compounds could not be completely separated via the analytic methods applied.

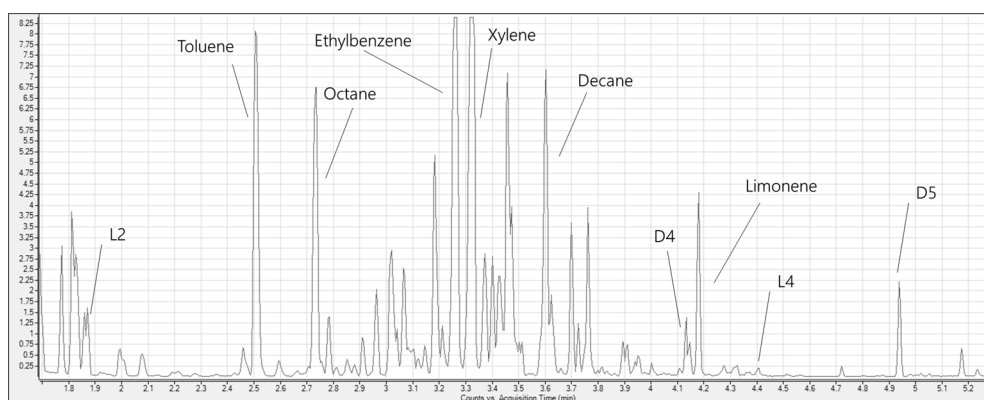


**Figure 7.2** GC-MS chromatograms obtained from the analysis of the THF extraction of exhausted Airpel samples used in biogas filters

The predominant compounds extracted include alkanes such as octane, nonane and decane, and cycloalkenes like toluene, xylene and ethylbenzene and limonene. Regarding siloxanes, D4, D5 and L2 were extracted in relatively high concentrations, although the extracted fraction does not need to match the total adsorbed due to the transformation of pristine siloxanes to non-extractable or non-detectable compounds. On the other hand, lineal siloxanes like L4 and L3, which were not detected in the biogas samples, were identified in the THF extraction as well as notable amounts of D6 and D7 that presumably were formed by ring-opening polymerization. On the other hand,  $\alpha$ - $\omega$ -silanediols could not be detected.

### 7.3.3 Effectiveness of thermal desorption

Thermal desorption of the exhausted Airpel samples was attempted at 100°C with 0.25 g of exhausted AC using an air flow of 200 ml min<sup>-1</sup> in order to regenerate the adsorbent. The outlet flow was analyzed by GC-MS so as to detect the variation of the desorbed compounds at different times. Neither D4 nor D5 were desorbed, and L2 was the only siloxane detected in the outlet flow, indicating that larger siloxanes are not desorbed by dry air at 100°C, presumably due to the formation of higher molecular weight siloxane polymers.

Figure 7.3 shows the chromatograms obtained after 10, 55 and 220 min of desorption, and the main compounds that could be identified are marked. Toluene disappears almost completely in the 55 min chromatogram, while ethylbenzene and xylene are the longest remaining compounds in the outflow gas. After 4 hours of this thermal treatment, Airpel samples were treated with THF to extract the remaining compounds and compare the results with the extraction before the thermal regeneration. The intensity of the peaks was greatly reduced, indicating that the remaining compounds after thermal treatment were not extractable with THF or not detectable by GC-MS.

D4 dynamic adsorption tests, were carried out after the air thermal desorption to assess the efficiency of the thermal regeneration in terms of D4 adsorption, in the same conditions applied in the high concentration experiments described in Chapter 4. The adsorption capacity obtained was 84 mg g<sup>-1</sup>, corresponding to a 26% of the original adsorption capacity results (Table 4.1).

Although large amounts of alkanes and cycloalkenes could be desorbed, the adsorption capacity was not recovered because of the presence of non-desorbed VOCs and siloxanes remaining in the AC surface, together with the plausible siloxane polymers formed due to the ring-opening reactions (described in section 4.3.4) that hamper the recovery of the adsorption sites of the AC. Therefore the thermal desorption with dry air at 100 °C was only partially successful. However, alternative thermal treatments, such as the use of steam, should also be considered in order to improve the regeneration results. Hot steam is proposed to improve the desorption of siloxane molecules attached to AC surface due to the hydrolysis reactions proposed.

Based on the experience arising from this dissertation (Chapter 5), AOP-driven regeneration of siloxane exhausted is not completely successful. AC are prone to oxidation by AOPs, their structure and chemical properties are affected by the oxidative treatment so they cannot be efficiently reused after wet regeneration. Zeolites, as adsorbents resistant to oxidation, are promising materials for the sequential adsorption/oxidation processes for the removal of volatile compounds susceptible to oxidation, but the high regeneration efficiencies were only obtained when the ratio of water soluble compounds formation was pronounced, i.e. in successive cycles the performance dropped (Chapter 6). Moreover, the price of a synthetic zeolite such as Fe-BEA (the most efficient in the adsorption/oxidation sequential processes) is up to 20 € per kg, which triplicates the price of a chemical activated carbon. Therefore, the use of this materials should be discarded for the application in siloxane filters for biogas treatment in WWTP power cogeneration because of the comparative high costs.

The change of the AC for a best performing AC can be the best alternative to increase the life of the adsorbent beds. The performance of the currently used Airpel in the AC filters was compared to the phosphoric activated Nuchar, which is a more expensive AC but may present advantages, since it was the best performing AC in the D4 dynamic adsorption tests performed at a high concentration (see Chapter 4). Therefore, in the following section the performance of both AC in different conditions, approaching to realistic ones, is studied.

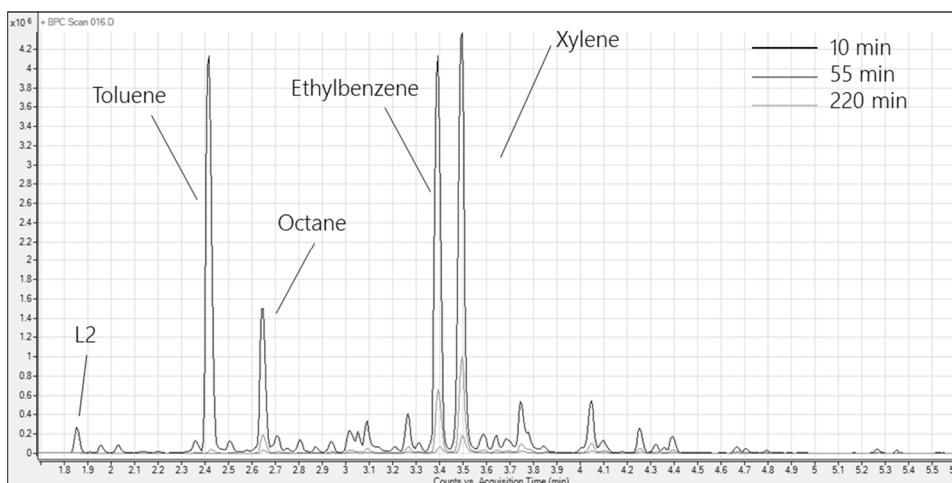


**Figure 7.3** GC-MS chromatograms obtained in the analysis of the outlet flow during the thermal desorption of real exhausted Airpel after 10, 55 and 220 minutes.

## 7.4 Approaching a real scenario

---

### 7.4.1 Influence of the D4 concentration

Adsorption isotherms were obtained to assess the D4 adsorption capacity of Airpel compared to Nuchar at low inflow concentrations in dry N<sub>2</sub> matrix. Thus, D4 static adsorption tests were performed following the experimental set up described in section 3.3 for both Airpel and Nuchar ACs. In order to confirm the results obtained in fast static adsorption tests, several dynamic breakthrough tests were carried out at range of 18 – 2350 mg m<sup>-3</sup> (1.45, 40, 120 and 180 ppm v/v). At these conditions the tests last up to 45 days, and the results were in agreement of those obtained statically, which validates the faster method. Therefore a wide range of results were obtained by static adsorption experiments.

The D4 adsorption isotherms obtained for both ACs are compared in Figure 7.4. and both AC fitted well to the Langmuir model, described by Equation 5:

$$\frac{C_e}{x/M} = \frac{1}{b_A \cdot Q_M} + \frac{C_e}{Q_M} \quad (\text{Eq. 5})$$

Where  $C_e$  is the D4 equilibrium concentration,  $Q_M$  is the maximum sorption uptake [mg g<sup>-1</sup>] and  $b_A$  is Langmuir adsorption constant of adsorbate [m<sup>3</sup> mg<sup>-1</sup>].

Both adsorption isotherms were adjusted to the Langmuir model and the constants are reported in Table 7.1.  $Q_M$  values reported in the literature range from 29 to 460 mg g<sup>-1</sup> (Boulinguez and Le Cloirec, 2010; Nam *et al.*, 2013) depending on the textural development of the ACs tested. Therefore, while Airpel  $Q_M$  can be considered as a conventional value, Nuchar results are outstanding since it is 5.7 times higher than Airpel. However, the  $x/M$  of both AC decreased significantly at D4 concentrations below 2000 mg m<sup>-3</sup>.

Therefore, the tendency shown in the results obtained at high D4 concentration dynamic adsorption tests, where chemically-AC present the highest  $x/M$ , is maintained at lower concentrations. Thus, in the lowest  $C_e$  tests, the  $x/M$  of Nuchar is still more than 3 times higher than Airpel.

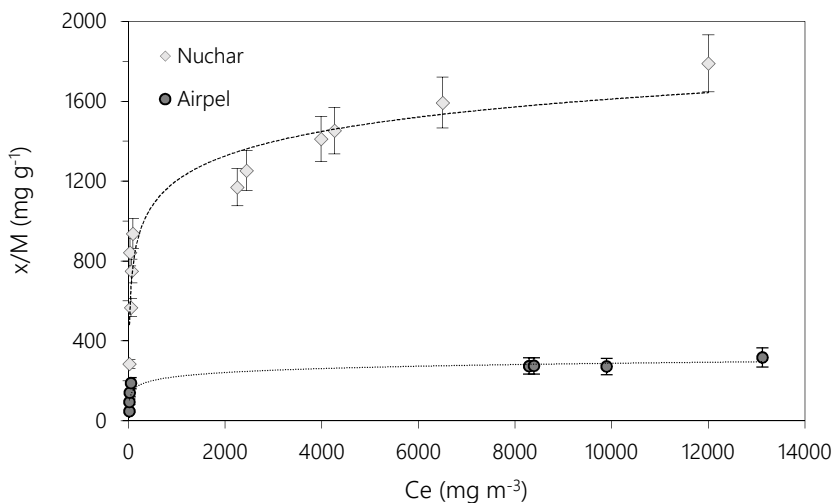


**Figure 7.4** D4 adsorption isotherms obtained in static adsorption tests with Airpel and Nuchar AC, fitting the Langmuir model.

**Table 7.1**

Isotherm equation constants of Langmuir model of D4 adsorption at 22 °C.

AC	Langmuir equation	$Q_M$ [mg g <sup>-1</sup> ]	$b_A$ [m <sup>3</sup> mg <sup>-1</sup> ]	$R^2$
Airpel	$x/M = (0.0034 + 0.5764/C_e)^{-1}$	294	0.0059	0.990
Nuchar	$x/M = (0.0006 + 0.2096/C_e)^{-1}$	1667	0.0028	0.988

#### 7.4.2 Effect of the gas matrix composition

From all the commercial ACs tested at high D4 dynamic adsorption tests, Nuchar showed the highest D4 uptake (see Table 4.1). For this reason, Nuchar was the adsorbent chosen for further experiments presented in this last section.

The first set of experiments was devoted to ascertain the influence of different, more realistic matrices on the adsorption results. Thus the presence of biogas main constituents and other important species such as oxygen (air) and water (moisture) were considered. For this reason, the D4 adsorption on Nuchar was studied using air and synthetic biogas as carriers, with different relative humidity (RH) contents. The adsorption breakthrough

curves of  $13000 \text{ mg m}^{-3}$  D4 on Nuchar in a matrix of air with 20% of RH, air with 80% RH, dry synthetic biogas, synthetic biogas with 80% RH and dry nitrogen were compared (Figure 7.5). The adsorption capacity in an air flow with 20% RH is  $1760 \pm 23 \text{ mg g}^{-1}$ , which is essentially the same obtained when using dry nitrogen as carrier ( $1732 \pm 93 \text{ mg g}^{-1}$ ). However, if the RH value raises up to an 80%, a significant decrease of the AC capacity is observed ( $1450 \pm 51 \text{ mg g}^{-1}$ , corresponding to a reduction of 17% in the x/M value).

For experiments with synthetic biogas as a D4 carrier gas, D4 adsorption capacity decreases to  $1423 \pm 37 \text{ mg g}^{-1}$ . This result suggests that  $\text{CH}_4$  and  $\text{CO}_2$  are competitively adsorbed and/or their presence reduces the diffusivity of the D4 into the AC. When the biogas contained 80% of relative humidity, the D4 x/M was reduced down to  $1172 \pm 84 \text{ mg g}^{-1}$ , which also corresponds to a 17% reduction respect to the value obtained with the dry biogas. The decrease on the performance in presence of humidity may be caused by the formation of hydrogen bonds with the oxygen functional groups which block the adsorption sites. Hence a preliminary gas drying to reduce the humidity content may increase the performance of the AC for the removal of siloxanes, especially when working at low D4 concentrations.

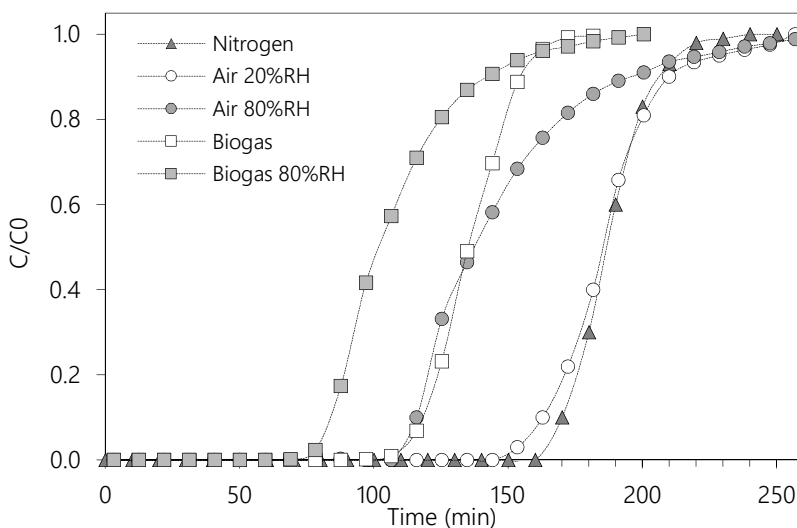


**Figure 7.5.** Adsorption breakthrough curves obtained for MVW-2 with a  $1000 \text{ ppm v/v}$  D4 flow with nitrogen, wet and dry air and synthetic biogas as carrier gases. Experiments were carried out with a stream of  $200 \text{ ml min}^{-1}$  at room temperature with  $0.250 \text{ g}$  of MVW-2.

### 7.4.3 Adsorption of other siloxanes

The knowledge gained in D4 adsorption was extended to perform L2 and D5 in dynamic adsorption tests. Five ACs of those tested in Chapter 4 were selected to carry out the adsorption tests with other siloxanes taking into account their different properties, origin and activation processes undergone (see Table 3.1 and 4.1). Furthermore, at his stage of the siloxane removal research, Cabot Corporation requested us for testing their recently developed products in our research project. Therefore Silpure and Silpure W, two chemically-activated carbons were included in further investigation. The pore volume of these ACs is 0.85 and 1.22 cm<sup>3</sup> g<sup>-1</sup> respectively (see Table 7.2).

**Table 7.2**

Origin, activation process and textural properties of Silpure and Silpure W.

Commercial name	Origin	Activation	$S_{\text{BET}}$ [cm <sup>2</sup> g <sup>-1</sup> ]	$V_t$ [cm <sup>3</sup> g <sup>-1</sup> ]	$V_{\text{DR}_{\text{N}_2}}$ [cm <sup>3</sup> g <sup>-1</sup> ]	$V_{\text{meso}}$ [cm <sup>3</sup> g <sup>-1</sup> ]
Silpure	Wood	H <sub>3</sub> PO <sub>4</sub>	1616	0.85	0.70	0.15
Silpure W	Wood	H <sub>3</sub> PO <sub>4</sub>	1854	1.22	0.79	0.43

Steam-AC Airpel, RB3 and Centaur, besides chemically-AC Nuchar, Aquasorb, Silpure and Silpure W were tested in single component L2 and D5 dynamic adsorption tests at 380 and 2060 mg m<sup>-3</sup> respectively using 200 ml min<sup>-1</sup> of dry N<sub>2</sub> as carrier gas using 250 mg fixed bed AC. Moreover, the D4 concentration in dynamic adsorption tests for all this AC was 1890 mg m<sup>-3</sup>.

The D4 adsorption capacities determined in Chapter 4 for a wide range of AC were highly dependent on the porosity development of the materials. The same tendency was observed in the adsorption of other siloxanes, such as L2 and D5.

Positive relation were found with both micropore and mesopore volume, however the best correlation were obtained with total pore volume in all cases. As discussed in section 4.3.2, siloxanes are expected to be adsorbed in larger micropores due to their molecular size. Nonetheless, the mesoporosity values showed great importance in the molecular diffusion to the larger micropore network, and it is also expected to allocate quantities of siloxanes. The relation between  $V_t$ , including micro and mesopores, and L2, D4 and D5 is shown in Figure 7.6.

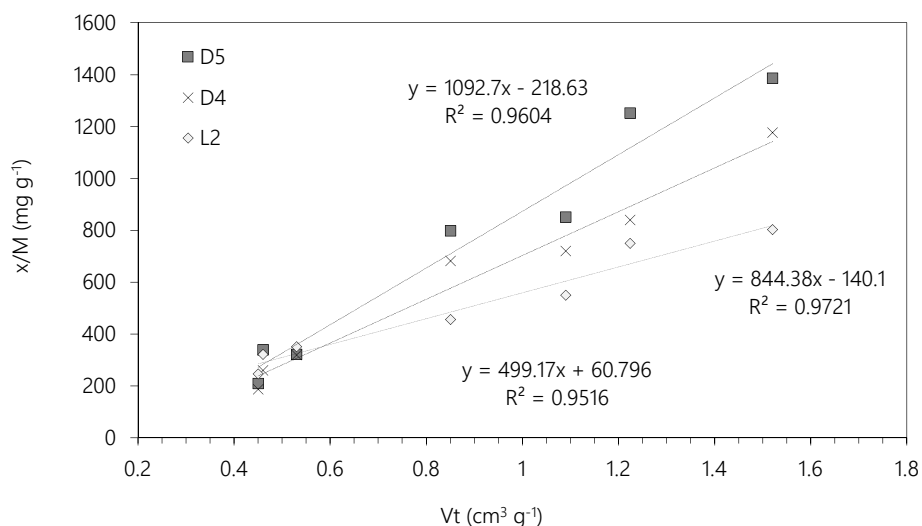


**Figure 7.6** Correlation between total pore volume of the AC tested and D5, D4 and L2 adsorption capacities in mono-component dynamic adsorption tests for D5 (2060 mg m<sup>-3</sup>), D4 (1890 mg m<sup>-3</sup>) and L2 (380 mg m<sup>-3</sup>)

#### 7.4.4 Competitive multicomponent adsorption

The siloxane single component adsorption under the test condition used, i.e. a dry N<sub>2</sub> stream, showed that Nuchar, and the other chemical-AC tested, performed better than steam-AC such as Airpel. Further, the siloxane adsorption in the presence of volatile organic compounds was evaluated in multicomponent dynamic adsorption tests with three siloxanes (L2, D4 and D5) and two VOCs (toluene and limonene) which is representative for the usual biogas trace composition. The tests were performed following the experimental set described in Section 3.3.1. The gas test was prepared by mixing 5 different streams of L2, D4, D5, toluene and limonene at different flow rates in order to adjust the concentrations to the values reported in Table 7.3.

As expected, higher molecular weight compounds (D5 and limonene) are the most strongly adsorbed. On the other hand, the smaller compounds (L2 and toluene) present earlier breakthrough times. Dynamic adsorption breakthrough curves obtained with Airpel and Nuchar are shown in Figure 7.7 and Figure 7.8 respectively. This two curves exemplify the behavior of the curves obtained for the two types of carbon as function of the activation process.

The adsorptive behavior of each compound depends on the adsorbent, since Nuchar had better performance for siloxanes than for VOCs, as opposite to Airpel. In this sense, the breakthrough curves obtained follow a different pattern in the competitive adsorption: in the case of Nuchar while the weakest adsorbed compound is toluene, the strongest is D5, and so happens with the other chemically activated carbons tested. In the case of Airpel (and the other steam activated carbons), the weakest adsorbed compound is L2 and the strongest adsorbed compound is limonene. In all cases, rolling up of toluene, L2 and D4 in the breakthrough curves appear because the displacement and desorption promoted by the most strongly adsorbed molecule.

**Table 7.3**  
Multicomponent test gas composition, 200 ml min<sup>-1</sup> N<sub>2</sub> carrier.

Compound	Test gas concentration	
	[mg m <sup>-3</sup> ]	[ppm v/v]
L2	380	57
D4	1892	501
D5	2064	567
Toluene	3886	1029
Limonene	752	199
Total siloxane	4336	1125
Total VOCs	4638	1324

The performance of the adsorbents must be assessed before the first siloxane breaks up, when the siloxane concentration after the AC is under the limit tolerated by the ERS manufacturers. L2 is the first siloxane that breaks up in all cases and due to roll up in all tests, its x/M at bed exhaustion tends to almost zero. Therefore the adsorption capacities are reported both at bed exhaustion (BE) and when the L2 arrives to 0.5 ppm v/v (BT). Figure 7.9 resumes the results of the competitive adsorption tests of the ACs tested. Thus, the adsorption capacities for each compound are reported at both BE and at L2-BT, which is range from 35 to 42 min for steam-ACs and from 94-161 for chemical-ACs in the conditions tested.

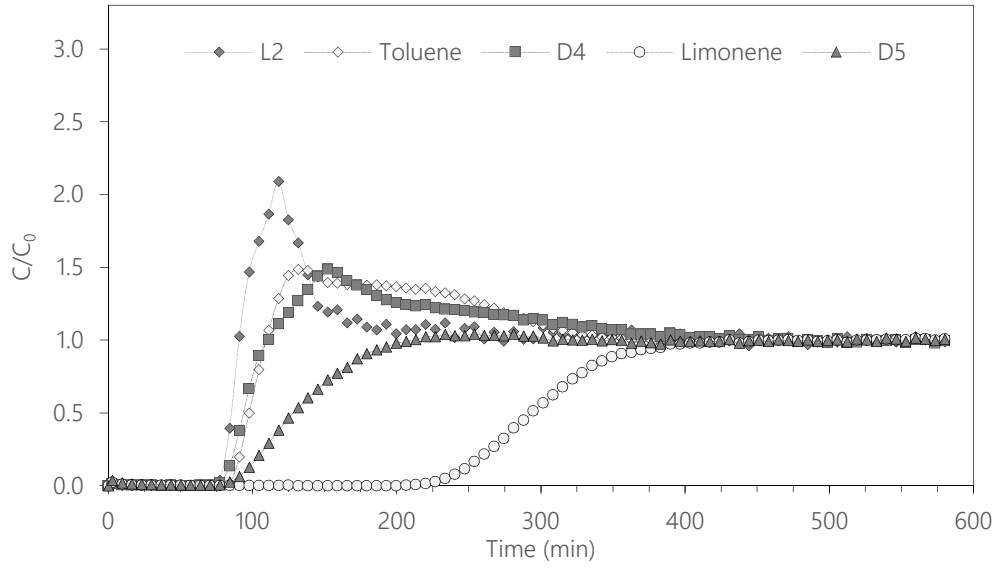


**Figure 7.7** Dynamic multicomponent adsorption breakthrough curves obtained for Airpel.

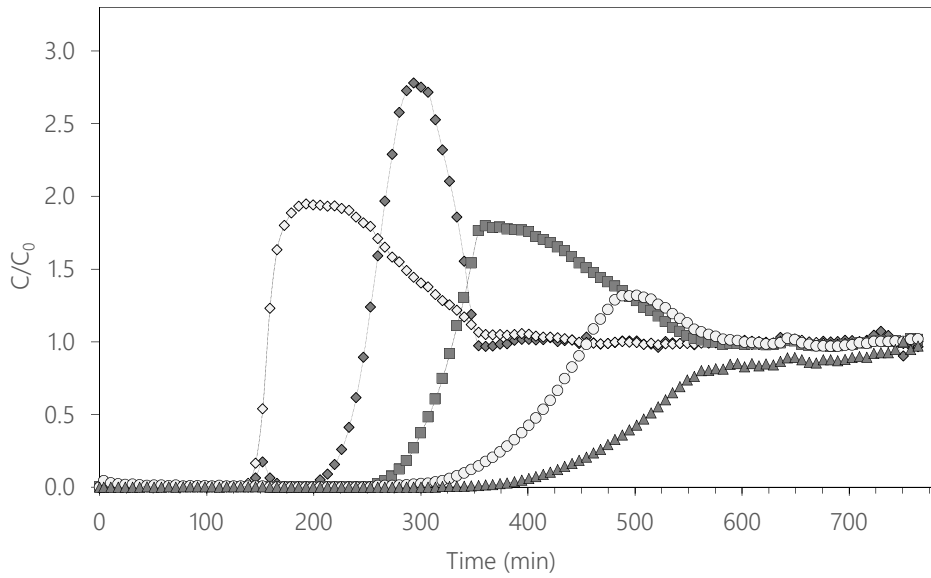


**Figure 7.8** Dynamic multicomponent adsorption breakthrough curves obtained for Nuchar.

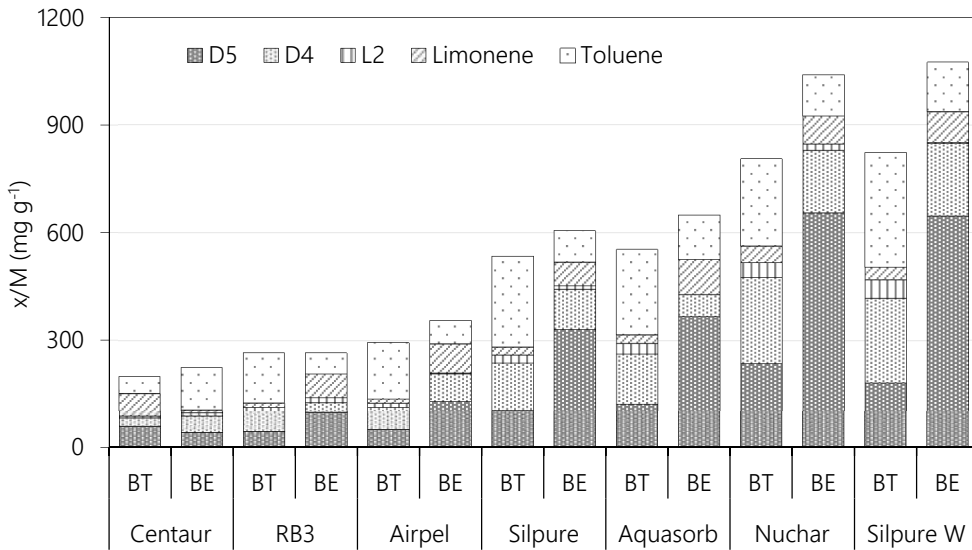


**Figure 7.9** Competitive adsorption capacities reported at L2 breakthrough (BT) and at bed exhaustion (BE).

Comparing the results of the ACs in terms of mass of adsorbate per mass of adsorbent, Silpure W is the best performing AC. Nevertheless, the adsorption capacity for real application in AC filters must be reported in terms of adsorbent volume, since it is the parameter which rules the quantity of adsorbent included in the AC vessels. The term bed volumes (BV) is defined as Eq. 6 and allows the comparison of the breakthrough curves regardless the bed size:

$$BV = \frac{V_W}{V_F} \quad (\text{Eq. 6})$$

where  $V_w$  is the volume of gas treated and  $V_f$  is the volume of the adsorbent bed.

In this sense, comparative results of the currently used Airpel and the best performing Nuchar are shown in Table 7.4. The apparent density of Nuchar is lower than Airpel, which results in a volume of beds treated of 37996 for Nuchar and 17370 for Airpel. Considering this results, the use of the Nuchar enlarged the BV treated a 120%.

**Table 7.4**

Results of the multicomponent removal efficiency expressed in BV for the set of AC

	RB3	Airpel	Centaur	Silpure	Aquasorb	Silpure W	Nuchar
Breakthrough time [min]	39	42	35	94	127	142	161
Apparent density [kg m <sup>-3</sup> ]	493	517	733	365	320	301	295
BV	15382	17371	20524	27448	32512	34194	37996

Finally, the competitive adsorption was investigated in the presence of humidity in the gas flow. To perform these tests, water was injected in the multicomponent gas test using a syringe pump in order to obtain a RH of 35%. The results, expressed as BV treated are shown in Figure 10 compared to the dry test gas discussed before. The outcome differs depending on the AC considered so far. There is a clear reduction on the adsorption capacity of Aquasorb, Centaur and RB3, while the performance of Airpel and Silpure is not decreased by the presence of humidity.

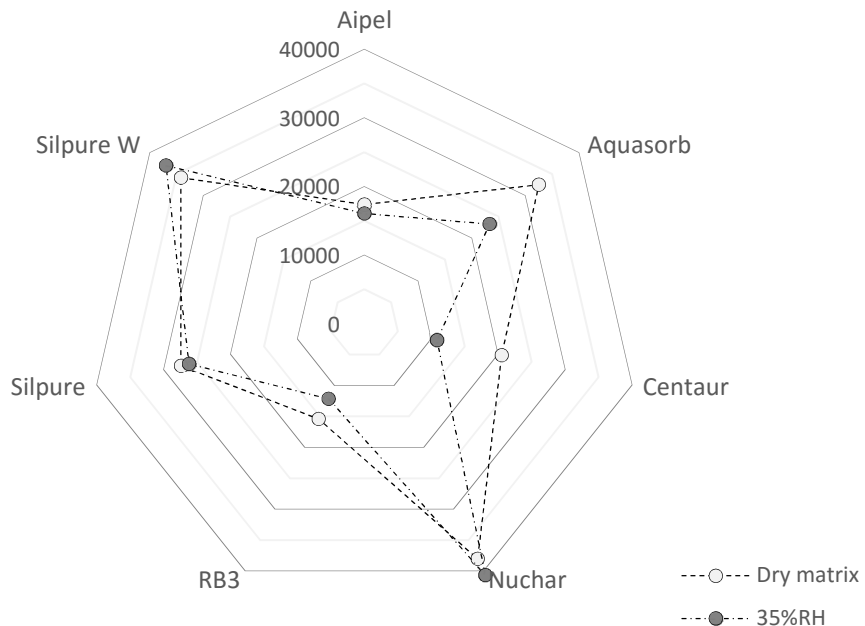


**Figure 7.10** Multicomponent adsorption in N<sub>2</sub> dry matrix vs in presence of 35% humidity. Results expressed in BV treated at L2 breakthrough.

On the other hand, Nuchar and Silpure W, phosphoric activated carbons, slightly increase their adsorption capacity where there is water in the multicomponent gas matrix. This finding, which needs further investigation, points out to some catalytic reactions that may enhance the siloxane removal when water is available in the carbon surface.

Taking into account that the AC price of steam-AC<sup>1</sup> range from 1.5 to 4 € kg<sup>-1</sup> and chemical-AC range from 4 to 8 € kg<sup>-1</sup>, and the siloxane removal efficiencies obtained, the cost of the biogas treatment as function of the AC used is shown in Figure 7.11. It can be concluded that, although the price of chemical-AC is higher, their yield is higher in terms of gas volume treated.

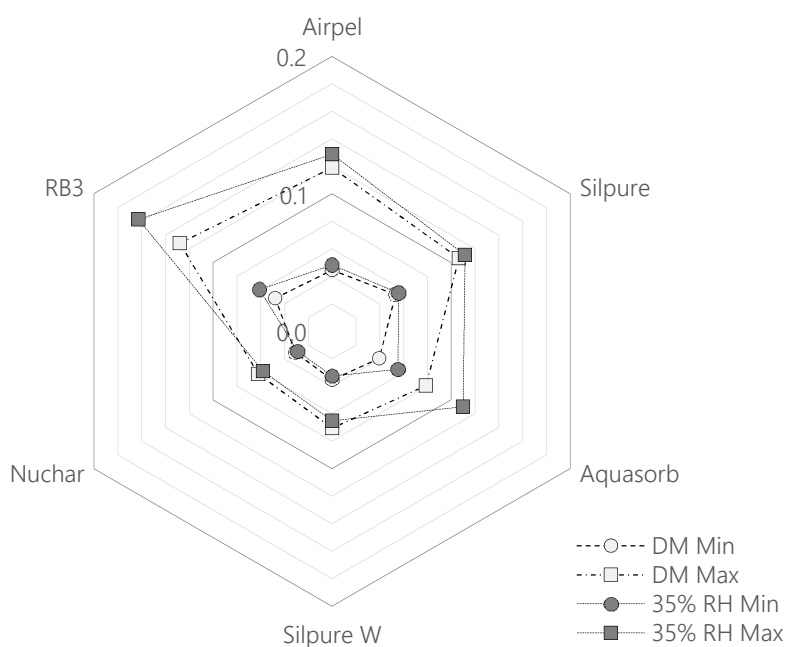


**Figure 7.11** Comparative cost of siloxane removal per volume of biogas treated [€ m<sup>-3</sup>] at the conditions tested at dry N<sub>2</sub> matrix gas (BD) (void symbols) and with 35% humidity (full symbols). Minimum (round) and Maximum (square) costs calculated as function of the AC price (steam-AC: 1.5-4€ kg<sup>-1</sup>, chemical-AC: 4-8€ kg<sup>-1</sup>).

<sup>1</sup> Personal communication from AC producers in the USA

## 7.5 Finals remarks

---

The biogas analyzed in the case of study WWTP contains an average siloxane concentration of up to  $100 \text{ mg m}^{-3}$  together with a wide variety of VOCs. Thermal desorption was attempted in order to regenerate the Airpel AC currently used for siloxane abatement with low efficiency results. Therefore, the use of a chemically-activated carbons is considered, and its performance in realistic conditions is assessed and compared to Airpel.

The presence of 20% humidity in the carrier gas did not show relevant effects on D4 adsorption. Nevertheless, higher humidity content, up to 80%, led to a reduction on the adsorption capacity, most likely as a result of the formation of hydrogen bonds between water molecules and the oxygen functional groups of the carbon surface, which blocked the adsorptive sites. Further, a mix of  $\text{CH}_4$  and  $\text{CO}_2$  was used as synthetic biogas matrix, concluding that the D4 removal performance in these cases was reduced up to 33% with respect to the adsorption under dry nitrogen experiments.

D4 adsorption isotherms were obtained to ascertain the influence of the adsorbate concentration. As expected, in the concentrations found in the biogas samples, the  $x/M$  was notably reduced, however, the D4 removal at this condition of Nuchar still triplicates the results of Airpel. Therefore, the higher performance of this AC in high concentration tests is validated at low concentration.

The conclusion drawn about the relation between textural development of the AC and the D4 adsorption capacity were also applicable to the L2 and D5 removal, since the best performing AC are also the chemically activated.

In competitive adsorption of various siloxanes with VOCs, L2 is the weakly adsorbed siloxane. Nevertheless, the behavior of chemical-AC differs from steam-AC since the first ones have more affinity for siloxanes than VOCs. The removal efficiencies are assessed at L2 breakthrough time, since is the first siloxane breaking up. The chemical-AC are the best performing, in particular Nuchar is the AC that treats a higher number of bed volumes, leading to a 120% enlargement of the adsorbent bed live time compared to the currently used Airpel. Although more research is required, humidity increased the performance of multicomponent adsorption for the phosphoric-activated carbons Nuchar and Silpure W.

To sum up, Table 7.5 shows the advantages and disadvantages identified for each material. Taking into account that the regeneration methods have to be further improved, the change of the adsorbent to use a chemical-activated carbon would suppose great saving on the AC consumed.

**Table 7.5**

Advantages and weaknesses of the adsorbent materials tested.

Adsorbent	Siloxane removal	Adsorbent costs	Thermal regeneration	AOP regeneration
Steam activated carbon	++	++++	+	-
Chemical activated carbon	++++	++	-	-
Synthetic zeolite	+	-	-	++

---

## Chapter 8

# GENERAL DISCUSSION



## General discussion

---

Siloxanes, which are consumed in huge quantities in a wide range of applications and consumer products, are considered the most harmful components for the energy use of the biogases produced in landfills and wastewater treatment plants. Therefore siloxane removal is a mandatory step before the biogas combustion. This removal process can be performed with the help of several technologies including adsorption, absorption, condensation, membrane separation and biological degradation. These technologies have been extensively reviewed in the literature (see Ajhar *et al.* (2010); Soreanu *et al.* (2011); Arespacochaga *et al.* (2015)). These studies agree that non-regenerative adsorption onto activated carbon is, so far, the most efficient removal technology from both technical and economical points of view. Nevertheless, the processes involved in the siloxane adsorption have not been properly defined to date and the chemical processes taking place on the carbon surface have received little scholarly attention.

This thesis constitutes a step forward in bridging this knowledge gap since it explores and determines the mechanisms of interaction of siloxanes with both activated carbon and zeolites surfaces, with the aim to improve the performance of the adsorption for siloxane removal and the regeneration technologies of the exhausted adsorbents. In order to consider the technical implications of the fundamental knowledge reported on Chapter 4, 5 and 6, the results have been discussed in a context as realistic as possible. To reach this goal, in the framework of Chapter 7 we applied our findings in a real case study and performed multicomponent adsorption tests.

### *Adsorption of siloxanes*

Adsorption on porous materials is the most common technique for removing siloxanes from biogases (Arespacochaga *et al.* (2015)). This thesis establishes the D4 adsorption mechanisms on activated carbons and zeolites. For this purpose, a wide set of commercial activated carbons (Chapter 4) and zeolites (Chapter 6) were tested in dynamic adsorption tests in order to determine the relation of the adsorption capacity with the textural and chemical properties of both types of adsorbents.

In Chapter 4, we report on the results of tests performed on a total of 12 commercial activated carbons used for the removal of D4, including chemically activated wood based carbons. Following the study of Yu *et al.* (2007) and Matsui *et al.* (2010), we found that the D4 adsorption capacity of the AC tested is positively correlated with the specific surface area and the pore volume. We also analyzed the narrower micropore volumes (<0.7 nm), which diameter is smaller than D4 molecular size (1.08-1.03 nm). As expected, no correlation was observed, concluding that only large micropores are relevant for D4 adsorption. At the same time, we found that a compromise between the meso and micropore volumes is desirable so as to enhance the adsorption capacity, not only for the possibility to allocate quantities of D4 but also in order to facilitate the diffusion of D4 into the larger micropore network.

Wood-based chemically activated carbons were included in the tests described in Chapter 4. We saw that the porosity development of this type of AC was higher than others reported before in the literature, therefore they allowed higher D4 adsorption capacities than steam activated carbons. However, the high amount of oxygen functionalities resulting from the chemical activation also led to high polymerization ratios, which are discussed in section 7.2, that hamper the thermal desorption for the regeneration of the exhausted adsorbents.

Inorganic materials were investigated for the removal of siloxanes, including silica gel and alumina (Sigot *et al.* 2014; Finocchio *et al.* 2009; Jiang *et al.* 2016) working with mesoporous aluminosilicates found a correlation between porosity and D4 adsorption capacity, although the pore volume of their materials is up to  $0.27 \text{ cm}^3 \text{ g}^{-1}$ , that is five times lower than the best AC described in Chapter 4 of the present work. Nevertheless, the D4 uptake of the zeolites we tested (see Chapter 6) was clearly not depending on the pore size. By studying a set of three different zeolite framework types, it was concluded that BEA type zeolites perform better than Y zeolites, which present larger pore diameter. Given the catalytic properties of BEA zeolites towards D4 ring-opening, silanediols are formed, narrow enough to diffuse in the channel structure, thus increasing the D4 uptake. Therefore, we can assert that the D4 adsorption capacity of D4 onto inorganic materials, which present narrower pore sizes than AC, depends on the capacity to transform cyclic siloxanes into narrower molecules.

All the materials considered for D4 removal were tested in lab-scale experiments conducted with dry N<sub>2</sub> gas matrix and high D4 concentration, leading to high adsorption capacities. To assess the adsorption in more realistic conditions, similar to those found in real biogases, several tests were performed at different settings with wood-based chemically-activated carbon, the best performing of all the adsorbents tested and compared to the anthracite-based steam-activated carbon currently used in the case of study WWTP described in Chapter 7.

In the experiments carried out with the chemically-AC Nuchar, the presence of humidity in the carrier gas led to a reduction on the adsorption capacity, most likely as a result of the formation of hydrogen bonds between water molecules and the oxygen functional groups of the carbon surface, hence blocking the adsorptive sites. Further, a mix of CH<sub>4</sub> and CO<sub>2</sub> was used as synthetic biogas matrix, concluding that the D4 diffusivity into the AC porosity is scarce. The D4 removal performance in these cases was reduced up to 33% with respect to the adsorption under dry nitrogen experiments.

Moreover, both Airpel and Nuchar ACs were tested in D4 adsorption tests at low concentration. At concentrations similar to those found in real biogas (20 mg m<sup>-3</sup>) the adsorption capacity of the AC is reduced to 72 and 226 mg g<sup>-1</sup> respectively. These results are in accordance to those obtained by Boulinguez and Le Cloirec (2010) working in static D4 low concentration adsorption with a wood-based carbon, the best performing adsorbent for siloxane reported in the state of the art literature.

In competitive adsorption, D4 is strongly adsorbed than smaller molecules such as L2 and toluene, but it is rolled up by limonene only in the case of Airpel. Phosphoric-activated carbons showed higher uptakes of siloxanes than VOCs, while steam-activated behave oppositely. However, further research is needed in order to establish the uptake mechanisms taking place in competitive adsorption.

#### *Octamethylcyclotetrasiloxane ring-opening transformation*

The study of Finocchio *et al.* (2009) investigating the thermal regeneration of siloxane-exhausted AC, showed that polymerization products of cyclic hexamethyltrisiloxane were found in the AC surface by FT-IR analysis. It was suggested that besides physical adsorption, chemical interactions could take place on the adsorbents surface. In this

dissertation, we prove that D4 undergoes ring-opening reactions catalyzed by the acidic groups of both AC and zeolites, which are discussed in this section.

Using the FT-IR spectra of the D4-spent AC, the presence of other siloxanes than D4 was detected in the double bands that appeared at  $1100\text{ cm}^{-1}$  (Figure 4.12), and it was further proven by the GC-MS analysis of the hexane extraction of the samples. Although we proposed  $\alpha$ - $\omega$ -silanediols as intermediate molecules of the ring-opening polymerization leading to the formation of larger cyclic siloxanes (Figure 4.17), the hexane-based extraction method followed (see Chapter 4, section 3.3.2) did not allow us to detect them in the spent carbon analysis. We proposed the ring-opening polymerization as a time-dependent phenomena, since only the  $\alpha$ - $\omega$ -silanediols condensation products (i.e. D5, D6, and D7) were found and their concentration varied depending on the time passed before the extraction.

On the short term, the presence of these cyclic siloxanes was only noticeable in chemically activated carbons, which present a higher amount of acidic functionalities, which catalyze the ring-opening hydrolysis reaction. When the hexane extraction was carried out after 30 days of contact, a higher amount of cyclic siloxanes was found, indicating the condensation of silanediols. The polymerization ratio, defined as Equation 4 (Section 4.3.4), was found to be clearly dependent on the concentration of oxygen functionalities, specially phenolic and carboxylic groups. In the case of AC, since their porous structure is large enough to fit the D4 molecules, the adsorption capacity was not affected by this polymerization. However, the formation of larger molecular weight siloxanes hampers the thermal regeneration of the exhausted adsorbents.

Further, when working with zeolites, we used anhydrous THF to extract the molecules adsorbed on the zeolites. In this case, since THF is a suitable solvent for both polar and non-polar compounds,  $\alpha$ - $\omega$ -silanediols could be identified in the GC-MS analysis of the extract. The compounds identified resulting from the D4 ring-opening, scission and condensation include the cyclic siloxanes and silanediols listed in Table 6.2.

Since the pore size of the zeolites considered is lower than the molecular size of D4, a high ratio of transformation to silanediols is required in order to obtain high adsorption capacities. BEA type zeolites display the highest amount of both Brønsted and Lewis acidic sites of the tested zeolites, and they also have a channel size large enough to fit the

silanediols. Therefore, we can assert that silanediols formed on BEA zeolites surface can diffuse into the channel structure, increasing the adsorption capacity and thus displaying the best D4 removal performance so far.

### *Regeneration of spent adsorbents*

This dissertation examines the polymerization leading to the formation of non-volatile higher molecular weight silicon polymers during D4 adsorption on AC and zeolites. In the specialized literature, this phenomenon is reported to occur irrespective of the adsorbent type, including silica gel, molecular sieves or mesoporous aluminosilicates (Kajolinna *et al.*, 2015; Sigot *et al.*, 2015; Jiang *et al.*, 2016), and it is known to trigger the ineffectiveness of the thermal regeneration of the adsorbents (Finocchio *et al.* (2009). Therefore, the adsorbent beds must be replaced regularly, generating high costs (Dewil *et al.*, 2006). Thus, although adsorption is regarded as a viable solution for siloxane removal from biogas, future trends will focus on regenerative and more selective systems to reduce costs for media renewal, as reported in the exhaustive reviews by Ajhar *et al.* (2010) and more recently by Arespacochaga *et al.* (2015).

In this dissertation, we propose the sequential application of adsorption/oxidation for the removal of siloxanes. The AOP-driven regeneration of exhausted adsorbents is an emerging technology that involves the sequential synergetic use of two reliable and well-established treatment technologies: contaminant adsorption onto porous materials and oxidation using AOPs. Although the simultaneous combination of both processes (i.e., catalytic heterogeneous AOPs) is a prominent industrial technology and a very active field for research, its sequential application has not been thoroughly investigated so far (Georgi *et al.*, 2010; Huling *et al.*, 2012; Anfruns *et al.*, 2013).

We applied H<sub>2</sub>O<sub>2</sub> and O<sub>3</sub> for the regeneration of both siloxane-exhausted AC, Fe-amended AC and Fe-zeolites. As revealed by the FT-IR analysis of the regenerated adsorbents, the oxidative wet treatments were successful in removing a substantial part of the siloxane adsorbed. Nevertheless, the loss of catalytic activity of the adsorbents led to a reduction of the regeneration efficiency. As pointed out by Huling *et al.* (2007, 2009, 2010) the iron amendment increased the overall performance of the adsorption/oxidation process using H<sub>2</sub>O<sub>2</sub>, achieving a complete regeneration after the first use. However, in the

following cycles of regeneration, both by Fenton-like treatment or ozonation, the induced changes in the carbon material, the iron leaching and/or the increasing accumulation of non-reacted D4 or D4 by-products contributed to the decrease in the performance.

Zeolites were considered for adsorption/oxidation processes to overcome the propensity of AC to oxidation and iron leaching. As aluminosilicate materials, zeolites are resistant to oxidation and therefore they were expected to work well as long-lived recyclable adsorbents. Nevertheless, the D4 uptake of zeolites depends on the catalytic transformation of the pristine molecules to narrower silanediols. The formed silanediols are water-soluble, therefore more easily removable from the zeolite; yet, in following adsorption/oxidation cycles, the catalytic activity of the zeolite towards the ring-opening of D4 is reduced, leading to the decrease of the overall performance.

Overall, the yield of the process is substantially higher for the Fe-BEA zeolite, which can be reused five times while adsorbing up to the 50% of the original D4 adsorption capacity (Chapter 6). In turn, Fe-Nuchar (Chapter 5) was used four times with similar regeneration efficiency. Notwithstanding, we should take into account that the D4 uptake of that activated carbon is 10 times higher than the one of zeolites. For the same reason, the optimum H<sub>2</sub>O<sub>2</sub> dosage needed for the optimum regeneration of Fe-Nuchar is higher than the one for the zeolite.

In conclusion, regeneration efficiencies obtained are restricted for both type of materials, but the understanding of the retention and transformation mechanisms accomplished in this thesis should facilitate further investigation of efficient regeneration processes.

#### *Further research*

In the light of the results obtained and discussed in the present dissertation, further research should be performed focusing on the enhancement of the siloxane uptake while improving the regenerability of the adsorbents. In this sense, concerning the use of AC, the mechanisms of multicomponent competitive adsorption must be deeply investigated provide that this knowledge will guide the modification of AC surfaces in order to reach higher siloxane uptake. We found that phosphoric-activated carbons present higher uptake of siloxanes than VOCs, on the contrary of steam-activated, which suggests that surface properties given by the chemical activation catalyze siloxane transformation

reactions leading to the enhancement of the siloxane uptake. The formation of silanediols, as a result of cyclic siloxanes ring-opening, that could be detached and removed by wet treatments for the regeneration of the material, may be enhanced by the modification of the adsorbent surface. To achieve so, zeolites are also promising materials given their catalytic properties. The performance of tailored natural zeolites, whose price is inexpensive compared to the synthetic ones tested before, should be further investigated in real scenario conditions, since they can be considered as alternative materials as long as could be easier regenerated.

Alternative regeneration techniques must maintain the AC surface properties, which ensure the siloxane uptake, in the pristine conditions. Therefore, the use of high temperature steam flow is suggested to be explored as a cost-effective technology. The combination of water-based and hot air desorption in mild conditions should be possible. The humidity may help in the detachment of siloxanes, since water is needed in the hydrolysis reactions that lead to siloxane bonds scissions forming higher vapor pressure siloxanes, which should be more easily desorbed by thermal treatment at mild conditions.

The multicomponent adsorption must be also assessed in the presence of humidity and synthetic biogas gas-matrix before the implementation of the improved materials to real biogas of the lab-scale tests.  $H_2S$  should also be considered in further research. Hereof Centaur is an AC specifically developed for the removal of this compound usually present in biogas in considerable concentrations. The siloxane removal results of Centaur are in the low range, but the possibility of the abatement of  $H_2S$  together with siloxanes should be considered. To test the adsorbents in real biogas, on-site experimentation must be considered since the storage under pressure and transport of raw biogas is not an alternative because of the difficulty of maintain the integrity of the samples and the occasional composition fluctuations.

The field tests, economically feasible and without inversions costs, will validate the lab-scale results obtained. Therefore, the enhancement of the bed adsorbents lifetime proposed in this dissertation would be validated in on site experimentations substituting the currently used AC for an already commercial phosphoric-activated carbon, such as Nuchar or Silpure W.



---

## Chapter 9

# GENERAL CONCLUSIONS



## General conclusions

---

Regarding D4 adsorption onto activated carbon:

- Textural development rules the D4 adsorption capacity; thus the performance of an activated carbon can be predicted by its pore volume. Accordingly, chemically activated carbons are the best performing at siloxane removal.
- Wood-based carbons activated with  $\text{H}_3\text{PO}_4$  possess the highest amount of phenolic and carboxylic functional groups, leading to a higher D4 ring-opening polymerization.

Regarding the regeneration of D4-exhausted activated carbon:

- $\text{O}_3$  has a limited efficiency, recovering 31-40% of the x/M due to the  $\text{O}_3$ -induced modifications of the textural and chemical properties of the AC. The different textural and chemical properties of the AC did not show differences on the regeneration efficiency.
- Iron deposition on the AC increased the overall performance of the adsorption/oxidation process using  $\text{H}_2\text{O}_2$  since an almost complete recovery of the D4 adsorption capacity could be achieved after the first regeneration step. The catalytic activity of the iron plausibly promoted the  $\cdot\text{OH}$  formation and a higher ratio of D4 oxidation.
- In three successive cycles, the iron leaching of the carbon, the induced changes in the carbon material itself and/or the increasing accumulation of non-reacted D4 contributed to the decrease in the regeneration performance.

Regarding the performance of zeolites:

- BEA zeolites, due to their high content of Brønsted and Lewis acidic sites, show the highest catalytic activity for the siloxane ring-opening and the formation of  $\alpha$ - $\omega$ -silanediols, narrow enough to diffuse into the channels, enhancing the removal efficiency for D4.

- Soluble silanediols formed during D4 adsorption are easily removed in wet regeneration treatments by using only water; however, the regeneration is incomplete.
- Adding H<sub>2</sub>O<sub>2</sub> in a heterogeneous Fenton-like regeneration treatment leads to a complete regeneration of the Fe-BEA zeolite in the first cycle. The regeneration efficiency obtained with oxidation by 10 min ozonation is similar. The recyclability of the zeolite in successive cycles is hampered by the accumulation of carbonaceous material that cause a loss of catalytic activity, affecting both the adsorption and the regeneration stages.
- The block of LAS and BAS reduces the D4 transformation into silanediols, the fundamental step that rules D4 uptake. Zeolites could be considered as an alternative adsorbents for AC as long as their catalytic activity towards silanediols formation could be largely enhanced, thus being efficiently regenerable with wet treatments at long term.

Regarding the implementation of the results:

- High humidity content, CH<sub>4</sub> and CO<sub>2</sub> instead of N<sub>2</sub> matrix, and low concentration of siloxane, reduce the performance of the adsorbents at different magnitude. However the tendencies found were validated under such conditions at lab-scale, pointing out that best materials siloxane removal are phosphoric-activated carbons.
- The knowledge gained is directly transferable to field application since the materials proposed to upgrade the siloxane removal system are already commercial, like Nuchar and Silpure W.

---

## Chapter 10

# REFERENCES



## References

---

- Abatzoglou, N. and Boivin, S. (2009). "A review of biogas purification processes." *Biofuels, Bioproducts and Biorefining* 3 (1): 42-71.
- Ajhar, M., Bannwarth, S., Stollenwerk, K. H., Spalding, G., Yüce, S., Wessling, M. and Melin, T. (2012). "Siloxane removal using silicone-rubber membranes." *Separation and Purification Technology* 89: 234-244.
- Ajhar, M. and Melin, T. (2006). "Siloxane removal with gas permeation membranes." *Desalination* 200 (1-3): 234-235.
- Ajhar, M., Travesset, M., Yuce, S. and Melin, T. (2010). "Siloxane removal from landfill and digester gas - A technology overview." *Bioresource Technology* 101 (9): 2913-2923.
- Álvarez, P. M., Beltrán, F. J., Gómez-Serrano, V., Jaramillo, J. and Rodríguez, E. M. (2004). "Comparison between thermal and ozone regenerations of spent activated carbon exhausted with phenol." *Water Research* 38 (8): 2155-2165.
- Alvarez, P. M., Beltran, F. J., Masa, F. J. and Pocostales, J. P. (2009). "A comparison between catalytic ozonation and activated carbon adsorption/ozone-regeneration processes for wastewater treatment." *Applied Catalysis B-Environmental* 92 (3-4): 393-400.
- Andreyev, M. K. and Zubkov, O. L. (2012). *Zeolites: Synthesis, chemistry and applications*
- Anfruns, A., García-Suárez, E. J., Montes-Morán, M. A., Gonzalez-Olmos, R. and Martin, M. J. (2014). "New insights into the influence of activated carbon surface oxygen groups on H<sub>2</sub>O<sub>2</sub> decomposition and oxidation of pre-adsorbed volatile organic compounds." *Carbon*.
- Anfruns, A., Montes-Morán, M. A., Gonzalez-Olmos, R. and Martin, M. J. (2013). "H<sub>2</sub>O<sub>2</sub>-based oxidation processes for the regeneration of activated carbons saturated with volatile organic compounds of different polarity." *Chemosphere* 91 (1): 48-54.
- Appels, L., Baeyens, J. and Dewil, R. (2008). "Siloxane removal from biosolids by peroxidation." *Energy Conversion and Management* 49 (10): 2859-2864.
- Bacenetti, J., Negri, M., Fiala, M. and González-García, S. (2013). "Anaerobic digestion of different feedstocks: Impact on energetic and environmental balances of biogas process." *Science of the Total Environment* 463-464: 541-551.
- Bach, A. and Semiat, R. (2011). "The role of activated carbon as a catalyst in GAC/iron oxide/H<sub>2</sub>O<sub>2</sub> oxidation process." *Desalination* 273 (1): 57-63.

- Bansal, R. C., Goyal, M. (2005). *Activated Carbon Adsorption*, Taylor&Francis.Taylor&Francis
- Becke, A. D. (1993). "Density-functional thermochemistry. III. The role of exact exchange." *The Journal of Chemical Physics* 98 (7): 5648-5652.
- Bletsou, A. A., Asimakopoulos, A. G., Stasinakis, A. S., Thomaidis, N. S. and Kannan, K. (2013). "Mass loading and fate of linear and cyclic siloxanes in a wastewater treatment plant in Greece." *Environmental Science and Technology* 47 (4): 1824-1832.
- Boulinguez, B. and Le Cloirec, P. (2010). "Adsorption on Activated Carbons of Five Selected Volatile Organic Compounds Present in Biogas: Comparison of Granular and Fiber Cloth Materials." *Energy & Fuels* 24: 4756-4765.
- C.M. Baerlocher, L. B. O., D.H. (2007). "Atlas of Zeolite Framework Types."
- Carlsson, M., Lagerkvist, A. and Morgan-Sagastume, F. (2012). "The effects of substrate pre-treatment on anaerobic digestion systems: A review." *Waste Management* 32 (9): 1634-1650.
- Cavinato, C., Bolzonella, D., Pavan, P., Fatone, F. and Cecchi, F. (2013). "Mesophilic and thermophilic anaerobic co-digestion of waste activated sludge and source sorted biowaste in pilot- and full-scale reactors." *Renewable Energy* 55: 260-265.
- Coelho, C., Oliveira, A. S., Pereira, M. F. R. and Nunes, O. C. (2006). "The influence of activated carbon surface properties on the adsorption of the herbicide molinate and the bio-regeneration of the adsorbent." *Journal of Hazardous Materials* 138 (2): 343-349.
- De Arespacochaga, N., Valderrama, C., Raich-Montiu, J., Crest, M., Mehta, S. and Cortina, J. L. (2015). "Understanding the effects of the origin, occurrence, monitoring, control, fate and removal of siloxanes on the energetic valorization of sewage biogas-A review." *Renewable and Sustainable Energy Reviews* 52: 366-381.
- Dewil, R., Appels, L. and Baeyens, J. (2006). "Energy use of biogas hampered by the presence of siloxanes." *Energy Conversion and Management* 47 (13-14): 1711-1722.
- Dewil, R., Appels, L., Baeyens, J., Buczynska, A. and Van Vaeck, L. (2007). "The analysis of volatile siloxanes in waste activated sludge." *Talanta* 74 (1): 14-19.
- Domínguez, C. M., Quintanilla, A., Ocón, P., Casas, J. A. and Rodriguez, J. J. (2013). "The use of cyclic voltammetry to assess the activity of carbon materials for hydrogen peroxide decomposition." *Carbon* 60: 76-83.
- Dudzina, T., von Goetz, N., Bogdal, C., Biesterbos, J. W. H. and Hungerbühler, K. (2014). "Concentrations of cyclic volatile methylsiloxanes in European cosmetics and

- personal care products: Prerequisite for human and environmental exposure assessment." *Environment International* 62 (0): 86-94.
- Fairén-Jiménez, D., Carrasco-Marín, F. and Moreno-Castilla, C. (2007). "Adsorption of benzene, toluene, and xylenes on monolithic carbon aerogels from dry air flows." *Langmuir* 23 (20): 10095-10101.
- Faria, P. C. C., Órfão, J. J. M. and Pereira, M. F. R. (2005). "Mineralisation of coloured aqueous solutions by ozonation in the presence of activated carbon." *Water Research* 39 (8): 1461-1470.
- Figueiredo, J. L. and Pereira, M. F. R. (2010). "The role of surface chemistry in catalysis with carbons." *Catalysis Today* 150 (1-2): 2-7.
- Figueiredo, J. L., Pereira, M. F. R., Freitas, M. M. A. and Órfão, J. J. M. (1999). "Modification of the surface chemistry of activated carbons." *Carbon* 37 (9): 1379-1389.
- Finocchio, E., Montanari, T., Garuti, G., Pistarino, C., Federici, F., Cugino, M. and Busca, G. (2009). "Purification of Biogases from Siloxanes by Adsorption: On the Regenerability of Activated Carbon Sorbents." *Energy & Fuels* 23 (8): 4156-4159.
- Flanigen, E. M., Jansen, J. C. and van Bekkum, H. (1991). *Introduction to Zeolite Science and Practice*. E. Sevier.
- Frisch, M. J., Pople, J. A. and Binkley, J. S. (1984). "Self-consistent molecular orbital methods 25. Supplementary functions for Gaussian basis sets." *The Journal of Chemical Physics* 80 (7): 3265-3269.
- Genualdi, S., Harner, T., Cheng, Y., MacLeod, M., Hansen, K. M., van Egmond, R., Shoeib, M. and Lee, S. C. (2011). "Global Distribution of Linear and Cyclic Volatile Methyl Siloxanes in Air." *Environmental Science & Technology* 45 (8): 3349-3354.
- Georgi, A., Gonzalez-Olmos, R., Koehler, R. and Kopinke, F.-D. (2010). "Fe-Zeolites as Catalysts for Wet Peroxide Oxidation of Organic Groundwater Contaminants: Mechanistic Studies and Applicability Tests." *Separation Science and Technology* 45 (11): 1579-1586.
- Georgi, A. and Kopinke, F.-D. (2005). "Interaction of adsorption and catalytic reactions in water decontamination processes: Part I. Oxidation of organic contaminants with hydrogen peroxide catalyzed by activated carbon." *Applied Catalysis B: Environmental* 58 (1-2): 9-18.
- Giraudet, S., Boulinguez, B. and Le Cloirec, P. (2014). "Adsorption and electrothermal desorption of volatile organic compounds and siloxanes onto an activated carbon fiber cloth for biogas purification." *Energy and Fuels* 28 (6): 3924-3932.
- Gislon, P., Galli, S. and Monteleone, G. (2013). "Siloxanes removal from biogas by high surface area adsorbents." *Waste Management* 33 (12): 2687-2693.

- Gonzalez-Olmos, R., Holzer, F., Kopinke, F. D. and Georgi, A. (2011). "Indications of the reactive species in a heterogeneous Fenton-like reaction using Fe-containing zeolites." *Applied Catalysis a-General* 398 (1-2): 44-53.
- Gonzalez-Olmos, R., Kopinke, F. D., Mackenzie, K. and Georgi, A. (2013). "Hydrophobic Fe-zeolites for removal of MTBE from water by combination of adsorption and oxidation." *Environmental Science and Technology* 47 (5): 2353-2360.
- Gonzalez-Olmos, R., Roland, U., Toufar, H., Kopinke, F. D. and Georgi, A. (2009). "Fe-zeolites as catalysts for chemical oxidation of MTBE in water with H<sub>2</sub>O<sub>2</sub>." *Applied Catalysis B-Environmental* 89 (3-4): 356-364.
- Hamelink, J. L., Simon, P. B. and Silberhorn, E. M. (1996). "Henry's law constant volatilization rate, and aquatic half-life of octamethylcyclotetrasiloxane." *Environmental Science and Technology* 30 (6): 1946-1952.
- Hornig, R. S. and Tseng, I. C. (2008). "Regeneration of granular activated carbon saturated with acetone and isopropyl alcohol via a recirculation process under H<sub>2</sub>O<sub>2</sub>/UV oxidation." *Journal of Hazardous Materials* 154 (1-3): 366-372.
- Huling, S. G., Arnold, R. G., Sierka, R. A., Jones, P. K. and Fine, D. D. (2000). "Contaminant adsorption and oxidation via Fenton reaction." *Journal of Environmental Engineering* 126 (7): 595-600.
- Huling, S. G. and Hwang, S. (2010). "Iron amendment and Fenton oxidation of MTBE-spent granular activated carbon." *Water Research* 44 (8): 2663-2671.
- Huling, S. G., Jones, P. K., Ela, W. P. and Arnold, R. G. (2005). "Fenton-driven chemical regeneration of MTBE-spent GAC." *Water Research* 39 (10): 2145-2153.
- Huling, S. G., Jones, P. K. and Lee, T. R. (2007). "Iron optimization for fenton-driven oxidation of MTBE-spent granular activated carbon." *Environmental Science & Technology* 41 (11): 4090-4096.
- Huling, S. G., Kan, E., Caldwell, C. and Park, S. (2012). "Fenton-driven chemical regeneration of MTBE-spent granular activated carbon - A pilot study." *Journal of Hazardous Materials* 205-206: 55-62.
- Huling, S. G., Kan, E. and Wingo, C. (2009). "Fenton-driven regeneration of MTBE-spent granular activated carbon—Effects of particle size and iron amendment procedures." *Applied Catalysis B: Environmental* 89 (3-4): 651-658.
- Hwang, S., Huling, S. G. and Ko, S. (2010). "Fenton-like degradation of MTBE: Effects of iron counter anion and radical scavengers." *Chemosphere* 78 (5): 563-568.
- Ince, N. H. and Apikyan, I. G. (2000). "Combination of activated carbon adsorption with light-enhanced chemical oxidation via hydrogen peroxide." *Water Research* 34 (17): 4169-4176.

- Jansen, J. C., Creyghton, E. J., Njo, S. L., Van Koningsveld, H. and Van Bekkum, H. (1997). "On the remarkable behaviour of zeolite Beta in acid catalysis." *Catalysis Today* 38 (2): 205-212.
- Jaramillo, J., Gómez-Serrano, V. and Álvarez, P. M. (2009). "Enhanced adsorption of metal ions onto functionalized granular activated carbons prepared from cherry stones." *Journal of Hazardous Materials* 161 (2-3): 670-676.
- Jiang, S., Qiu, T. and Li, X. (2010). "Kinetic study on the ring-opening polymerization of octamethylcyclotetrasiloxane (D4) in miniemulsion." *Polymer* 51 (18): 4087-4094.
- Jiang, T., Zhong, W., Jafari, T., Du, S., He, J., Fu, Y. J., Singh, P. and Suib, S. L. (2016). "Siloxane D4 adsorption by mesoporous aluminosilicates." *Chemical Engineering Journal* 289: 356-364.
- Kajolinna, T., Aakko-Saksa, P., Roine, J. and Káll, L. (2015). "Efficiency testing of three biogas siloxane removal systems in the presence of D5, D6, limonene and toluene." *Fuel Processing Technology* 139: 242-247.
- Katada, N. and Niwa, M. (2004). "Analysis of acidic properties of zeolitic and non-zeolitic solid acid catalysts using temperature-programmed desorption of ammonia." *Catalysis Surveys from Asia* 8 (3): 161-170.
- Kulprathipanja, S. (2010). *Zeolites in Industrial Separation and Catalysis*
- Kwan, W. P. and Voelker, B. M. (2003). "Rates of Hydroxyl Radical Generation and Organic Compound Oxidation in Mineral-Catalyzed Fenton-like Systems." *Environmental Science & Technology* 37 (6): 1150-1158.
- Kwiatkowski, J. F. (2011). *Activated carbon: Classifications, properties and applications*
- Lercher, J. A., Gründling, C. and Eder-Mirth, G. (1996). "Infrared studies of the surface acidity of oxides and zeolites using adsorbed probe molecules." *Catalysis Today* 27 (3-4): 353-376.
- Li, Y., Zhang, W. and Xu, J. (2014). "Siloxanes removal from biogas by a lab-scale biotrickling filter inoculated with *Pseudomonas aeruginosa* S240." *Journal of Hazardous Materials* 275: 175-184.
- Liu, X., Yu, G. and Han, W. (2007). "Granular activated carbon adsorption and microwave regeneration for the treatment of 2,4,5-trichlorobiphenyl in simulated soil-washing solution." *Journal of Hazardous Materials* 147 (3): 746-751.
- Mantzavinos, D., Kassinos, D. and Parsons, S. A. (2009). "Applications of advanced oxidation processes in wastewater treatment." *Water Research* 43 (16): 3901.
- Marsh, H. and Rodríguez-Reinoso, F. (2006). *Activated Carbon*
- Matsui, T. and Imamura, S. (2010). "Removal of siloxane from digestion gas of sewage sludge." *Bioresource Technology* 101: S29-S32.

- McBean, E. A. (2008). "Siloxanes in biogases from landfills and wastewater digesters." *Canadian Journal of Civil Engineering* 35 (4): 431-436.
- McLachlan, M. S., Kierkegaard, A., Hansen, K. M., Van Egmond, R., Christensen, J. H. and Skjøth, C. A. (2010). "Concentrations and fate of decamethylcyclopentasiloxane (D5) in the atmosphere." *Environmental Science and Technology* 44 (14): 5365-5370.
- Montanari, T., Finocchio, E., Bozzano, I., Garuti, G., Giordano, A., Pistarino, C. and Busca, G. (2010). "Purification of landfill biogases from siloxanes by adsorption: A study of silica and 13X zeolite adsorbents on hexamethylcyclotrisiloxane separation." *Chemical Engineering Journal* 165 (3): 859-863.
- Moreno-Castilla, C. (2004). "Adsorption of organic molecules from aqueous solutions on carbon materials." *Carbon* 42 (1): 83-94.
- Mourand, J. T., Crittenden, J. C., Hand, D. W., Perram, D. L. and Notthakun, S. (1995). "Regeneration of spent adsorbents using homogeneous advanced oxidation." *Water Environment Research* 67 (3): 355-363.
- Nam, S., Namkoong, W., Kang, J. H., Park, J. K. and Lee, N. (2013). "Adsorption characteristics of siloxanes in landfill gas by the adsorption equilibrium test." *Waste Management*.
- Newsam, J. M., Treacy, M. M. J., Koetsier, W. T. and De Gruyter, C. B. (1988). "Structural characterization of zeolite beta." *Proceedings of The Royal Society of London, Series A: Mathematical and Physical Sciences* 420 (1859): 375-405.
- Ohannessian, A., Desjardin, V., Chatain, V. and Germain, P. (2008). Volatile organic silicon compounds: The most undesirable contaminants in biogases. 58: 1775-1781.
- Ortega, D. R. and Subrenat, A. (2009). "Siloxane treatment by adsorption into porous materials." *Environmental Technology* 30 (10): 1073-1083.
- Oshita, K., Ishihara, Y., Takaoka, M., Takeda, N., Matsumoto, T., Morisawa, S. and Kitayama, A. (2010). "Behaviour and adsorptive removal of siloxanes in sewage sludge biogas." *Water Science and Technology* 61 (8): 2003-2012.
- Parker Jr, W. O., De Angelis, A., Flego, C., Millini, R., Perego, C. and Zanardi, S. (2010). "Unexpected destructive dealumination of zeolite beta by silylation." *Journal of Physical Chemistry C* 114 (18): 8459-8468.
- Piechota, G., Haggmann, M. and Buczkowski, R. (2012). "Removal and determination of trimethylsilanol from the landfill gas." *Bioresource Technology* 103 (1): 16-20.
- Popat, S. C. and Deshusses, M. A. (2008). "Biological removal of siloxanes from landfill and digester gases: Opportunities and challenges." *Environmental Science and Technology* 42 (22): 8510-8515.

- Raich-Montiu, J., Ribas-Font, C., de Arespacochaga, N., Roig-Torres, E., Broto-Puig, F., Crest, M., Bouchy, L., Cortina, J. L. (2014). "Analytical methodology for sampling and analysing eight siloxanes and trimethylsilanol in biogas from different wastewater treatment plants in europe." *Analytica Chimica Acta* 812: 83-91.
- Rasi, S., Lantela, J. and Rintala, J. (2011). "Trace compounds affecting biogas energy utilisation - A review." *Energy Conversion and Management* 52 (12): 3369-3375.
- Rasi, S., Lantela, J., Veijanen, A. and Rintala, J. (2008). "Landfill gas upgrading with countercurrent water wash." *Waste Management* 28 (9): 1528-1534.
- Rasi, S., Lehtinen, J. and Rintala, J. (2010). "Determination of organic silicon compounds in biogas from wastewater treatments plants, landfills, and co-digestion plants." *Renewable Energy* 35 (12): 2666-2673.
- Rey, A., Faraldos, M., Bahamonde, A., Casas, J. A., Zazo, J. A. and Rodriguez, J. J. (2008). "Role of the Activated Carbon Surface on Catalytic Wet Peroxide Oxidation." *Industrial & Engineering Chemistry Research* 47 (21): 8166-8174.
- Rey, A., Zazo, J. A., Casas, J. A., Bahamonde, A. and Rodriguez, J. J. (2011). "Influence of the structural and surface characteristics of activated carbon on the catalytic decomposition of hydrogen peroxide." *Applied Catalysis a-General* 402 (1-2): 146-155.
- Ribeiro, R. S., Silva, A. M. T., Figueiredo, J. L., Faria, J. L. and Gomes, H. T. (2013). "The influence of structure and surface chemistry of carbon materials on the decomposition of hydrogen peroxide." *Carbon* 62: 97-108.
- Rivera-Utrilla, J., Sanchez-Polo, M., Ferro-García, M. ., Prados-Joya, G. and Ocampo-Perez, R. (2013). "Pharmaceuticals as emerging contaminants and their removal from water. A review." *Chemosphere* 93 (7): 1268-1287.
- Sanchez-Polo, M., Rivera-Utrilla, J., Prados-Joya, G., Ferro-García, M. A. and Bautista-Toledo, I. (2008). "Removal of pharmaceutical compounds, nitroimidazoles, from waters by using the ozone/carbon system." *Water Research* 42 (15): 4163-4171.
- Schweigkofler, M. and Niessner, R. (2001). "Removal of siloxanes in biogases." *Journal of Hazardous Materials* 83 (3): 183-196.
- Seredych, M. and Badosz, T. J. (2008). "Desulfurization of digester gas on wood-based activated carbons modified with nitrogen: Importance of surface chemistry." *Energy and Fuels* 22 (2): 850-859.
- Serp, P. and Figueiredo, J. L. (2008). *Carbon Materials for Catalysis*
- Shahbazi, A., Gonzalez-Olmos, R., Kopinke, F. D., Zarabadi-Poor, P. and Georgi, A. (2014). "Natural and synthetic zeolites in adsorption/oxidation processes to remove surfactant molecules from water." *Separation and Purification Technology* 127: 1-9.

- Sigot, L., Ducom, G. and Germain, P. (2015). "Adsorption of octamethylcyclotetrasiloxane (D4) on silica gel (SG): Retention mechanism." *Microporous and Mesoporous Materials* 213: 118-124.
- Simon-Masseron, A., Marques, J. P., Lopes, J. M., Ribeiro, F. R., Gener, I. and Guisnet, M. (2007). "Influence of the Si/Al ratio and crystal size on the acidity and activity of HBEA zeolites." *Applied Catalysis A: General* 316 (1): 75-82.
- Soreanu, G., Béland, M., Falletta, P., Edmonson, K., Svoboda, L., Al-Jamal, M. and Seto, P. (2011). "Approaches concerning siloxane removal from biogas - A review." *Canadian Biosystems Engineering / Le Genie des biosystems au Canada* 53: 8.1-8.18.
- Stavitskaya, S. S., Goba, V. E. and Tsyba, N. N. (2002). "Comparison of various procedures for regeneration of activated carbons used for recuperation of ethyl acetate." *Russian Journal of Applied Chemistry* 75 (12): 1956-1959.
- Tansel, B. and Surita, S. C. (2014). "Oxidation of siloxanes during biogas combustion and nanotoxicity of Si-based particles released to the atmosphere." *Environmental Toxicology and Pharmacology* 37 (1): 166-173.
- Toledo, L. C., Silva, A. C. B., Augusti, R. and Lago, R. M. (2003). "Application of Fenton's reagent to regenerate activated carbon saturated with organochloro compounds." *Chemosphere* 50 (8): 1049-1054.
- Urban, W., Lohmann, H. and Gómez, J. I. S. (2009). "Catalytically upgraded landfill gas as a cost-effective alternative for fuel cells." *Journal of Power Sources* 193 (1): 359-366.
- Vaidya, A. A. and Kumar, V. G. (1998). "Silica-alumina catalysts for polymerization of cyclic siloxanes." *Journal of Applied Polymer Science* 70 (4): 629-635.
- Valdés, H. and Zaror, C. A. (2006a). "Heterogeneous and homogeneous catalytic ozonation of benzothiazole promoted by activated carbon: Kinetic approach." *Chemosphere* 65 (7): 1131-1136.
- Valdés, H. and Zaror, C. A. (2006b). "Ozonation of benzothiazole saturated-activated carbons: Influence of carbon chemical surface properties." *Journal of Hazardous Materials* 137 (2): 1042-1048.
- Varaprath, S. and Lehmann, R. G. (1997). "Speciation and quantitation of degradation products of silicones (silane/siloxane diols) by gas chromatography-mass spectrometry and stability of dimethylsilanediol." *Journal of Environmental Polymer Degradation* 5 (1): 17-31.
- Vega, E., Lemus, J., Anfruns, A., Gonzalez-Olmos, R., Palomar, J. and Martin, M. J. (2013). "Adsorption of volatile sulphur compounds onto modified activated carbons:

- Effect of oxygen functional groups." *Journal of Hazardous Materials* 258-259: 77-83.
- Von Gunten, U. (2003). "Ozonation of drinking water: Part I. Oxidation kinetics and product formation." *Water Research* 37 (7): 1443-1467.
- Wang, D. G., Norwood, W., Alaei, M., Byer, J. D. and Brimble, S. (2013). "Review of recent advances in research on the toxicity, detection, occurrence and fate of cyclic volatile methyl siloxanes in the environment." *Chemosphere* 93 (5): 711-725.
- Warner, N. A., Evenset, A., Christensen, G., Gabrielsen, G. W., Borga, K. and Leknes, H. (2010). "Volatile Siloxanes in the European Arctic: Assessment of Sources and Spatial Distribution." *Environmental Science & Technology* 44 (19): 7705-7710.
- Whelan, M. J., Estrada, E. and Van Egmond, R. (2004). "A modelling assessment of the atmospheric fate of volatile methyl siloxanes and their reaction products." *Chemosphere* 57 (10): 1427-1437.
- Wheless, E., Pierce, J. (2004). Siloxanes in Landfill and Digester Gas Update. SWANA 27th Landfill Gas Conference. San Antonio, Texas.
- Xiao, F. S. and Meng, X. (2015). Zeolites in sustainable chemistry: Synthesis, characterization and catalytic applications
- Xu, L., Shi, Y. and Cai, Y. (2013). "Occurrence and fate of volatile siloxanes in a municipal Wastewater Treatment Plant of Beijing, China." *Water Research* 47 (2): 715-724.
- Yashiro, T., Kricheldorf, H. R. and Schwarz, G. (2010). "Polymerization of cyclosiloxanes by means of triflic acid and metal triflates." *Macromolecular Chemistry and Physics* 211 (12): 1311-1321.
- Yu, J., Yang, M., Lin, T.-F., Guo, Z., Zhang, Y., Gu, J. and Zhang, S. (2007). "Effects of surface characteristics of activated carbon on the adsorption of 2-methylisobornel (MIB) and geosmin from natural water." *Separation and Purification Technology* 56 (3): 363-370.
- Yu, M., Gong, H., Chen, Z. and Zhang, M. (2013). "Adsorption characteristics of activated carbon for siloxanes." *Journal of Environmental Chemical Engineering* 1 (4): 1182-1187.
- Zazo, J. A., Casas, J. A., Mohedano, A. F. and Rodriguez, J. J. (2006). "Catalytic wet peroxide oxidation of phenol with a Fe/active carbon catalyst." *Applied Catalysis B-Environmental* 65 (3-4): 261-268.



---

Chapter 11

APPENDICES



## A. Calibration curves GC-FID

---

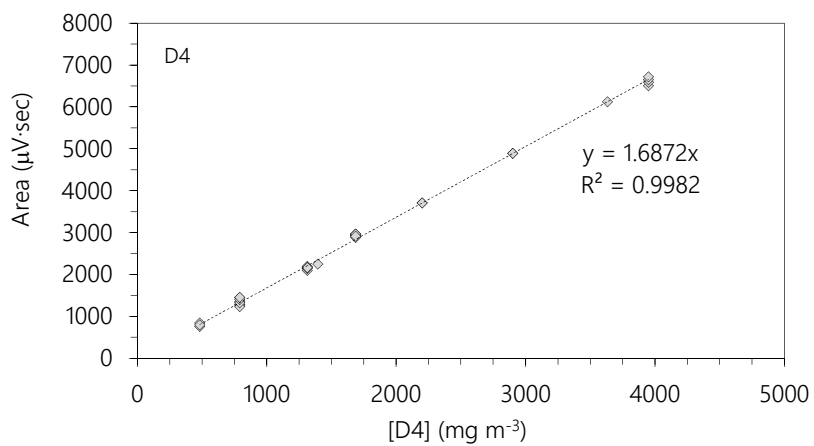


**Figure 11.1** Calibration curve of D4 in N<sub>2</sub> gas matrix

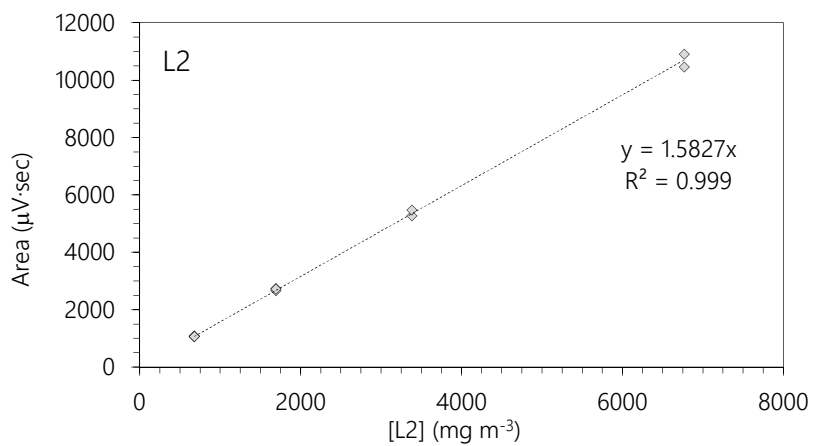


**Figure 11.2** Calibration curve of L2 in N<sub>2</sub> gas matrix

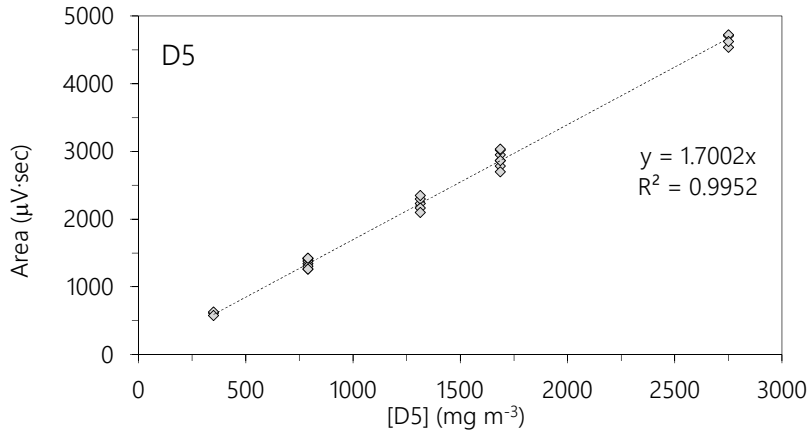


**Figure 11.3** Calibration curve of D5 in  $\text{N}_2$  gas matrix

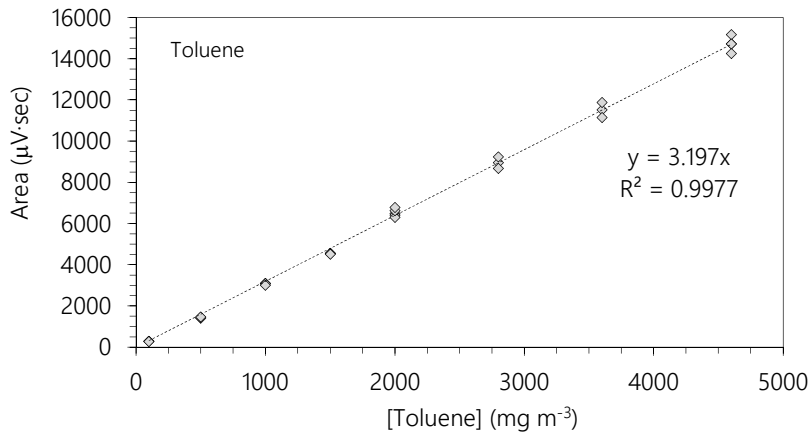


**Figure 11.4** Calibration curve of Toluene in  $\text{N}_2$  gas matrix

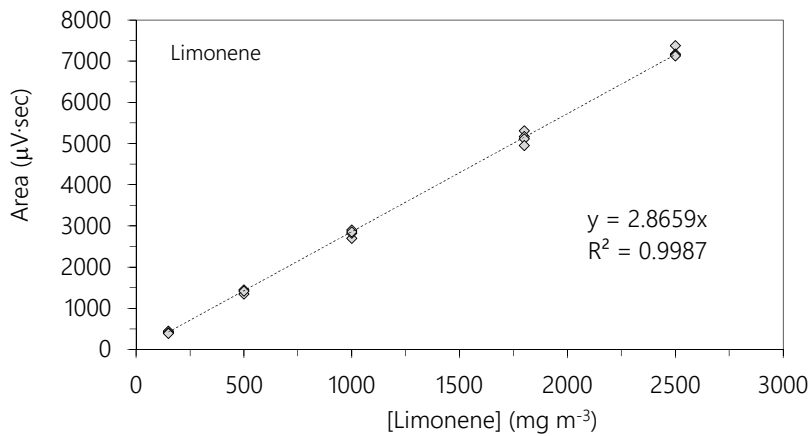


**Figure 11.5** Calibration curve of Limonene in  $\text{N}_2$  gas matrix

## B. Calibration curves GC-MS

---

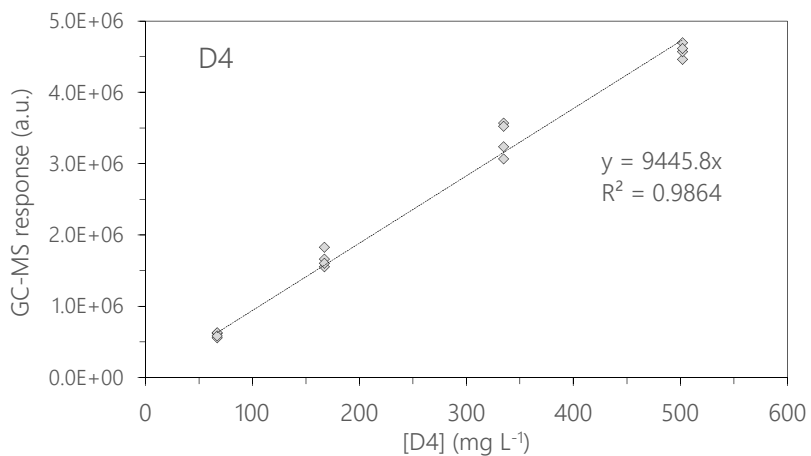


Figure 11.6 Calibration curve of D4 in THF dissolution

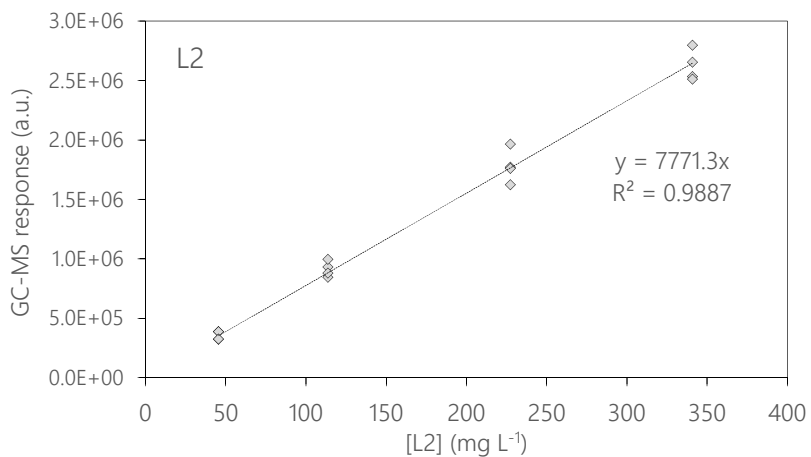
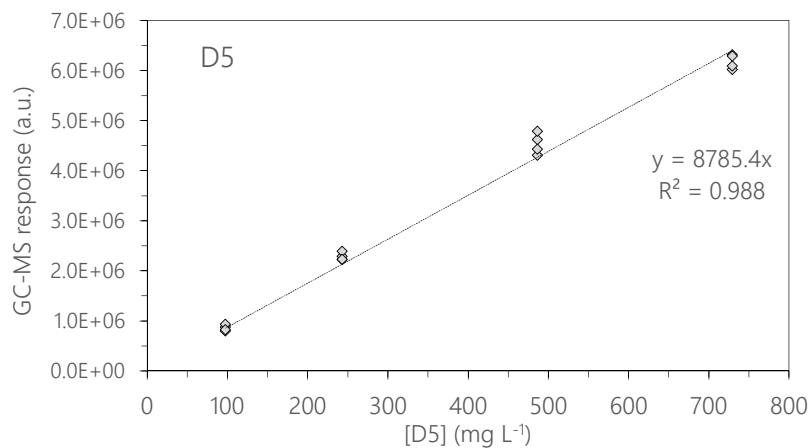
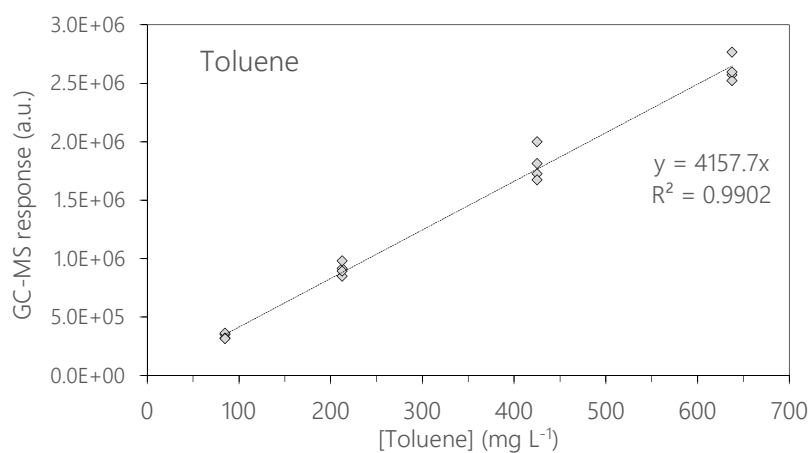


Figure 11.7 Calibration curve of L2 in THF dissolution



**Figure 11.8** Calibration curve of D5 in THF dissolution



**Figure 11.9** Calibration curve of Toluene in THF dissolution

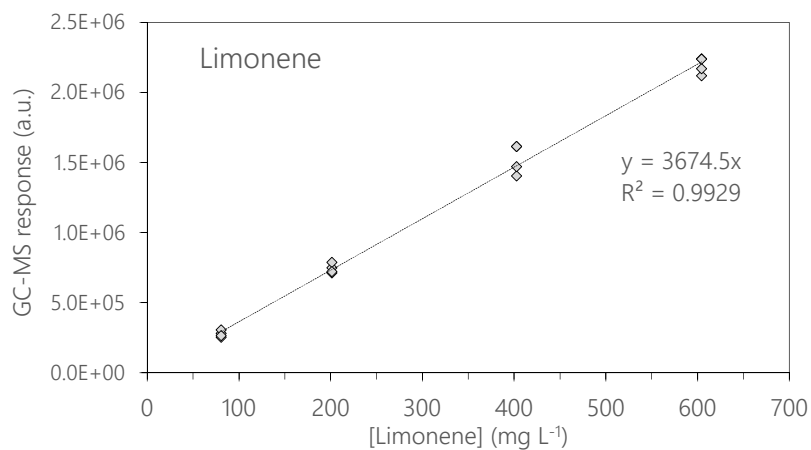


**Figure 11.10** Calibration curve of limonene in THF dissolution

### C. Calibration curves UV-VIS spectroscopy

---

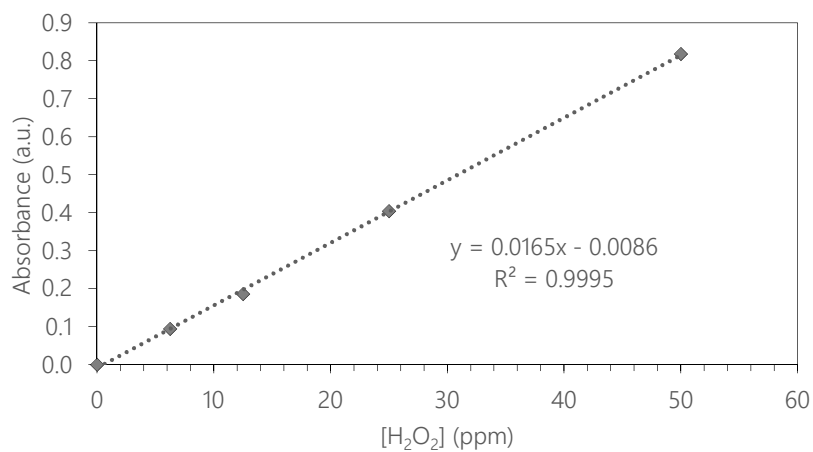


**Figure 11.11** Calibration curve of H<sub>2</sub>O<sub>2</sub> ( $\lambda=410$  nm)

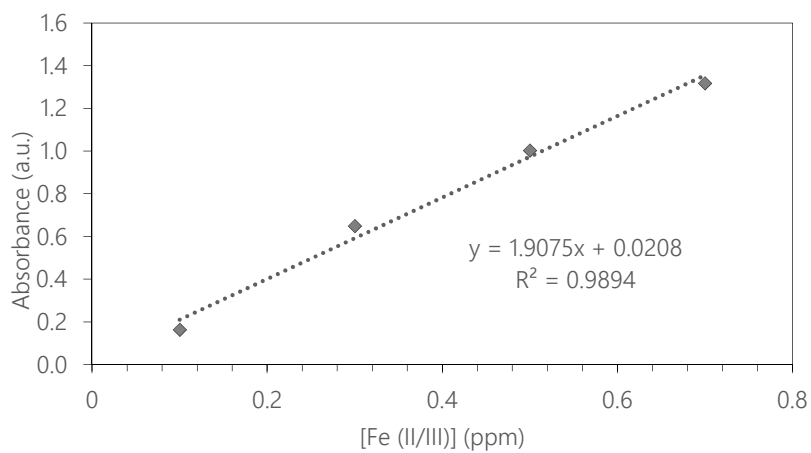


**Figure 11.12** Calibration curve of Fe(II/III) ( $\lambda=504$  nm)

## D. AC characterization

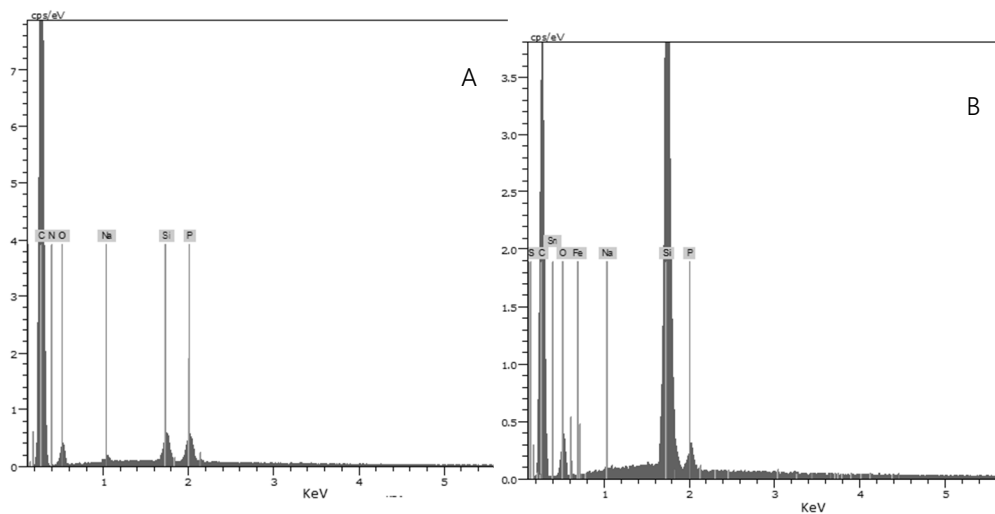


Figure 11.13 EDX spectra of A) fresh MWV-2 B) D4-saturated MWV-2.

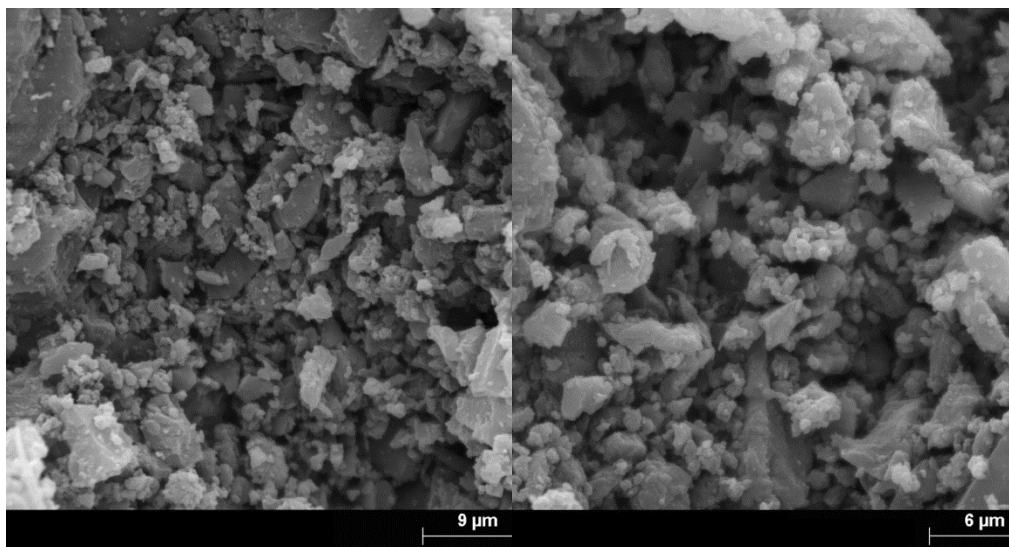
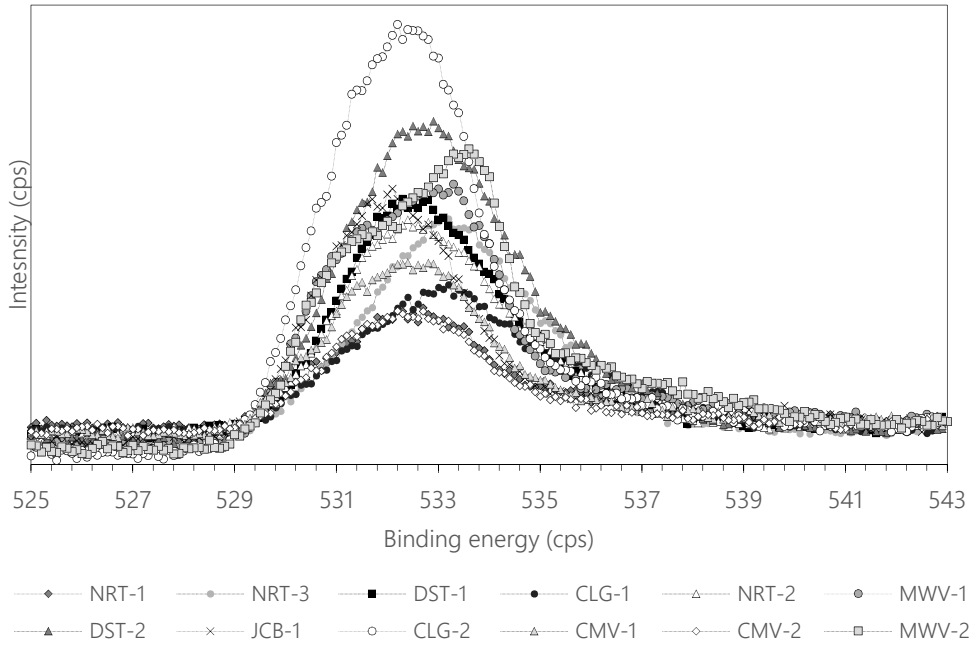
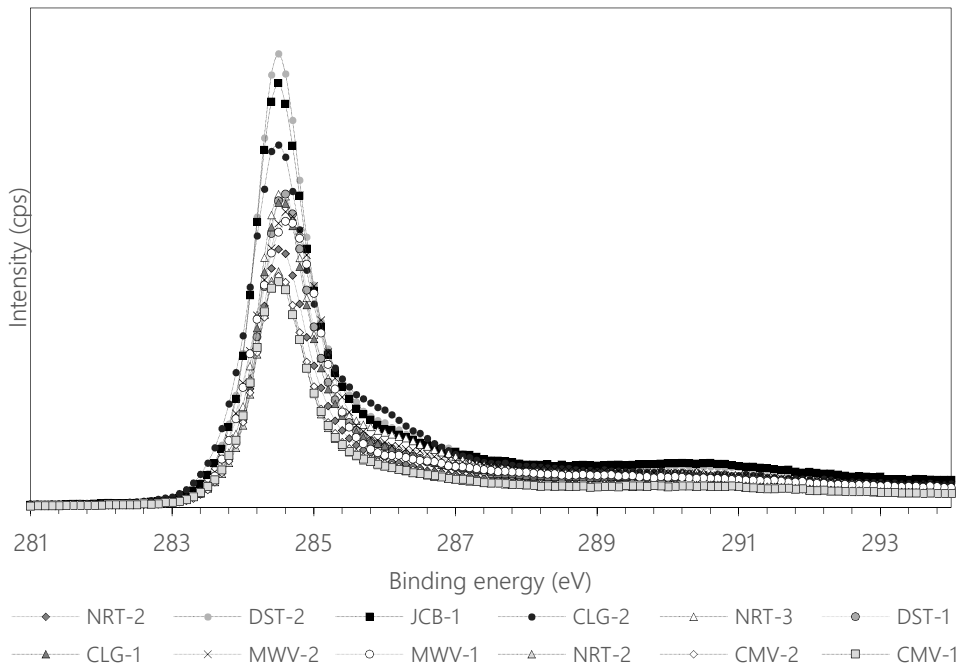


Figure 11.14 SEM image of A) fresh MWV-2 and B) D4-saturated MWV-2.



**Figure 11.15** XPS oxygen (1s) spectrum of activated carbons.



**Figure 11.16** XPS carbon (1s) spectrum of activated carbons.

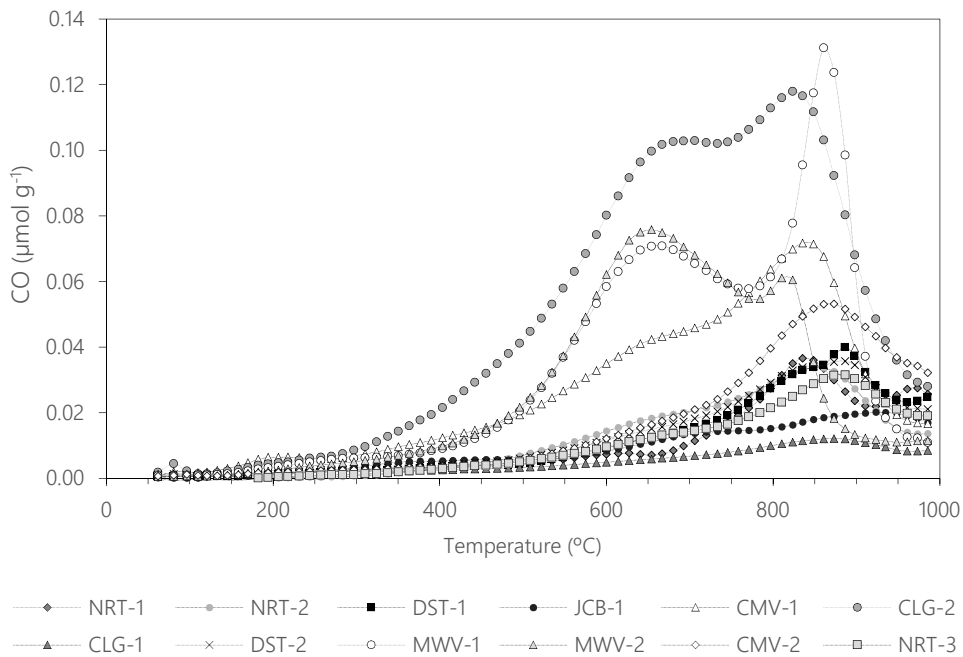


Figure 11.17 CO desorption curve for all the activated carbons considered.

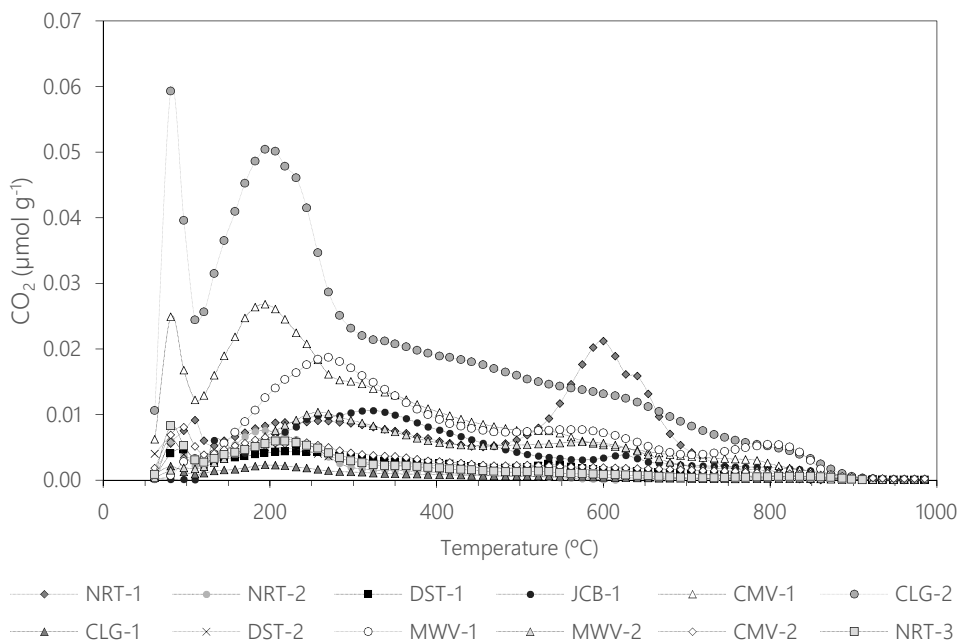


Figure 11.18 CO<sub>2</sub> desorption curve for all the activated carbons considered.